

## Early Cambrian Small Shelly Fossils from northwest Mexico: Biostratigraphic implications for Laurentia

Léa Devaere, Sébastien Clausen, Jesús Porfirio Sosa-Leon,  
Juan José Palafox-Reyes, Blanca Estela Buitrón-Sánchez, and Daniel Vachard

### ABSTRACT

The early Cambrian record of Small Shelly Fossils (or SSFs) of Laurentia has been relatively poorly studied despite their major importance for understanding the Cambrian explosion. They represent key biostratigraphic tools for the subdivision and correlation of the Terreneuvian and Cambrian Series 2 at regional and global scales. This study is aimed at improving our knowledge of SSF stratigraphic ranges of Laurentia by focusing on the Puerto Blanco Formation of the Cerro Rajón section, near Caborca in northwestern Sonora, Mexico. Four SSF assemblages have been recovered that include sclerites of chancelloriids (*Archiasterella hirundo*, *A. charma*, *A. cf. A. pentactina*, *Allonnia erromenosa*, *A. tetrathallis* and *Chancelloria* spp.), hyolithelminths (*Hylolithellus* spp.), hyoliths (*Cupitheca* cf. *C. mira*, *Petasothea* sp., Hyolithid sp. and *Parkula bounites*), micromolluscs (*Mackinnonia corrugata*, *Xianfengella* sp., *Pelagiella* sp. and *Pojetaia* sp.), brachiopods (*Eoobolus* sp. and *Rajonia ornata*), sclerites of the lobopod *Microdictyon multicavus*, one unidentified bradoriid and an indeterminate fossil. Distribution of the SSFs that extend below the first trilobite and archaeocyathan demonstrates that most of the Puerto Blanco Formation is Cambrian Age 3 to 4. The SSFs provide additional clues to correlate Ediacaran-Cambrian sedimentary successions in Sonora with the southern Great Basin (USA). The described assemblages are also compared with SSF assemblages of other localities of the American Cordillera and southeastern Laurentia. At the global scale, they support faunal connections with Australia and possibly China.

Léa Devaere. Museum für Naturkunde, Leibniz-Institut für Evolutions- und Biodiversitätsforschung, Invalidenstr. 43, 10115 Berlin, Germany. lea.devaere@mfn-berlin.de and Univ. Lille, CNRS, UMR 8198 - Evo-Eco-Paleo, F-59000 Lille, France. lea.devaere@univ-lille.fr

Sébastien Clausen. Univ. Lille, CNRS, UMR 8198 - Evo-Eco-Paleo, F-59000 Lille, France. sebastien.clausen@univ-lille1.fr

Jesús Porfirio Sosa-Leon. Universidad de Sonora, Departamento de Geología, Boulevard Luis Encinas y Rosales, 83000 Hermosillo, Sonora, Mexico. sosa@geologia.uson.mx

Devaere, Léa, Clausen, Sébastien, Porfirio Sosa-Leon, Jesús, Palafox-Reyes, Juan José, Buitrón-Sánchez, Blanca Estela, and Vachard, Daniel. 2019. Early Cambrian Small Shelly Fossils from northwest Mexico: Biostratigraphic implications for Laurentia. *Palaeontologia Electronica* 22.2.41A 1-60. <https://doi.org/10.26879/880>  
[palaeo-electronica.org/content/2019/2600-early-cambrian-ssfs-of-mexico](http://palaeo-electronica.org/content/2019/2600-early-cambrian-ssfs-of-mexico)

Copyright: July 2019 Paleontological Society.

This is an open access article distributed under the terms of Attribution-NonCommercial-ShareAlike 4.0 International (CC BY-NC-SA 4.0), which permits users to copy and redistribute the material in any medium or format, provided it is not used for commercial purposes and the original author and source are credited, with indications if any changes are made.  
[creativecommons.org/licenses/by-nc-sa/4.0/](http://creativecommons.org/licenses/by-nc-sa/4.0/)

Juan José Palafox-Reyes. Universidad de Sonora, Departamento de Geología, Boulevard Luis Encinas y Rosales, 83000 Hermosillo, Sonora, Mexico. [juan\\_palafox@hotmail.com](mailto:juan_palafox@hotmail.com)

Blanca Estela Buitrón-Sánchez. Universidad Nacional Autónoma de México, Instituto de Geología, Departamento de Paleontología, Ciudad Universitaria, Delegación Coyoacán, 14510 México D.F. [blancab@unam.mx](mailto:blancab@unam.mx)

Daniel Vachard. 1 Les Tilleuls, 59152 Gruson, France. [daniel.vachard@univ-lille1.fr](mailto:daniel.vachard@univ-lille1.fr)

Keywords: Small Shelly Fossils; Laurentia; Mexico; Cambrian Series 2; biostratigraphy

Submission: 18 April 2018. Acceptance: 17 May 2019.

## INTRODUCTION

Small Shelly Fossils (or SSFs as named by Matthews and Missarzhevsky in 1975) is an umbrella term that refers to a polyphyletic assemblage of skeletonized organisms that thrived during the early Cambrian. They are typically preserved as phosphatic microfossils. They can be extracted relatively easily through acid digestion of carbonate rocks. Documenting SSFs is particularly important because they contribute to an increased understanding of the earliest phases of bilaterian radiation at the beginning of the Cambrian. Along with their phylogenetic (e.g., Shu et al., 2014), palaeobiogeographic (e.g., Yang et al., 2015) and palaeoecologic (e.g., Budd and Jackson, 2016) significance, SSFs can play a pivotal role in establishing the chronology of the different events occurring during the Cambrian explosion. They are reported during the early and middle Cambrian, but most importantly during the Terreuneuvian, the Cambrian interval devoid of trilobites and agnostoids, which are the main biostratigraphic tools for the rest of the System. The International Subcommission on the Cambrian Stratigraphy has emphasized the high potential of SSFs for biostratigraphic subdivision of the early Cambrian and SSF First Appearance Data (FAD) have been proposed for the definition of the base of several Cambrian stages (summary in Peng et al., 2012; Devaere et al., 2013; Clausen et al., 2015; Zhang et al., 2017). Two FAD of SSFs are proposed for the definition of the base of the Cambrian stage 2: the FAD of the micromollusc *Watsonella crosbyi* or the FAD of *Aldanella attleboensis*. Trilobites are first recorded in the Cambrian stage 3 along with SSFs. In this time interval, FAD of the latter can be considered for the definitions of the stage boundaries, such as the FAD of *Pelagiella subangulata*, the FAD of *Microrodictyon effusum* along with other guides such as *Rhombocorniculum cancellatum*, species of the *Lapworthella cornu* group and *Mobergella radiolata*, but can also be used as complementary bio-

stratigraphic tools to further test and correlate the trilobite biozones, which are otherwise largely affected by diachroneity (Peng et al., 2012) and provincialism (Álvaro et al., 2013). However, for the Cambrian stage 3, FAD of SSFs are not entirely satisfactory and need further investigation.

Due to their great biostratigraphic potential, lower Cambrian SSFs have been largely studied in major palaeocontinents, but remain relatively poorly studied in Laurentia. Recent studies have mainly focused on the upper lower Cambrian of the southeastern palaeomargin of Laurentia, especially from Greenland (Skovsted and Peel, 2001; Skovsted, 2003a; Skovsted and Holmer, 2003; Skovsted, 2004, 2005; Skovsted and Holmer, 2005; Peel and Skovsted, 2005; Skovsted, 2006a; Skovsted et al., 2010; Peel et al., 2016; Skovsted, 2016), eastern USA (Landing and Bartowski, 1996; Skovsted and Peel, 2010), western Newfoundland (Skovsted, 2003b; Skovsted and Peel, 2007; Skovsted et al., 2017), Quebec (Landing et al., 2002) and Labrador (Spencer, 1980; Skovsted et al., 2010; Skovsted et al., 2017). But SSF data are severely lacking from older Cambrian strata and from the northern and western palaeomargins of this palaeocontinent, where successions are often dominated by dolostones, sandstones and shales that are unfavourable for SSF preservation. Very few SSFs have thus been reported from northern Laurentia in northwestern Canada (Conway-Morris and Fritz, 1984; Nowlan et al., 1985; Voronova et al., 1987), Nevada and California (Tynan, 1980, 1981a, 1981b, 1983; Skovsted, 2006b; Skovsted and Holmer, 2006; Wotte and Sundberg, 2017).

So far, no detailed biostratigraphic subdivisions have been proposed for the “pre-trilobitic” interval of Laurentia (Babcock et al., 2011; Peng et al., 2012). The trilobite biozonations for the Cambrian Series 2 are still difficult to establish, and the support of a complementary biostratigraphic tool is necessary to test correlations (Webster, 2011). In addition, most potential international chronostrati-

graphic SSF guide taxa have not yet been reported in Laurentia. However, a promising SSF assemblage has been described by McMenemy (1984) from mixed carbonate-siliciclastic deposits of northwestern Mexico (Sonora) that could help in filling this gap. Unfortunately, this important work did not provide stratigraphic intervals of the recovered fauna.

Dating the Ediacarian-Cambrian succession in northwestern Sonora is also of prime importance to better constrain the regional geodynamic history. The break-up of Rodinia resulted in two main palaeocontinents, Gondwana and Laurentia, estimated to have ended at ~555-550 Ma, according to tectonic subsidence curves and palaeomagnetic data (Bond et al., 1984; Meert and Torsvik, 2003; Poole et al., 2005). However, the rifting most probably constituted multiple branches, along which associated transform-faults might have remained episodically active until 525 Ma along the southwest palaeomargin of Laurentia (Poole et al., 2005). This latter activity is mostly recorded by associated igneous activity and sedimentary infill of intracratonic graben systems or transform basins (Buffler and Thomas, 1994; Poole et al., 2005). In this context, the Ediacaran-Cambrian rocks in northwestern Sonora, located on the western margin of Cambrian Laurentia, is unique in recording a thick volcano-sedimentary episode marked by alternation of volcanic rocks and volcanoclastic deposits which attest for a still intense geodynamic activity in this area. Nevertheless, the exact duration and context of this episode remain poorly constrained. However, a detailed palaeontological study of these Cambrian-Ediacaran sedimentary rocks of northwestern Sonora would provide a unique opportunity to better biostratigraphically constrain this episode.

It is, therefore, proposed herein to detail the SSF assemblages of the Puerto Blanco Formation (PBF) in the Cerro Rajón section, near Caborca in northwestern Mexico that were first studied by McMenemy (1984). The stratigraphic range of the taxa identified is detailed to allow chronostratigraphic interpretation facilitating global correlations and to contribute baseline data for the future construction of an SSF-based biostratigraphic chart for Laurentia.

## GEOLOGICAL SETTING

This study focuses on the mixed sedimentary succession that includes rocks from the upper part of the Neoproterozoic and the Cambrian of the Cerro Rajón, a low hill located in the northwestern

part of Mexico, in the Sonora State, 40 km SSE to the city of Caborca (Figure 1.1-3). This Neoproterozoic-Cambrian also outcrops in other hills and ranges of the area (some are reported in Figure 1.3, see Stewart and Poole, 2002 for latest review).

The Neoproterozoic-Cambrian of Caborca can be correlated with the southern Great Basin of southwestern USA, and particularly with California (Death Valley succession) and Nevada (Stewart et al., 1984, Loyd et al., 2012). They all belong to the American Cordillera and are interpreted to have been deposited along the rifted northern margin of Laurentia (Eardley, 1951; Stewart, 1970; Dickinson, 1981; Stewart et al., 1984; Stewart and Poole, 1975; Stewart et al., 2002; Stewart, 2005). Today, the Neoproterozoic-Cambrian successions of the Mojave Desert of California and of the Caborca area (northwestern Sonora) are offset. This offset has been tentatively explained by, or used to support the Mojave-Sonora megashear hypothesis (Stewart, 2005). The Mojave-Sonora megashear was originally hypothesized by Silver and Anderson (1974) and further supported by Anderson and Schmidt (1983), Anderson and Silver (2005), Nourse et al. (2005) and Stewart (2005) to explain an apparent disjunct distribution of U-Pb ages of Proterozoic basements in the Mojave Desert and northwestern Sonora (Silver and Anderson, 1974; Amato et al., 2009). It was modelled as a large-scale, cryptic, NW-SE-trending, mid-Mesozoic system of left-lateral strike-slip faults extending from the Mojave Desert across Sonora. In Sonora, different Proterozoic crystalline provinces have been described, based on distinct chronological histories, and later, on isotopic determination (U-Pb zircons geochronology by Anderson and Silver, 2005; U-Pb zircons geochronology and Nd isotopic data by Farmer et al., 2005). Among these, existence of the Caborca block, and its affinities with major provinces of the southwestern United States have been argued since the early work of Silver and Anderson (1974), and Campa and Coney (1983). However, even if such affinities and their consistency with the megashear hypothesis have been reaffirmed recently (Farmer et al., 2005; Solari et al., 2018), they do not provide a definitive demonstration of this model, and an autochthonous origin of the Caborca terrane still remains possible (as supported by Vachard et al., 2017 and the “wrap-around” model of Stewart, 2005). In such a case, the distance between the Caborca block successions and the correlative successions in southwestern USA may only be due to an eastward curvature of the Cordilleran margin of Laurentia into northern

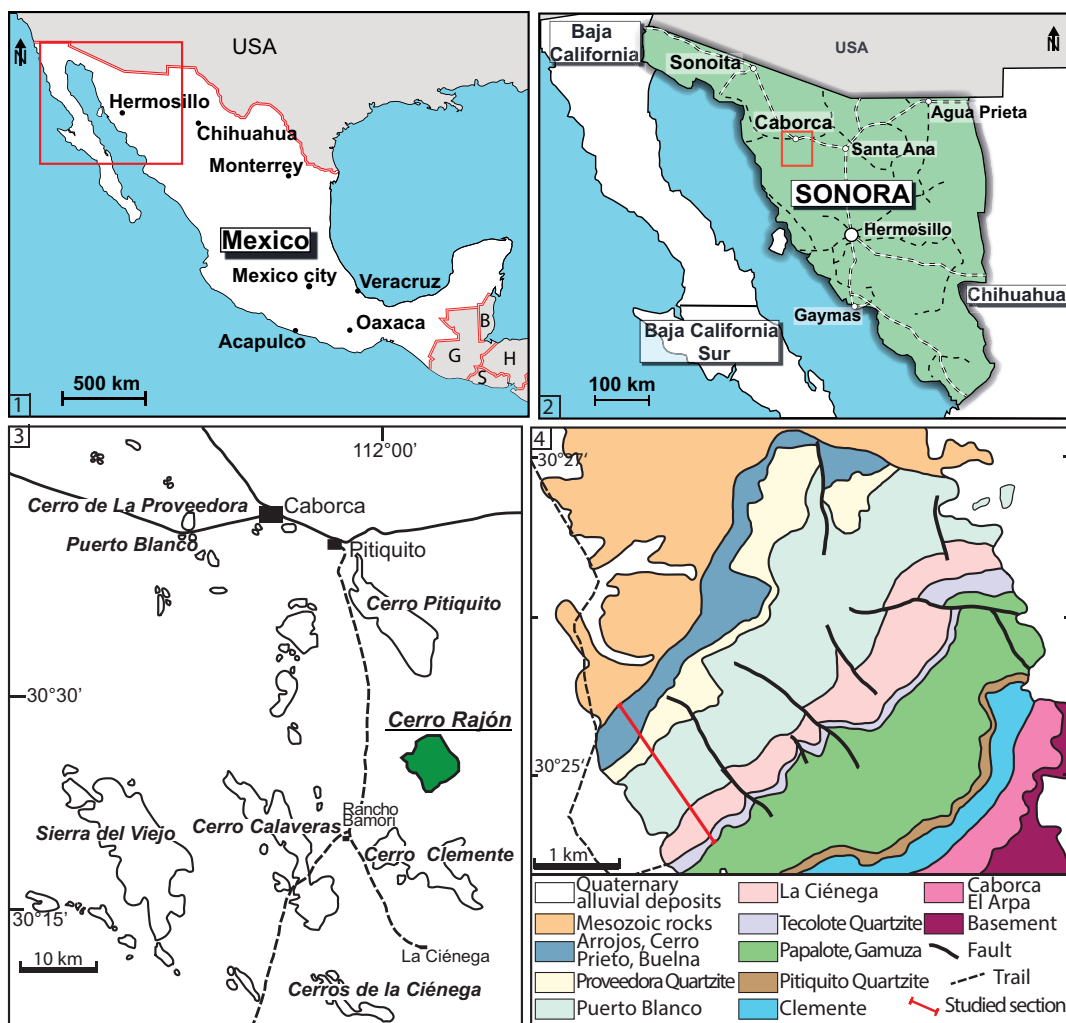


**FIGURE 1.** Geological setting. 1. Mexico and neighbouring countries (B for Belize, G for Guatemala, H for Honduras and S for El Salvador); area in the square is magnified in 2. 2. Main cities and roads of Sonora State, red square delimiting the area represented in 3. 3. Studied area. Indicated are the main roads (plain lines), trails (dashed lines) and cerros with Ediacaran/Cambrian succession outcrops, after Stewart et al. (1984), McMenamin (1987) and Sour-Tovar et al. (2007). 4. Geological map of Cerro Rajón reporting the distribution of basement rocks, Ediacaran and Cambrian formations, Mesozoic rocks and Quaternary alluvial deposits, after McMenamin (1984) and Stewart et al. (1984).

Mexico (Eardley, 1951; Stewart and Poole, 1975; Peiffer-Rangin, 1979; Stewart et al., 1984; Poole et al., 2005; Stevens et al., 2005; Iriondo et al., 2005; Molina-Garza and Iriondo, 2007; Amato et al., 2009). The age, orientation, and magnitude of possible fault displacements and the subsequent sutures between blocks have also been debated (see e.g., Iriondo et al., 2005; Poole et al., 2005; Amato et al., 2009). Mexico has a very complex geological history resulting from the merging of a number of terranes with Gondwanan, Laurentian or Rheic affinities, during the formation of Pangea. The latter resulted in the closure of the Rheic ocean and the Ouachita-Marathon-Sonora oro-

gen, a 3000-km-long belt bordering the southern margin of the Laurentian (North American) craton (Poole et al., 2005). The geological history leading to this puzzling structure is still highly debated.

The present study focuses on the Puerto Blanco Formation (PBF), which has been suggested to include Ediacaran and Cambrian strata (Sour Tovar et al., 2007) with a diverse early Cambrian macrofauna and microfauna (Cooper and Arellano, 1952; McMenamin, 1984; Stewart et al., 1984; Debrenne, 1987; McMenamin, 1987; Debrenne et al., 1989; McMenamin, 1992; McMenamin et al., 1994; McMenamin, 2008). The PBF is underlain by the Neoproterozoic La

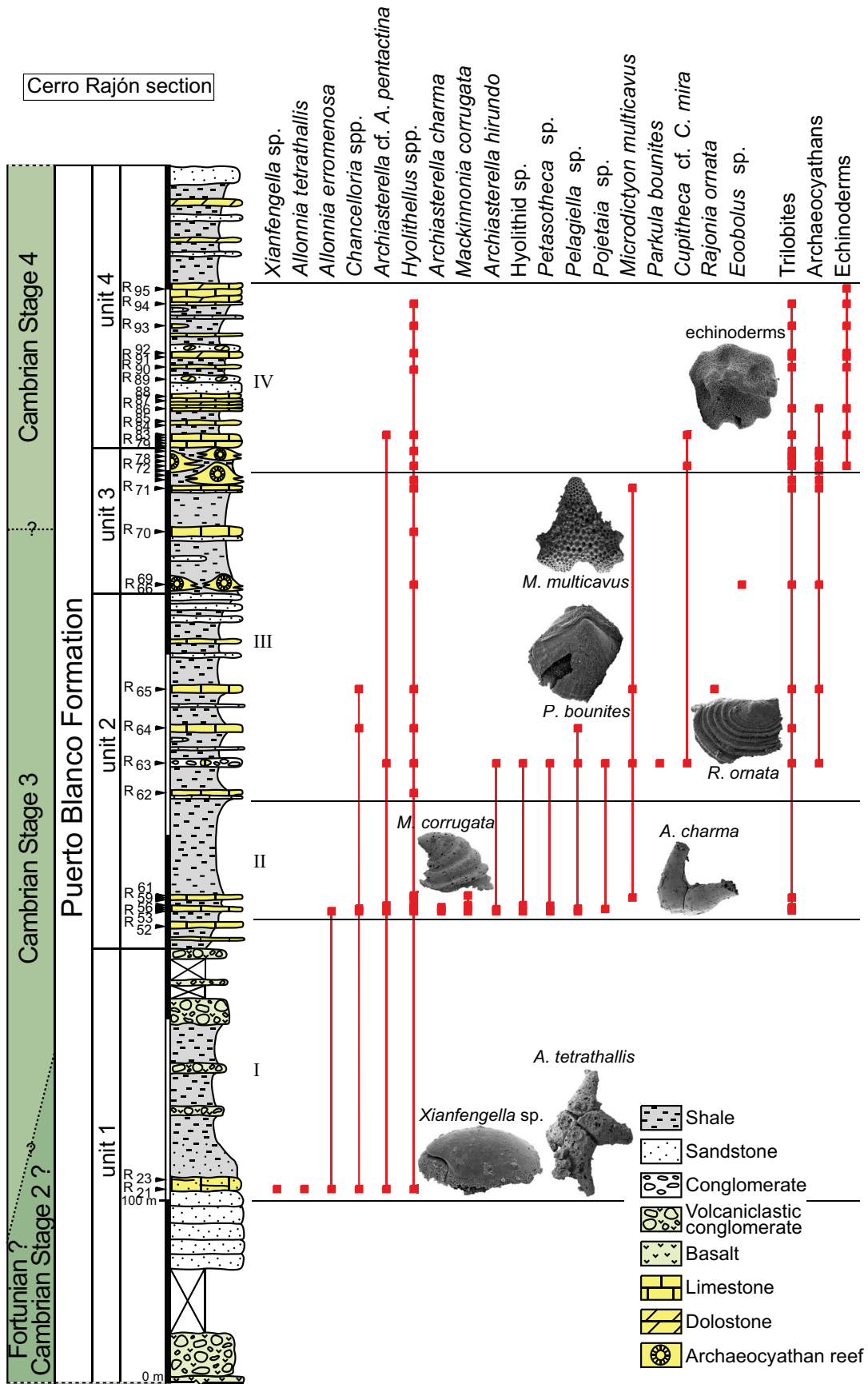
Ciénega Formation. The La Ciénega Formation was introduced by Stewart (1984) as a 178 m succession of sedimentary rocks dominated by dolostones that alternate with quartzites and siltstones at the type section of the Cerro Rajón (reported in Figure 1.3). It was here re-evaluated at about 130 m thick. However, due to the content of the formation and the absence of clearly defined boundaries along the observed gradual change from the underlying Tecolote Formation, precise recognition of this unit is in practice very difficult. It is also to be noted that the type section studied by Stewart (1984) was composite and slightly discontinuous (see Stewart et al., 1984, figure 3), which might have introduced errors in description and measurement. The formation that overlies the PBF in the Caborca area is the Proveedora Quartzite and is composed of prominent, poorly stratified quartzite with a thickness varying between 200 m and 225 m (Stewart et al., 1984). As summarized by Stewart et al. (1984), the PBF was first defined by Cooper and Arellano (1952) at the type section of the Cerro de la Proveedora (reported in Figure 1.3) as ~293 m of green shale, limestone and sandstone containing archaeocyathans, hyoliths, trilobites and brachiopods. However, the basal contact of the formation was unknown at this locality (Cooper and Arellano, 1952). Arellano (1956) reported a more complete succession in a range to the southeast of the village of Pitiquito that he named Cerro Rajón (reported in Figure 1.3). Eells (1972) later investigated another, more complete succession in the Cerros Calaveras (reported in Figure 1.3) and in small hills, east to the Cerros Calaveras. There, he similarly defined the PBF as a succession of siltstone, quartzite and limestone, but deposited stratigraphically between a thick (~200 m) volcanoclastic unit below and the overlying Proveedora Quartzite. The volcanoclastic units, associated with basalts, were included within the PBF by Longoria (1981), a statement followed by Stewart et al. (1984, p. 15-16) who argued that "basalt (greenstone) and volcanoclastic rocks are interstratified with siltstone and quartzite similar to these included by Eells (1972) in his Puerto Blanco Formation" in the Cerro Rajón section which was first described by Arellano (1956). Our observations in different hills of the area question this argumentation. However, this latter definition is followed pending further investigation. In the absence of a defined lower boundary, this formation is considered to start, in Cerro Rajón, at the base of the first volcanoclastic horizon. Such a thick volcanoclastic unit, suggested to include the Ediacaran-Cambrian transition by

some authors (Sour-Tovar et al., 2007), is unique along the western palaeomargin of Laurentia. However, its precise stratigraphic extent remains undetermined.

The Cerro Rajón section was selected for this study of the PBF because it is well exposed, continuous and not, or very little, affected by deformation. The PBF has been informally subdivided into four lithological units based on observations by Stewart et al. (1984) in the Cerro Rajón. Such a subdivision into four units is grossly supported by the present study, only the boundary between unit 3 and 4 is slightly revised as the microbial-archaeocyathan reefs levels are considered to be strictly restricted to unit 3 (Figure 2). Unit 1 is ~275 m thick and is delimited by the first and last occurrence of volcanic/volcanoclastic beds. It is dominated by volcanoclastic sandstones and conglomerates with rare interstratified basalt flows. Rare shales are intercalated between the sets of coarser, volcanic-related material. Sandstone beds with oblique laminations, thin limestone nodules and beds alternating with shales are intercalated in the middle part of the unit without any volcanic-related material. Unit 2 is ~190 m thick, composed exclusively of sedimentary material and is dominated by shales. Intercalation of fine, laminated sandstone and limestone laminated beds and nodules are present. The ~80 m unit 3 is delimited by two levels of microbial-archaeocyathan limestone separated by calcareous shales with thin intercalations of sandstone and limestone. Although unit 3 is slightly extended herein, its thickness is significantly different from Stewart's evaluation (80 m vs about 117.5 m). This difference may reflect lateral variations or error due to study through composite sections by Stewart et al. (1984, figure 3). Unit 4 is ~155 m thick and composed of finely bedded and laminated sandy limestone to dolostone, nodular limestone and laminated sandstone alternating with shale.

## MATERIALS AND METHODS

Forty-four carbonate samples (average weight of 1.2 kg) were collected directly from the beds of a continuous section at the Cerro Rajón (Figures 1.3, 2). They were broken into fragments and dissolved, either with ~10% acetic acid when dealing with limestone or with ~8% formic acid for the slightly dolomitic limestone. The acid-resistant residues were sifted (>50 µm), dried and the microfossils were picked from the residues under a stereomicroscope. The SSFs were coated with palladium and observed and imaged with a Scanning



Electron Microscope FEI Quanta 200 at University Lille. The described and figured material is housed in the collections of University Lille (acronym USTL for Université des Sciences et Technologie de Lille) following the recommendation of the International Commission on Zoological Nomenclature.

## BIOSTRATIGRAPHIC ASSESSMENT AND CORRELATION

### Age of Recovered SSF Assemblages

This new study of the SSFs of the PBF at the Cerro Rajón provides detailed stratigraphic ranges of the taxa, allowing illustration of the evolution of the microfauna along the section through four distinct assemblages (Figure 2). The first assemblage comes from the sandy limestone nodules intercalated within fine shales from the otherwise mostly siliciclastic and volcanoclastic unit 1 of the PBF (sample R21; Figure 2). *Xianfengella* sp. and *Allonnia tetrathallis* are characteristic of this first assemblage. The second assemblage, from the lowermost limestone beds of unit 2 of the PBF (samples R53 to R61, Figure 2), is differentiated by the presence of *Mackinnonia corrugata* and *Archiasterella charma*. *Parkula bounites* and *Rajonia ornata* are restricted to the third assemblage that occurs in the middle of unit 2 (samples R62 to R65; Figure 2). *Microdictyon multicavus* is also quite characteristic of the third assemblage, even if one fragment has also been recovered in the second assemblage. Mickwitziid valves and fragments are very abundant (but not described in this paper) in the third assemblage which also includes rare, small archaeocyathan fragments although the first microbial-archaeocyathan reefs occur in unit 3 of the PBF. Our interpretation of mickwitziid characters differs from that proposed by McMenamin (1984, 1992), with important implications for our understanding of early brachiopod evolution. Such phylogenetic discussion is out of the scope of the present study and a detailed study of mickwitziid valves and fragments will be presented in a later publication. The last assemblage is differentiated by the first occurrence of echinoderm ossicles and

corresponds to the upper reefal interval of unit 3 and to unit 4. The echinoderm ossicles are associated with *Hyolithellus* spp., trilobites and mickwitziids.

*Hyolithellus* spp. occur throughout the PBF. *Allonnia erromenosa*, *Archiasterella* cf. *A. pentactina* and *Chancelloria* spp. are present in, but not restricted to, the first assemblage. In addition to taxa from the first assemblage, different taxa occur from the second assemblage upward: *Archiasterella hirundo*, *Petasotheca* sp., *Pelagiella* sp., *Pojetaia* sp., Hyolithid sp., *Microdictyon multicavus* (only one specimen) and trilobite fragments. Mickwitziids are rarely found in the second assemblage and occur only as fragments; they are more abundant and better preserved in the third assemblage. They last occur a few meters below the base of the fourth assemblage. The first occurrence of *Cupithea* cf. *C. mira* is recorded in the third assemblage but its stratigraphic range extends to the fourth assemblage.

Some of the taxa reported in the different assemblages described above had already been described by McMenamin (1984) such as *Microdictyon multicavus*, *Chancelloria* spp., *Pelagiella* sp. and *Rajonia ornata*. In some cases, taxonomic interpretations might slightly differ: taxa referred to various species of *Hyolithellus* (*H. mexicanus*, *H. micans*, ?*Hyolithellus* sp.) by McMenamin (1984) are here referred to *Hyolithellus* spp. due to the poor taxonomic resolution of the genus. ?*Paragloborilus* cf. *P. mirus* described by McMenamin (1984) is here assigned to *Cupithea* cf. *C. mira*. Most probably, the specimens described as *Bemella mexicana* McMenamin, 1984 in the plate legend and as *Bemella pauper* (Billings, 1872) in the text by McMenamin (1984) corresponds to *Mackinnonia corrugata* but the poor preservation of the material figured by McMenamin (1984) prevents any definite synonymy. *Lapworthella filigrana* Conway Morris and Fritz, 1984 reported in the PBF unit 3 at the Cerro Rajón by McMenamin (1984) was not recovered in this study despite a very detailed sampling. The high abundance and diversity of chancelloriid sclerites occurring along the

**FIGURE 2** (figure on previous page). Stratigraphic section through the Puerto Blanco Formation at Cerro Rajón with the range of identified SSFs and other fossils. The transition between the underlying La Ciénega Formation and the PBF is not represented as well as the lowermost part of the PBF as no limestone beds suitable for SSF studies were identified and sampled. The upper limit of the PBF illustrated corresponds to the transition between the PBF and the overlying Proveedora Quartzite. The four identified microfaunal assemblages are indicated by Roman numerals. The characteristic microfossils are figured without scale. The characteristic microfossils are, for assemblage I: *Xianfengella* sp. and *Allonnia tetrathallis*; assemblage II: *Mackinnonia corrugata* and *Archiasterella charma*; assemblage III: *Microdictyon multicavus*, *Parkula bounites* and *Rajonia ornata*; assemblage IV: echinoderm ossicles).

PBF at Cerro Rajón was not reflected in the study by McMenamin (1984). *Parkula bounites*, *Petastotheca* sp., *Xianfengella* sp. and the bradoriid species had not been previously reported from the area. With the description of the SSFs first assemblage, this paper represents the first report of fossils from unit 1 of the PBF. These are also the oldest SSFs ever described in Mexico. Finally, in McMenamin's (1984) work, the detailed stratigraphic range of the taxa in the Cerro Rajón section had not been reported, preventing analysis of the evolution of the microfaunal assemblages and their use for biostratigraphy and chronostratigraphic interpretations. Only the composite stratigraphic range of some of the SSFs was reported by Stewart et al. (1984).

Some of the taxa formally identified in the PBF at the Cerro Rajón have a wide palaeogeographic distribution and a relatively well-described stratigraphic range that enable their use for biostratigraphic interpretation of the section (Figure 3). It appears that the sampled and fossiliferous part of the PBF corresponds mainly to the Cambrian stage 3 to Cambrian stage 4 based on the SSFs global stratigraphic range. Indeed, the age of the PBF based on the SSFs distribution can be inferred here only from their lowest occurrence in the middle part of unit 1 (sample R21). Among the taxa that occur in this sample, only the formally identified *Allonnia tetrathallis* and *A. erromenosa* have a global stratigraphic range that can be used for biostratigraphic interpretation (Figure 3). *A. erromenosa* occurs in the Cambrian stage 2 and Cambrian stage 3 of China and India and so does *A. tetrathallis* worldwide (see other occurrences in Systematic Palaeontology and Figure 3), except for a possible occurrence in the Cambrian stage 4 of Antarctica (Wrona, 2004). Therefore, the carbonate level intercalated between the volcanoclastic rocks of unit 1 of the PBF is interpreted to date most probably of Cambrian Age 2 to Age 3. *Archiassterella charma*, which occurs in unit 2, is restricted to the Cambrian stage 2 of China, while *Archiassterella hirundo*, *Mackinnonia corrugata* and *Parkula bounites* extend from Stage 3 to Cambrian stage 4 (see other occurrences in Systematic Palaeontology and Figure 3). No SSFs restricted to the Cambrian stage 4 have been identified that could help interpreting the position of the Cambrian Age 3-4 limit (Figure 3). So, based on the SSFs, the upper half of the PBF (from the base of unit 2) is interpreted to be of Cambrian Age 3 to 4.

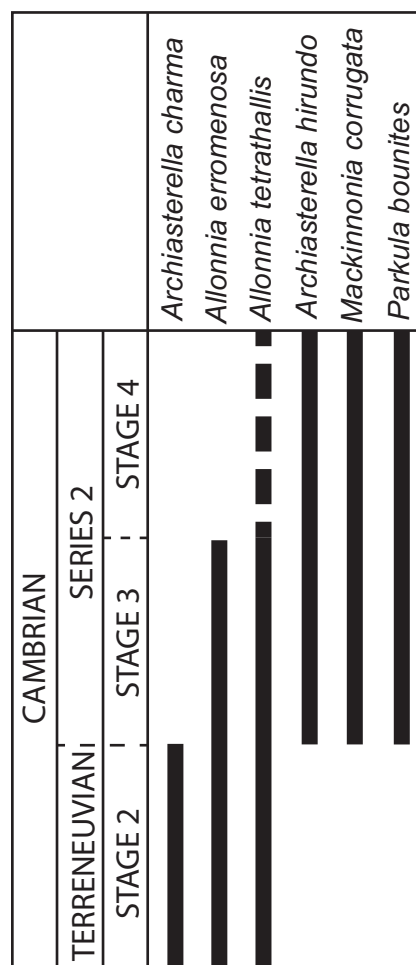


**FIGURE 3.** Range of globally distributed taxa recorded in the Puerto Blanco Formation. See Systematic Palaeontology ("other occurrences" of taxa) for references.

### Assessment of Previous Trilobite and Archaeocyath Biostratigraphic Interpretations

Different bio- and chronostratigraphic interpretations of the PBF have been proposed based on the distribution of various macrofossils. Cooper and Arellano (1946) reported that I.G. Gomez and L. Torres first discovered Cambrian trilobites in 1941 in the Caborca region. Trilobites have been described from the PBF around Caborca first by Lochman (1948, 1952) in the localities of Puerto Blanco, Cerro Prieto, Cerros de Los Difuntos and Cerros de La Proveedora. On the basis of the stratigraphic range of particular genera, Stewart et al. (1984) and McMenamin (1987) roughly recognized, following Fritz (1972, 1975): (1) the *Fallotaspis* zone, equivocally based on the occurrence of cf. *Fallotaspis* in unit 2 of the PBF at the Cerro Rajón (McMenamin, 1987); (2) the *Nevadella* Zone

in Sierra Agua Verde, ~100 km of Hermosillo in strata presumably correlated with the upper part of the PBF (McMenamin, 1987); and finally (3) the *Bonnia* – *Olenellus* Zone based on the occurrence of equivocal olenellid fragments and *Olenellus* sp. in unit 3 of the PBF in the Caborca area (Stewart et al., 1984) and in strata equivalent to the uppermost part of the PBF to the Proveedora quartzite at Sierra Agua Verde (Stewart et al., 1984) that are all defined in the North American Cordillera. However, as stated by Webster (2011), major systematic revisions have been proposed for these genera, considerably modifying their stratigraphic range, thus a revision of the trilobite biostratigraphy of *Laurentia* has been presented (Hollingsworth, 2007, 2011; Webster, 2011). It has been applied to the Sonoran sequences by Webster and Bohach (2014) and Cuen-Romero et al (2018). However, the trilobite biostratigraphy of Sonora has been based on the composite distribution of trilobites in the Puerto Blanco Formation from all over the Caborca area. From Cerro Rajón particularly, only McMenamin (1984, 1987) described cf. *Fallotaspis* from the base of unit 2 of the PBF and *Nevadia ovalis* McMenamin, 1987 and *Avefallotaspis? orbis* (McMenamin, 1987) in the middle portion of unit 3 (Webster and Bohach, 2014). *Avefallotaspis? orbis* indicates the Cambrian stage 3 *Avefallotaspis maria* Zone (part of the outdated *Nevadella* Zone; Webster and Bohach, 2014).

In addition to the trilobites, two levels of archaeocyathan-microbial buildups occur in unit 3 of the PBF in Cerro Rajón. Their systematics, palaeoecology and depositional settings have been studied by Debrenne (1987) and Debrenne et al. (1989). The identified archaeocyaths mainly occur in Cambrian Age 4 rocks worldwide, but some genera also occur in the Cambrian stage 3 (Debrenne et al., 1989). New archaeocyathan material has been collected along with the SSFs and is being studied; the preliminary data obtained confirm that unit 3 corresponds to the Cambrian stages 3-4 based on the occurrences of the species. In addition, McMenamin (1987, note added in proof) reports the occurrence of “Silicified fragments of irregular archaeocyathans [...] from a kutorginid brachiopod-rich, thin limestone bed 26 m above the base of unit 2 of the Puerto Blanco Formation,” indicating a Cambrian Age 3.

The regional bio(chrono)stratigraphic charts of Sonora based on trilobites and archaeocyathans are consistent with the biostratigraphic interpretation based on the newly determined SSF stratigraphic distribution at Cerro Rajón. Trilobites,

occurring before archaeocyaths, have a better biostratigraphic potential in the studied area. However, pending further study, trilobites have a restricted use for biostratigraphic interpretations in the area, and Cerro Rajón in particular, due to the absence of a methodologically detailed study of the systematics and ranges of the taxa. Nevertheless, while it is not possible to precisely place the base of the Cambrian stage 4 based on the SSFs distribution at Cerro Rajón, the first occurrence of olenellids in the middle part of unit 3 of the PBF in other localities indicates the possible position of the base of this stage (Stewart et al., 1984).

Hence, the SSFs are a more effective biostratigraphic tool in the studied area. SSFs indicative of the Cambrian stage 3 appear in unit 1 of the PBF, significantly below the first trilobite presumably occurring in the upper half of unit 2 (but the specimen was recovered in a float at Cerro Rajón by McMenamin, 1987, so most probably come from higher in the section, according to topography, strike and dip of beds). The new SSFs data herein sharpen our knowledge of the extent of the Cambrian stage 3 in the PBF and allow a better correlation of this interval at the regional scale. However, detailed micropalaeontological studies in similar sections are required to verify the patterns identified from the study at Cerro Rajón.

### **Implication for the Understanding of the Ediacaran-Cambrian Transition in North-Western Sonora**

The exact position of the Ediacaran/Cambrian boundary in the Sonoran sedimentary succession has been strongly discussed due to the thick volcanoclastic succession affecting the interval and its fossil record. The Ediacaran/Cambrian boundary has tentatively been placed by Sour-Tovar et al. (2007) within unit 1 of the PBF at the Cerro Rajón on the basis of the occurrence of the trace fossil *Treptichnus pedum* (Seilacher, 1955), the FAD of which is internationally used for the correlation of the base of the Fortunian (Brasier et al., 1994). They report the lowest occurrence of *T. pedum* ~260 m above the base of unit 1 of the PBF (Sour-Tovar et al., 2007). Bioturbation is frequently abundant in the upper part of unit 2, but we have been unable to find other specimens of *T. pedum* in different sections of the area, and only one specimen was tentatively identified by Sour-Tovar et al. (2007), which may require further investigation by an ichnofossil expert. In any case, Cambrian stage 3 SSFs are reported herein from the middle part of unit 1 of the PBF. This occurrence invalidates the

interpretation of Sour-Tovar et al. (2007). Most probably their report of *T. pedum* does not correspond to the first appearance of the ichnofossil, but to its first record, which is usually diachronous due to strong dependence to lithofacies (Babcock et al., 2014). These results contribute to the ongoing debate about the use of the FAD of *T. pedum* for the recognition of the base of the Cambrian.

McMenamin (2008) places the Ediacaran/Cambrian boundary at the top of the La Ciénega Formation or near the boundary between the La Ciénega and Puerto Blanco formations. This interpretation is based on the report of *Cloudina* in the La Ciénega Formation (McMenamin, 1985). The fossils of this formation were first identified as hyoliths, *Sinotubulites* and *Cambrotubulus* by McMenamin (1985) and the La Ciénega Formation as Terreneuvian in age. However, Grant (1990) later synonymized the specimens from La Ciénega Formation with *Cloudina*, assigning the containing levels to the Ediacaran, an interpretation followed by Sour-Tovar et al. (2007). In Cerro Rajón, detailed field work confirms that possible cloudinids (internal moulds and silicified tubes) are only found in the unit 1 of the La Ciénega Formation, as reported by McMenamin (McMenamin et al., 1983, 1994; McMenamin, 1996). Bed-plane bioturbation also locally occurs along this formation, as reported by McMenamin (1984) and Stewart (1984), which was not supported by Sour-Tovar et al. (2007). However, none of the observed ichnofossils indicate a Cambrian age. In addition, cloudinids were reported by Sour-Tovar et al. (2007) from Cerro La Ciénega in the eponymous formation, in unit 4. They would be deposited above basalt levels that the authors identified as unit 3. However, the GPS coordinates provided by Sour-Tovar et al. (2007) points to middle-upper part of unit 1 of PBF. Our preliminary investigation suggests that there are no basalt layers below the PBF unit 1, and that the numerous offsets of the sediments by faulting of the hills studied by Sour-Tovar et al. (2007) may have led to a misinterpretation of the succession and, thus the location of the reported cloudinids. Further investigations are in progress. However, SSF occurrences reported herein are congruent with the presence of *Cloudina* in the La Ciénega Formation and the interpretation of the Ediacaran/Cambrian boundary near the top of this formation (McMenamin, 1985). This interpretation is further supported by the  $\delta^{13}\text{C}$  curve constructed by Loyd et al. (2012), which presents a strong negative  $\delta^{13}\text{C}$  incursion most probably corresponding to the

well-recognized anomaly at the Precambrian-Cambrian boundary (Loyd et al., 2012).

To summarize, at Cerro Rajón, the Ediacaran/Cambrian boundary is located in the upper part of the La Ciénega Formation based on the occurrence of the negative  $\delta^{13}\text{C}$  excursion and of *Cloudina*. The Cambrian stages 2 and 3 are indicated by the occurrence of SSFs 125 m above the base of the PBF. On this basis, the lower part of the PBF would include the complete Terreneuvian and possibly the base of Cambrian Series 2, Stage 3. In this locality, the succession deposited during the Terreneuvian is mainly volcanoclastic. The corresponding volcanic event seems to be variably, and possibly diachroneously, recorded in the Ediacaran-Cambrian successions of the area. Therefore, the study of this interval in other localities of the Caborca area, in search of lower occurrence of carbonates within or below volcanoclastic deposits, would potentially provide Terreneuvian SSFs. They are necessary for the construction of a Sonoran and further Laurentian, SSF-based biostratigraphic chart.

### Regional to Global Correlations

Outcrops of the Ediacaran-Cambrian sedimentary succession, including the PBF, are numerous in the Caborca area, northwestern Sonora (reported in Figure 1; see Stewart and Poole, 2002 for detailed list). Lithostratigraphic correlations of the Ediacaran-Cambrian transition have, therefore, been established across Sonora (McMenamin et al., 1994; Stewart et al., 2002). However, previous work on the regional stratigraphy of the PBF (Cooper and Arellano, 1952; Eells, 1972; Longoria, 1981; Stewart et al., 1984; McMenamin et al., 1994; Stewart and Poole, 2002) points to major local to regional variations of this transition, an observation confirmed by the field explorations conducted by the authors of this paper. Detailed stratigraphic and sedimentological studies at the regional scale are required to document such facies changes and determine their origin (as also noticed by Stewart et al., 1984).

Fossil data have also been used as a correlation tool for the Cambrian successions of Sonora, but so far, they only rely tenuously on trilobites and follow the general lithological correlations (Lochman, 1948, 1952; Stewart et al., 1984; McMenamin, 1987). The SSF data from the present study in Cerro Rajón, therefore, constitute a novel instrument for evaluating the correlations based on lithology and trilobites between the successions of Sonora. SSFs have not been reported

from other localities in the Caborca area, but they have been observed by the authors in various limestones from the PBF, which crops out in a number of hills of the Caborca area that require investigation (Figure 1; Stewart and Poole, 2002).

Lithological correlations of the Cambrian successions of Sonora with Ediacaran-Cambrian successions of southwestern USA (San Bernardino Mountains and southern Great Basin - California and Nevada) have also been proposed (Stewart et al., 1984; McMenamin, 1984, 1996; Stewart et al., 2002; Stewart, 2005) and, more recently, chemostratigraphy was also used (Loyd et al., 2012). The PBF is generally roughly correlated with the Wood Canyon Formation of California and Nevada (McMenamin, 1996; Stewart et al., 2002; Stewart, 2005). Specifically, Stewart et al. (1984) correlate units 2, 3, and 4 of the PBF with the upper member of the Wood Canyon Formation of the Death Valley region, California and unit 3 with the Poleta Formation of Esmeralda County, Nevada. However, the detailed relationship between the successions remains unresolved, and it is necessary to improve our knowledge of the trends in stratigraphic patterns in the Caborca area (facies changes, thickness variations, palaeocurrents, etc.) to better compare them with trends in the southern Great Basin (Molina-Garza and Iriando, 2007).

Correlations between Sonora and southwestern USA (Signor, 1991) based on fossils, mainly trilobites (Fritz, 1972, 1975; Palmer and Halley, 1979; Stewart, 1982; Stewart et al., 1984; McMenamin, 1984, 1987; Hollingsworth, 2005, 2011) but also archaeocyathans (McMenamin, 1984, 1987; Debrenne, 1987; Debrenne et al., 1989), have been proposed. Using trilobites, McMenamin (1984, 1987) suggested that the upper part of the Montenegro Member in the White-Inyo Mountains (California) should be correlated with unit 3 of the PBF as they both include the *Nevadia* assemblage, the base of which is defined by the first occurrence of the genera *Holmia* and *Nevadia*. The microbial-archaeocyathan buildups in the lower part of unit 3 of the PBF at Cerro Rajón are correlated with buildups in the upper part of the Campito Formation. Buildups in the upper part of unit 3 are correlated with buildups in the lower part of the Poleta Formation (McMenamin, 1987; Debrenne et al., 1989).

So far, no comparisons of the SSF record have been proposed between Sonora and southwestern USA. Two studies focusing on the SSFs have been conducted in the Great Basin: Wotte and Sundberg (2017) described SSFs recovered

from nine sections in eastern California and southern Nevada while Skovsted (2006b) focused on a Cambrian stage 4 fauna from the basal Emigrant Formation of Nevada. The fossil assemblage described in the latter is endemic, preventing any comparisons with the SSF assemblages described in this paper. Only cancelloriid spicules and echinoderm ossicles similar to that of the Cerro Rajón are present, but do not support any correlation. The SSFs described by Wotte and Sundberg (2017) encompass a composite assemblage extracted from Cambrian stage 3 to 5 carbonates of different formations studied in nine different sections. From this composite assemblage, the fragments of *Microdictyon* sclerites, herein considered as belonging to the species *Microdictyon multicaucus* which occurs in the PBF, enable the correlation of successions from Sonora and the Great Basin. The fragments of *Microdictyon* sclerites are restricted to the sample M5 from carbonate lenses of the upper part of the Montenegro Member, Campito Formation cropping out in the Montezuma Range, Esmeralda County (Nevada) and dated as Cambrian Age 3. The fragments of *Microdictyon* sclerites also occur with *Pelagiella* aff. *P. subangulata*, *Microcornus* sp., *Parkula* sp., *Hyolithellus?* sp., *Allonia* sp. and *Chancelloria* sp. This assemblage is comparable to the assemblage co-occurring with *M. multicaucus* in Sonora. Indeed, *Pelagiella* sp., *Chancelloria* spp., *Parkula bounites* and very abundant *Hyolithellus* spp. co-occur with *M. multicaucus* in unit 2 of the PBF. Therefore, we suggest a correlation, based on SSFs, of unit 2 of the PBF with the top part of the Montenegro Member of the Campito Formation. This correlation differs from the correlation of unit 3 of the PBF with the upper part of the Montenegro Member in the White-Inyo Mountains proposed by McMenamin (1984) based on the trilobites.

Tynan (1980, 1981a, 1981b, 1983) also described SSFs from the Cambrian stage 3 of the Campito and Poleta Formations of the White-Inyo Mountains, California. Their archaeocyathan- and trilobite-bearing carbonates yielded helcionellids, hyolithids, hyolithelminths, foraminifers, cancelloriids, echinoderm ossicles, bradoriids, brachiopods, tommotiids and other problematical microfossils (Tynan, 1981a) that could probably be compared with the assemblages from Cerro Rajón. Even older possible molluscs have been recovered from the upper member of the Deep Spring Formation interpreted as Cambrian Age 2 (Tynan, 1981a). This occurrence would represent the oldest for SSFs in Laurentia (SSFs are herein defined

as early Cambrian skeletal microfossils so *Cloudina* is excluded). It is not possible to relate this occurrence with the SSFs of Cerro Rajón as the Cambrian stage 2 is mostly represented by volcanoclastic sediments.

Signor and Mount (1986) summarize the published literature on the stratigraphic distribution of lower Cambrian fossils in the White-Inyo Mountains. In addition to archaeocyathans, echinoderms, brachiopods and trilobites, *Chancelloria* sp., *Bemella* sp., *Hyolithellus* sp., *Lapworthella filigrina*, *Microdictyon* sp., *Hyolithes princeps* and species of *Cambrotubulus* and of *Pautibubulites* have been observed by the two authors in the upper part of the Montenegro Member of the Campito Formation and in the Poleta Formation. More analyses are necessary to formally correlate the data of Signor and Mount (1986) with data from this study, but the assemblages appear to be comparable. Problematic skeletal tubes described as *Nevadatubulus*, *Coleoloides*, *Sinotubulites* and *Salanytheca* have been reported from the lower member of the Deep Spring Formation of the White-Inyo Mountains of eastern California and in Esmeralda County, Nevada by Signor et al. (1983, 1987) who considered them as equivalent in age to the Tommotian Stage of Siberia. However, they were later synonymized with *Cloudina* by Grant (1990) and are, therefore, related to the Ediacaran fossils described in the La Ciénega Formation.

Skovsted and Holmer (2006) reported SSFs from the Cambrian stages 3 to 4 Harkless Formation of Gold Point, Esmeralda County. The brachiopods, sponge spicules and *Sphenotallus* described in their work have not been recovered in the PBF. Only *Hyolithellus insolitus* is very similar to some specimens referred to *Hyolithellus* spp. in this work. *Platysolenites antiquissimus* is reported from the Cambrian stage 3 middle member of the Poleta Formation in Esmeralda County (Streng et al., 2005), but was not recovered in the PBF equivalent to the Cambrian stage 3.

Other SSFs from the American Cordillera have been described in northwestern Canada (Nowlan et al., 1985; Voronova et al., 1987). The Vampire Formation of Yukon (Nowlan et al., 1985) yielded *Anabarites trisulcatus*, *Protohertzina anabarica*, *P. unguiformis*, *Hyolithellus* cf. *H. isiticus*, *Rushtonia?* sp. and maikhanellids that correspond to SSF assemblages from the Fortunian described in Siberia, China, Iran, Mongolia, India and Kazakhstan. As already stated, the SSF record of the Terreneuvian (Fortunian and Cambrian stage 2) is partly missing at Cerro Rajón, precluding any

comparison. *Lapworthella filigrina*, which was described by McMenamin (1984) from the PBF, also occurs in the Rosella Formation (*Nevadella* Zone) in the Cassiar Mountains (Conway-Morris and Fritz, 1984). *Lapworthella filigrina* was not recovered in the framework of the present study. The assemblage described by Voronova et al. (1987) from the Mackenzie Mountains in the Northwest Territories includes *Microdictyon* sp., cancelloriid sclerites with a possible specimen of *A. hirundo* and various *Hyolithellus* species that are comparable to the PBF assemblages.

SSF assemblages from southeastern Laurentia can also be compared with the SSFs of the PBF, although no direct correlation at the species level can be proposed. Indeed, the genera are comparable but the species differ and a number of taxa are described with open nomenclature from the PBF, preventing direct comparisons. Skovsted and Peel (2007) report the presence of a diverse Small Shelly Fossil fauna in the Cambrian stages 3 to 4 argillaceous facies of the Forteau Formation from western Newfoundland. It includes several genera (*Eoobolus*, *Pelagiella*, *Pojetaia*, *Parkula*, *Cupitheca*, *Archiasterella*, *Chancelloria*, and *Hyolithellus*) that are also found in the PBF. The Cambrian stages 3 to 4 Browns Pond Formation of New York State yielded 26 species of SSFs including species of *Pelagiella*, *Hyolithellus*, *Petasothea* and *Chancelloria* (Landing and Bartowski, 1996). *Pelagiella*, *Eoobolus*, cancelloriid sclerites and echinoderms ossicles are also recovered from the Cambrian stage 4 basal Kinzer Formation of Pennsylvania (Skovsted and Peel, 2010). The largest Small Shelly Fossil fauna of southeastern Laurentia has been described from the Cambrian stages 3 to 4 upper Bastion and Ella Island formations of northeast Greenland at Albert Heim Bjerge and Ostensfeld Nunatak (Skovsted and Peel, 2001; Skovsted, 2003a; Skovsted and Holmer, 2003; Skovsted, 2004; Peel and Skovsted, 2005; Skovsted, 2005; Skovsted and Holmer, 2005; Skovsted, 2006a, Skovsted, 2016). It is comparable to the Small Shelly Fossil assemblages of the PBF, with the occurrences of *Microdictyon* cf. *depressum* possibly synonym of *M. multicavus*, *Parkula bounites* and species of *Hyolithellus*, *Pelagiella*, *Pojetaia*, *Cupitheca*, *Eoobolus* and cancelloriid sclerites and echinoderm ossicles. SSFs from Québec (Landing et al., 2002) correspond to a much younger assemblage (Cambrian stage 5) than the assemblages of the PBF.

At the global scale, the SSF assemblages from the PBF at the Cerro Rajón exhibit relatively

strong affinities with assemblages described in China and Australia (Figure 4). Three species (*Archiasterella hirundo*, *Parkula bounites* and *Mackinnonia corrugata*) formally identified in the PBF are common to the sedimentary successions corresponding to the Cambrian stages 3 to 4 of South Australia (Figure 4) described by Bengtson et al. (1990) and Gravestock et al. (2001). In addition, *Archiasterella pentactina* (comparable to the specimens referred to *A. cf. A. pentactina* in this study), *Pojetaia runnegari* (comparable to the specimens referred to *Pojetaia* sp. in this study) and *Pelagiella subangulata* (comparable to the specimens referred to *Pelagiella* sp. in this study) have also been extensively reported in the Cambrian stage 3 to 4 of South Australia (Bengtson et al., 1990; Gravestock et al., 2001; Betts et al., 2016). *Parkula bounites* is also present in the neighbouring region of Australia (Figure 4): Antarctica (Wrona, 2004). Three species of cancelloriids are common between South China and Mexico: *Archiasterella charma*, *Allonnia erromenosa* and *A. tetrathallis* (Figure 4); however, the differentiation of the species is based on disarticulated sclerites and may reflect an artificially higher diversity and, therefore, an artificial biogeographical connection. Following the same reasoning, the similarity with Small Shelly Fossil fauna from Germany based on the two shared cancelloriid species *Archiasterella hirundo* and *Allonnia tetrathallis* might be either artificial or representing accurate connections (Figure 4). Loose connections with India, Pakistan, Turkey and Jordan are also observed based on cancelloriid sclerite occurrences (Figure 4).

## CONCLUSIONS

- Four distinct SSF assemblages are identified in the Puerto Blanco Formation at the Cerro Rajón (SE of Caborca, Sonora, Mexico). Assemblage I is characterized by *Xianfengella* sp. and *Allonnia tetrathallis*, assemblage II by *Mackinnonia corrugata* and *Archiasterella charma*, assemblage III by *Parkula bounites* and *Rajonia ornata* and assemblage IV by echinoderm ossicles. Mickwitziids, the cancelloriids *Allonnia erromenosa*, *Archiasterella hirundo*, *A. cf. A. pentactina* and *Chancelloria* spp., the hyolithelminths *Hyolithellus* spp., the hyoliths *Petasotheca* sp., *Cupithec* cf. *C. mira*, Hyolithid sp., the molluscs *Pelagiella* sp. and *Pojetaia* sp., the brachiopod *Eoobolus* sp., the sclerites of the lobopod *Microdictyon multicavus* and one unidentified bradoriid and an indeterminate fossil are also recovered in the Puerto Blanco Formation at the Cerro Rajón.

Faunal comparisons Taxa	Laurentia				Worldwide									
	Region	Mexico	SW USA	Canada	NE Greenland	Australia	Antarctica	S China	India	Pakistan	Turkey	Jordan	Germany	Spain
<i>Archiasterella hirundo</i>		x	x			x					x	x	x	x
<i>Archiasterella charma</i>		x					x							
<i>Allonnia erromenosa</i>		x					x	x						
<i>Allonnia tetrathallis</i>		x					?	x		x				x
<i>Parkula bounites</i>		x			x	x								
<i>Mackinnonia corrugata</i>		x				x								
<i>Microdictyon multicavus</i>		x	x	x	?									
<i>Rajonia ornata</i>		x												

**FIGURE 4.** Distribution of formally identified taxa in the Puerto Blanco Formation at Cerro Rajón and comparison with Laurentian and global distribution. See Systematic Palaeontology ("other occurrences" of taxa) for references.

- SSFs are reported for the first time from a carbonate bed intercalated within the dominant volcanoclastic deposits of unit 1 of the Puerto Blanco Formation. Taxa with a global distribution indicate that this bed corresponds to the Cambrian stages 2 to 3. This occurrence of SSFs is the oldest in Mexico. Units 2 to 4 of the Puerto Blanco Formation correspond to the Cambrian stages 3 to 4 based on the SSFs.
- SSFs in Sonora represent a new powerful palaeontological tool for correlations and for biostratigraphic interpretations of the early Cambrian sedimentary successions of the area, which complement and surpass trilobites and archaeocyathans. They allow better correlation of this interval at regional and international scales.
- SSFs further help improving knowledge of the Ediacaran-Cambrian transition in Sonora. Their occurrence in the middle part of unit 1 of the Puerto Blanco Formation invalidates the interpretation of Sour-Tovar et al. (2007) that the Ediacaran/Cambrian boundary occurs in the upper part of this unit based on the record of *Treptichnus pedum*. The SSFs support the placement of the Ediacaran/Cambrian boundary at the top of the La Ciénega Formation due to the presence of *Cloudina* and a strong negative  $\delta^{13}\text{C}$  incursion (Loyd et al., 2012).
- SSFs from the Puerto Blanco Formation enable revision of the correlation between early Cambrian successions of Sonora and southwestern USA. Unit 2 of the Puerto Blanco Formation is correlated with the top part of the Montenegro Member of the Campito Formation cropping out in the Montezuma Range, Esmeralda County (Nevada).
- The SSF assemblages of Cerro Rajón exhibit relatively strong affinities with assemblages in Australia. To a lesser extent, connections with South China

are also identified. Loose connections with Germany, India, Pakistan, Turkey and Jordan are also recognized.

7. Detailed micropalaeontological studies in other sections are required to verify the patterns identified from the study at Cerro Rajón. Such studies would further contribute to the ongoing work of the International Subcommittee on Cambrian Stratigraphy by providing the bases for the construction of a SSF-based biostratigraphic chart for *Laurentia* which is still lacking.

### SYSTEMATIC PALAEOLOGY

Phylum and Class uncertain

Order CHANCELLORIIDA Walcott, 1920

Family CHANCELLORIIDAE Walcott, 1920

**Remarks.** The taxonomy of cancelloriids in this study is based on disarticulated sclerites, which are the only available material. The taxonomic treatment of disarticulated cancelloriid sclerites has always represented a challenge and is considered unstable at best (Bengtson and Collins, 2015). Recently, Moore et al. (2014) proposed a method contributing to the identification of cancelloriid species on the basis of their disarticulated sclerites. According to their method, to determine if different sclerite morphotypes come from a single cancelloriid species, the significance of the differences in proportions of the sclerite morphotypes in different samples has to be tested by a chi-square or other statistical test. This method presents some limits discussed in the original publication (Moore et al., 2014), but we would recommend its consideration when dealing with disarticulated cancelloriid sclerites. One limit is that this method requires a significant number of complete disarticulated sclerites for the statistical tests (in the case-studies of Moore et al., 2014, samples with a minimum of 100 complete sclerites have been considered). Unfortunately, the low number of complete, disarticulated sclerites recovered from our various samples prevents the use of this method. Assignment to the species level is proposed, and some specimens are left in open nomenclature in order to figure and discuss in detail the material that could prove to be of use in spite of absence of articulated scleritome and sufficient number of sclerites for statistical analyses. The morphological terminology utilized herein to describe cancelloriid sclerites follows Moore et al. (2014) with additional references to Bengtson and Collins (2015). The configuration of marginal and central rays is described with the  $m+n$  system proposed by Sdzuy (1969) and modified by Qian and Bengtson (1989).

Genus ARCHIASTERELLA Sdzuy, 1969

**Type species.** *Archiasterella pentactina* Sdzuy, 1969, Cambrian stage 3, Cazalla de la Sierra/Sierra Morena, Spain.

**Diagnosis.** See Moore et al. (2014, p. 858).

*Archiasterella hirundo* Bengtson in Bengtson et al., 1990

Figure 5.1-17

- 1990 *Archiasterella hirundo* n. sp.; Bengtson in Bengtson et al., p. 54; figs. 29-30.
- 1994 *Archiasterella hirundo* Bengtson; Elicki, fig. 7.3.
- ?1998 *Archiasterella tetraspina* (Vassiljeva and Sayutina, 1988); Vassiljeva, p. 102, pl. 20, figs. 11, 12.
- ?1998 *Archiasterella quadriradiata* n. sp.; Vassiljeva, p. 102, pl. 21, figs. 2, 3.
- 2001 *Archiasterella quadratina* Lee, 1987; Demidenko in Gravestock et al., pl. VI, figs. 3-4.
- ?2001 *Archiasterella* cf. *hirundo* Bengtson; Fernández-Remolar, p. 59, figs. 3e-f, 8c-d, f.
- ?2001 *Archiasterella* cf. *hirundo* Bengtson; Sarmiento et al., p. 120, pl. 2, fig. 5.
- 2008 *Archiasterella hirundo* Bengtson; Porter, pl. 2, figs. 1-15.
- ?2010 *Archiasterella hirundo* Bengtson; Moore et al., fig. 11.1-3, 6, 7 (isolated rays from internal moulds, possibly from *Archiasterella hirundo*).
- ?2011 *Archiasterella* cf. *hirundo* Bengtson; Elicki, p. 161, figs. 5P-Q.
- 2017 *Archiasterella* cf. *hirundo* Bengtson; Wotte and Sundberg, p. 895, fig. 8.23

**Diagnosis.** See Bengtson et al. (1990, p. 54).

**Material.** 31 articulated sclerites including the three figured phosphatic internal moulds with phosphatic outer layer USTL3170-3, USTL3175-4, and USTL3177-2.

**Distribution.** Cerro Rajón section, samples R54 and R63 from unit 2 of the Puerto Blanco Formation.

**Description.** The articulated sclerites are bilaterally symmetrical and composed of four lateral rays (4+0 configuration; Figure 5.1-2, 5.6-7, 5.12-13) diverging at similar angle of 90°. They are preserved as phosphatic internal moulds associated with a phosphatic outer layer. Three rays are approximately parallel to the basal plane (horizontal rays according to Moore et al., 2014), whereas the principal ray (following Moore et al., 2014) is recurved away from the basal plane at ~85 to 115° (Figure 5.5, 5.8). The axis of symmetry of the sclerite bisects the principal ray and its opposite horizontal counterpart. Those rays meet at a sagittal suture and are also in contact with the two lat-

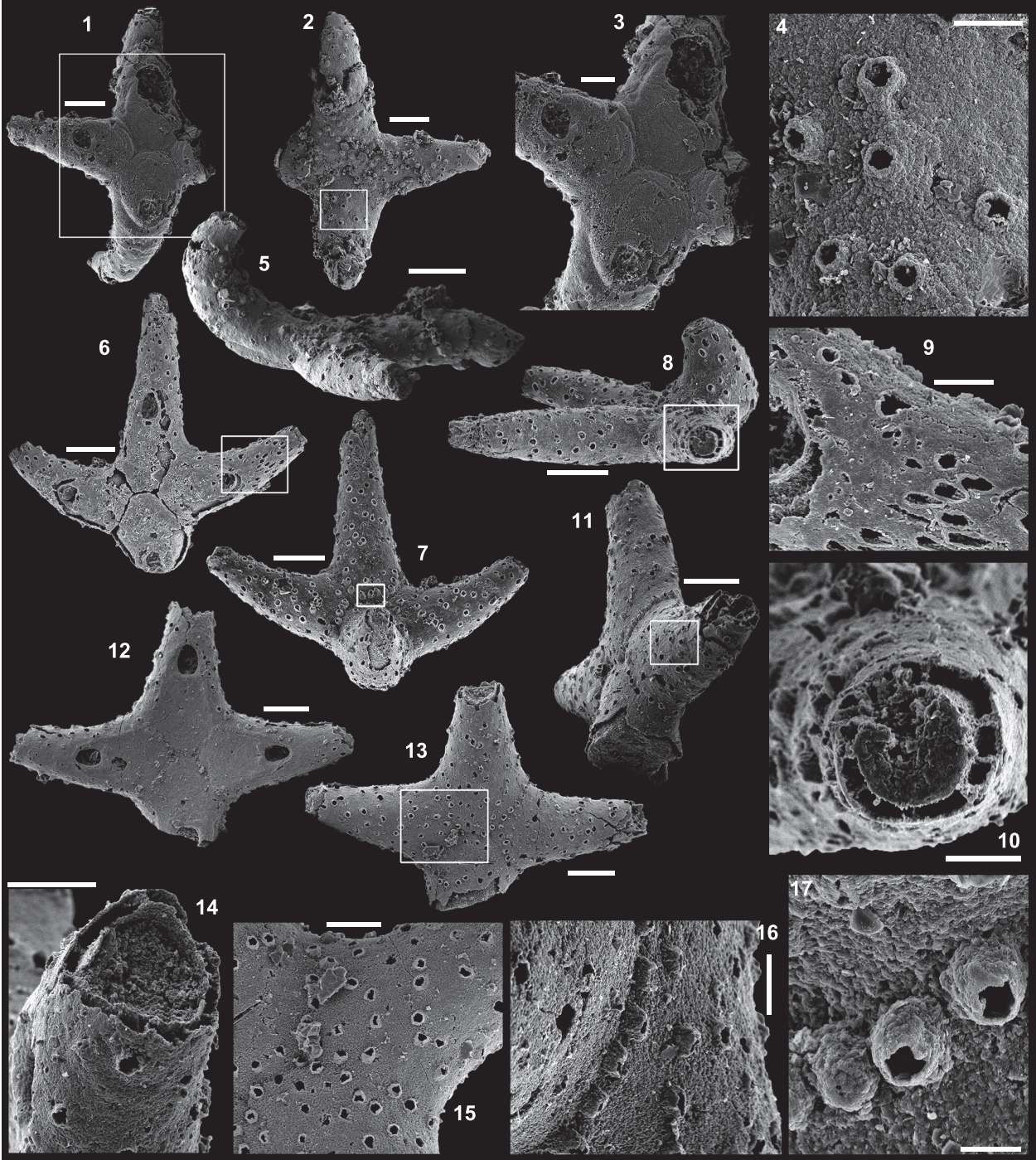


FIGURE 5. Caption on next page.

eral horizontal rays forming three articular facets. The lateral rays, perpendicular to the axis of symmetry, exhibit only two articular facets (Figure 5.1, 5.3, 5.6, 5.12-13). The rays are robust, slightly flattened at their proximal ends so that the basal plane is strongly developed with a broad, flat surface. The outer layer at the basal plane is either completely smooth (Figure 5.12) or with low, irregular, arched wrinkles near the ray sutures and around the foramina (Figure 5.1, 5.3). The foramina form perforations through the outer phosphatic layer and depressions on the internal mould; they have a circular (Figure 5.1, 5.3) to elongate shape (Figure 5.6, 5.12) and their maximum diameter is small (from 80 to 203  $\mu\text{m}$ ) relative to the sclerite size. They are located at the distalmost part of the basal plane. The thin, outer phosphatic layer, consistently present on the specimens, exhibits a smooth (Figure 5.9) to slightly rugose texture (Figure 5.4, 5.17) with hollow tubercles of  $\sim 20 \mu\text{m}$  in height on its surface (Figure 5.2, 5.4, 5.6-9, 5.11, 5.13-17). The tubercles are generally broken, leaving a circular (where the tubercle extends perpendicularly to the coating surface; Figure 5.4) to elongate (where the tubercle is inclined toward the distal end of the ray; Figure 5.9) perforation of  $\sim 25 \mu\text{m}$  diameter through the coating. The tubercles are randomly distributed over the entire surface of the external coating but completely absent from the basal plane (Figure 5.1, 5.3, 5.6, 5.12). In the central part of the sclerite abaxial surface, the tubercles are mostly randomly distributed, but some are aligned along the ray sutures (Figure 5.7, 5.11, 5.13, 5.16-17). The outer layer is separated from the internal mould by a 10 to 20  $\mu\text{m}$  gap (Figure 5.10, 5.14). The outer layer may continuously cover the entire sclerite (Figure 5.1-3, 5.11-13) or may be disrupted at the ray sutures (Figure 5.6).

Where the rays are broken, the phosphatic internal mould is visible. It can be massive (Figure 5.10) or granular with an external, thin phosphatic crust (Figure 5.14).

**Comparisons.** The sclerites described herein are assigned to *Archiasterella hirundo* Bengtson in Bengtson et al. (1990) as they exhibit the characteristic tubercles and basal plane of this 4+0 achiasterellid. Few negligible, yet remarkable differences are present between the Mexican specimens and other described specimens of *A. hirundo*. In the Mexican material, the rays that meet at the sagittal suture and, therefore, exhibit three articular facets are the principal, recurved ray and the facing horizontal ray, whereas the opposite configuration (horizontal rays meet at the sagittal suture with three articular facets) is described in other articulated specimens of the species. Moreover, the regular organization of tubercles described by Porter (2008) is not present in the Mexican specimens, which are more randomly organized.

Comparisons of the present specimens with any other 4+0 cancelloriids are constrained by the spatial configuration of the rays, the organization of the basal plane and the ornamentation. *Archiasterella tetraspina* specimens described by Vassiljeva (1998) are similar in morphology to *A. hirundo* possessing a characteristic short median recurved ray, the longer median one and two lateral recurved rays. However, poor illustration and description provided by Vassiljeva (1998) prevent the accurate observation of the foramina and of possible ornaments and, therefore, the confident synonymy with *A. hirundo*.

**Remarks.** The thin outer phosphatic layer on the Mexican *A. hirundo* (Figure 5.10) is closely comparable to the thin outer layer described by Porter

**FIGURE 5** (figure on previous page). Internal moulds of sclerites with outer layer of *Archiasterella hirundo* Bengtson in Bengtson et al., 1990, from the Puerto Blanco Formation of Cerro Rajón, Sonora, Mexico. 1-5. Specimen USTL3170-3 from sample R54: 1. Adaxial view, area in the square is magnified in 3; 2. Abaxial view, area in the square is magnified in 4; 3. Detail of the basal plane showing the foramina and intersections of the rays articular facets; 4. Detail of broken tubercles of the outer layer forming circular perforations; 5. Lateral view showing the recurved lateral ray. 6-10, 17. Specimen USTL3175-4 from sample R63: 6. Adaxial view, area in the square is magnified in 9; 7. Abaxial view, area in the square is magnified in 17; 8. Lateral view showing the recurved lateral ray, area in the square is magnified in 10; 9. Detail of the outer layer near the foramen with broken inclined tubercles forming elongated perforations; 10. Detail of a transversally broken ray shows the gap between the outer phosphatic layer and the phosphatic internal mould of the lumen; 11-16. Specimen USTL3177-2 from sample R63: 11. Lateral view, area in the square is magnified in 16; 12. Adaxial view; 13. Abaxial view, area in the square is magnified in 15; 14. Detail of a transversally broken ray showing the gap between the outer phosphatic layer and the phosphatic internal mould of the lumen, note that a thin phosphatic crust is present on the outer surface of the internal mould; 15. Detail of the abaxial surface covered with broken tubercles that form perforations through the outer layer; 16. Detail of aligned tubercles along the suture between two adjacent rays; 17. Detail of the granular outer layer and preserved to partially broken tubercles at rays suture. Scale bars are: 17, 20  $\mu\text{m}$ ; 4, 9, 10, 16, 50  $\mu\text{m}$ ; 3, 14-15, 100  $\mu\text{m}$ ; 1-2, 5-8, 11-13, 200  $\mu\text{m}$ .

(2008) in casts of *A. hirundo* sclerites from the Parara Limestone of Curramulka Quarry Section, South Australia (same smooth to slightly rugose texture, continuous extension on the entire sclerite, tubercles). In the Mexican sclerites, the layer is mostly separated from the phosphatic internal mould by a gap which varies between 10 to 20  $\mu\text{m}$ . It is difficult to assess the presence of this gap in the sclerites described by Porter (2008). We interpret this gap in the Mexican material as the former position of the dissolved carbonate wall of the sclerite. Porter (2008) interpreted the thin, outer phosphatic layer as a replacement of a possibly originally organic layer of the otherwise carbonate wall. Based on the present observations, the layer could alternatively be interpreted as a phosphatic outer coating that mimics the original carbonate surface of the sclerite. The consistent presence of the external coating in all the specimens observed in this study prevents the accurate observation of the internal mould and, therefore, the identification of indices of the other shell layers described by Porter (2008) such as, (1) the thin outer phosphatic layer, (2) the inner layer composed of aragonite fibres orientated parallel to the long axis of the sclerite, (3) aragonite fibres bundled into discrete "projections" that are commonly inclined from the vertical toward the distal tip of the sclerite and (4) a lower surface where the projections are absent.

**Other occurrences.** Cambrian stages 3-4 (*Abadiella huoi*, *Pararaia tatei*, *P. bunyeroensis* and *P. janea* trilobites zones) of Australia: Ajax Limestone, Mount Scott Range, Arrowie basin (Bengtson et al., 1990; Gravestock et al., 2001; Porter, 2008); Parara Limestone, Horse Gully, Curramulka, Minlaton-1 drill core (7 km east of Minlaton), SYC-101 drill core (south-west of Curramulka and 6 km north-east of Minlaton), Cur-D1B drill core (2.8 km east of Minlaton); Cobowie Limestone, Port Julia; Kulpara and Parara Limestones, CD-2 drill core (east of the Curramulka Quarry), Yorke Peninsula, Stansbury Basin (Gravestock et al., 2001). Cambrian stage 3 of the USA: Pioche Formation, Log Cabin Mine, Nevada (Wotte and Sundberg, 2017). Cambrian stage 3 of Germany: Upper Zwetau Carbonate Member, Doberlug-Torgau Synclinorium (Elicki, 1994). Possibly Cambrian stage 3 of Spain: Pedroche Formation, Jimenez Quarry and Cerro de las Ermitas, Córdoba (Fernández-Remolar, 2001). Possibly Cambrian stages 3 to 4 of Turkey: Çal Tepe Formation, Taurus Mountains (Sarmiento et al., 2001). Possibly Cambrian stage 4 of Jordan: lower Numayri Member, valley south of Wadi At Tayan (Elicki, 2011).

*Archiasterella charma* (Moore et al., 2014)

Figure 6.1-19

2014 *Archiasterella charma* n. sp.; Moore, Li and Porter, p. 859, fig. 3B-C, H, 11.

**Material.** 116 broken articulated sclerites including the figured five phosphatic internal moulds of sclerites USTL3166-4, USTL3172-9, USTL3167-7, USTL3169-6 and USTL3168-4, two phosphatic internal moulds with external phosphatic coating USTL3164-3 and USTL3168-6 and thousands of disarticulated rays including the figured USTL3189-6, USTL3167-3 and USTL3173-4.

**Distribution.** Cerro Rajón section, samples R53, R54 and R55 from unit 2 of the Puerto Blanco Formation.

**Description.** The isolated articulated sclerites, preserved as internal phosphatic moulds are fragmented (rays broken; Figure 6.1, 6.6, 6.11) and three specimens exhibit a partially (Figure 6.10) to completely (Figure 6.16-19) preserved external phosphatic coating. The sclerites are bilaterally symmetrical with three marginal rays (3+0 form; Figure 6.10). In lateral view, the two horizontal rays lie approximately in the basal plane with a slight angle up to 25° in the abaxial direction (Figure 6.2, 6.10, 6.12, 6.17-18). The principal ray is strongly abaxially recurved from the basal plane with an angle varying between 55° and 95° (Figure 6.2, 6.4-5, 6.10, 6.12, 6.15, 6.17-18). The size of sclerites is variable: basal plane diameter, which may be used as indication for the size, ranges from ~485 to 782  $\mu\text{m}$ . It is not possible to determine the size of sclerites based on the length of the rays which are broken. One disarticulated ray assigned to the species, although broken, exhibits the maximum length observed (~1900  $\mu\text{m}$ ; Figure 6.13). Cross-section of rays is circular (Figure 6.5, 6.15). Horizontal and principal rays are generally very similar in size (Figure 6.1, 6.5-7, 6.9-12, 6.14-17), but the principal ray differs considerably from the horizontal rays in one specimen (Figure 6.18, 6.19). Rays rapidly taper from the basal area and then more slightly distally (Figure 6.1, 6.6, 6.11, 6.13). In basal view, the angle of divergence between the two horizontal rays varies from slightly acute (minimum 80°; Figure 6.6, 6.9, 6.19) to strongly obtuse (maximum 155°; Figure 6.1, 6.11, 6.16). All rays meet at the basal plane in a Y-shaped junction underlined by narrow grooves between adjoining rays on internal moulds (Figure 6.1, 6.3, 6.6, 6.9, 6.11), but faded on external coatings (Figure 6.16, 6.19). The articulatory junction between adjoining rays is either straight (Figure 6.1, 6.3, 6.6) or irregular due to the presence of



FIGURE 6. Caption on next page.

faded tubercles on the edge of ray internal moulds corresponding to slight protrusions of the internal cavity (Figure 6.9, 6.11). The foramen is located at the centre of the basal facet of each ray. The diameter and shape of the foramen greatly varies depending on the preservation; nevertheless, in the best preserved specimens, they seem to be relatively small and elongate to circular (Figure 6.9). The rim of the foramen is swollen both on internal moulds and external coatings (Figure 6.3, 6.8-9, 6.11, 6.13, 6.16, 6.19).

**Comparisons.** The three-rayed sclerites described above all exhibit two rays in the basal plane and one ray that is recurved away from the basal plane typical of *Archiastrella* Sdzuy, 1969. In this genus, three-rayed sclerites have only been reported in the species *Archiastrella charma*. The characters observed in the present specimens are similar to those described in *A. charma* by Moore et al. (2014) with only two slight differences: the angle between the two horizontal rays is not always acute in the Mexican specimens as obtuse angles are also observed, and the rims around the foramina are swollen but smooth, not tooth-bordered. Possible synonyms of *A. charma* have been discussed by Moore et al. (2014).

**Other occurrence.** Cambrian stage 2 (*Sinosachites flabelliformis* – *Tannuolina zhangwentangi* Assemblage Zone), possibly Cambrian stage 3 of South China: Shiyantou Formation, Xiaotan, Yongshan County, Yunnan Province and possibly Guizhou and Sichuan provinces (Moore et al., 2014).

*Archiasterella* cf. *A. pentactina* (Sdzuy, 1969)  
Figure 7.1-15

**Material.** 56 articulated sclerites including six figured phosphatic internal moulds with partial phosphatic external coating USTL3164-6, USTL3166-

10, USTL3171-5, USTL3175-13 and USTL3167-4 and thousands of disarticulated rays.

**Distribution.** Cerro Rajón section, samples R21, R53, R54, R55, R63 and R83 from units 1 to 4 of the Puerto Blanco Formation.

**Description.** The articulated sclerites are preserved as fragmented (tips of rays broken) internal phosphatic moulds (Figure 7.1-7, 7.9-11, 7.14-15) and one specimen exhibits an external phosphatic coating (Figure 7.8, 7.12-13). The size of the sclerites is variable, the width across the mid-point of the basal plane (between the two pairs of horizontal rays, as described by Moore et al., 2014) ranges from ~360 to 600  $\mu\text{m}$ . The sclerites are bilaterally symmetrical; five massive marginal rays (5+0 form) of equivalent size (estimated with the diameter of the ray as they are incompletely preserved) are present although the principal ray may have a slightly larger diameter (Figure 7.1-2, 7.5-7, 7.12-14). The two abapical rays seem to taper gradually distally, which is not observed in the two adapical rays that narrow rapidly and are then sub-cylindrical. Four of the marginal rays extend in the basal plane, and one ray (principal), although incompletely preserved, protrudes in the abaxial direction with an angle with the basal plane ranging from 60° to 80° (Figure 7.3, 7.8-11). The boundaries between the different rays are variably expressed from very distinct (Figure 7.2, 7.4-5) to faded (Figure 7.1, 7.14). The principal ray is in contact with all the other rays and, therefore, has four articulatory facets. The two abapical rays exhibit only two articulatory facets, one in contact with the principal ray and the other in contact with the adjacent adapical rays which therefore have three articulatory facets (Figure 7.2, 7.4-5, 7.7, 7.13). Foramina are present on each marginal ray and situated at the centre of their basal facets. When best

**FIGURE 6** (figure on previous page). Articulated but broken internal moulds of sclerites of *Archiasterella charma* Moore, Li and Porter, 2014, from the Puerto Blanco Formation of Cerro Rajón, Sonora, Mexico. 1-3, 5. Specimen USTL3166-4 from sample R53: 1. Adaxial view showing the almost straight angle between the horizontal rays, area in the square is magnified in 3; 2, 5. Lateral views showing the curvature of the principal ray; 3. Detail of the basal plane showing the swollen rims of the foramina. 4. Disarticulated principal ray USTL3189-6 from sample R53 in lateral view showing the curvature and the swollen rim of the foramen. 6, 8. Specimen USTL3172-9 from sample R55: 6. Adaxial view; 8. Lateral view showing a relatively well-preserved (long) horizontal ray and the principal ray broken at the edge of the basal facet. 7, 9-10. Specimen USTL3168-4 from sample R54: 7. Lateral view from the principal ray; 9. Adaxial view showing the acute angle between the horizontal rays and the irregular junction between adjoining rays; 10. Lateral view showing the recurved principal ray partially covered by the external coating. 11, 14. Specimen USTL3167-7 from sample R53: 11. Adaxial view; 14. Lateral view. 12. Basal view of disarticulated principal ray USTL3167-3 from sample R53 showing the swollen rim of the foramen. 13. Adaxial view of one disarticulated horizontal ray USTL3173-4 from sample R55. 15. Lateral view of specimen USTL3169-6 R54b A\_018 from sample R54b. 16-17. Specimen USTL3164-3 preserved with external coating from sample R53a: 16. Adaxial view; 17. Lateral view showing horizontal rays diverging from the basal plane. 18-19. Specimen USTL3168-6 preserved with external coating from sample R54: 16. Adaxial view; 17. Lateral view. Scale bars are: 3, 12, 100  $\mu\text{m}$ ; 1-2, 4-11, 13-19, 200  $\mu\text{m}$ .

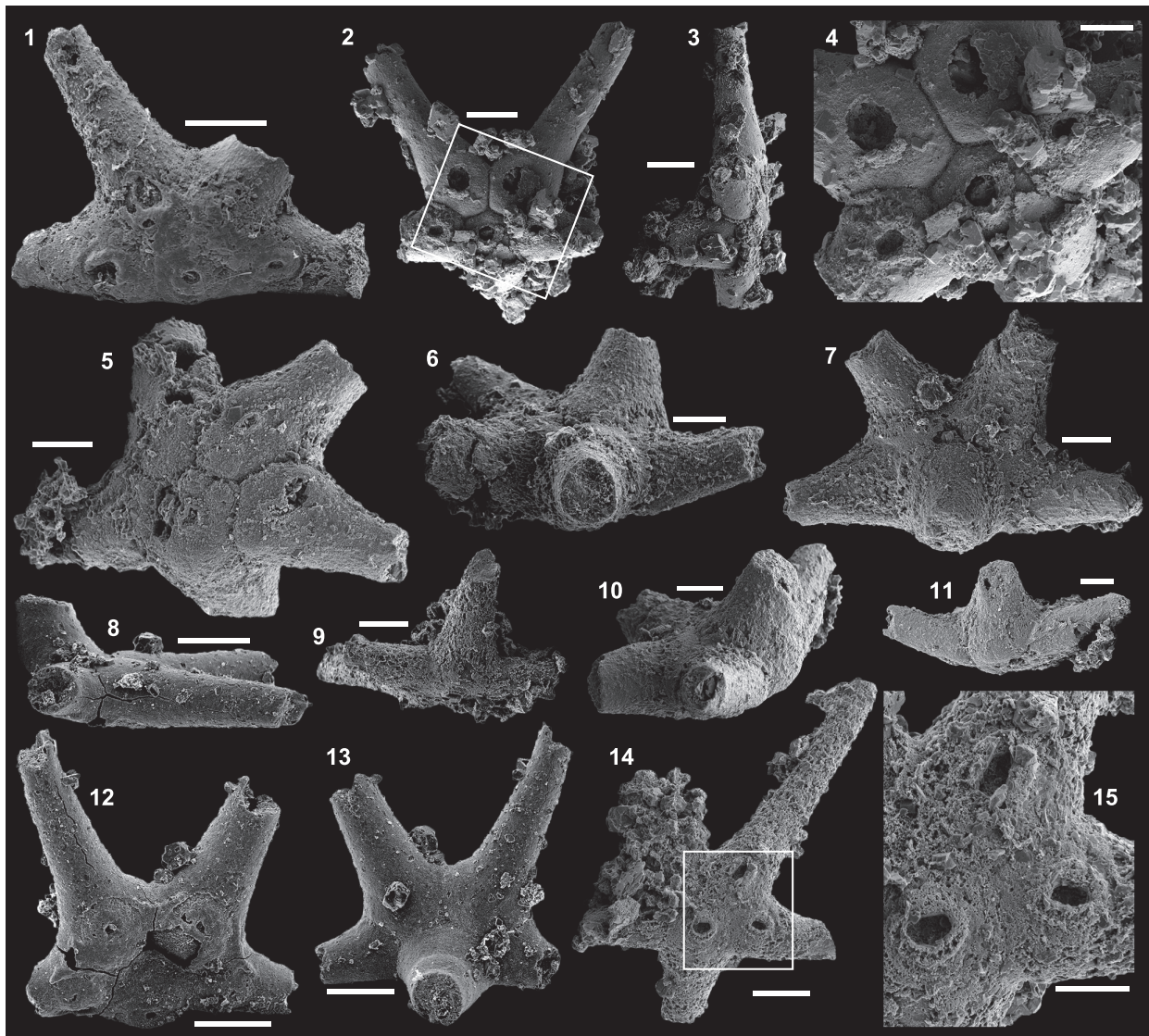


**FIGURE 7.** Internal moulds with partial external coating of sclerites of *Archiasterella* cf. *A. pentactina* Sdzuy, 1969 from the Puerto Blanco Formation of Cerro Rajón, Sonora, Mexico. 1. Specimen USTL3164-6 from sample R53a': Adaxial view; 2-4. Specimen USTL3166-10 from sample R53: 2. Adaxial view, area in the square is magnified in 4; 3. Lateral view; 4. Detail of the basal plane with the circular and large foramina. 5-7, 10-11. Specimen USTL3171-5 from sample R54: 5. Adaxial view; 6. Abapical view showing the circular cross-section of the protruding broken principal ray; 7. Abaxial view; 10-11. Lateral views. 8, 12-13. Specimen USTL3175-13 from sample R63: 8. Lateral view; 12. Adaxial view showing the small perforations of the external coating corresponding to the foramina; 13. Abaxial view. 9, 14-15. Specimen USTL3167-4 from sample R53: 9. Abapical view; 14. Adaxial view, area in the square is magnified in 15; 15. Detail of the basal surface with elongated foramina surrounded by a swollen ring. Scale bars are: 4-7, 10-11, 15, 100  $\mu\text{m}$ ; 1-3, 8-9, 12-14, 200  $\mu\text{m}$ .

preserved on internal moulds, foramina are circular to ovate and the rim is swollen (Figure 7.1, 7.5, 7.14-15). This swollen rim is sometimes broken and the foramina is round and wide (Figure 7.2, 7.4). A small perforation is seen on the external coatings at the position of the foramina (Figure 7.12).

**Comparisons.** The sclerites described above exhibit five lateral rays (no central), one of which is recurved away from the basal plane so they are similar to sclerites referred to *Archiasterella pentactina*. However, due to the lack of data on *Archiasterella pentactina* type material, the present specimens are only referred to *Archiasterella* cf. *A. pentactina*. A revision of the species type material



**FIGURE 8.** Articulated but broken internal moulds of sclerites of *Allonnia erromenosa* Jiang, in Luo et al., 1982 from the Puerto Blanco Formation of Cerro Rajón, Sonora, Mexico. 1-4. Specimen USTL3162-6 from sample R21: 1-2. Lateral view showing all the lateral rays recurved away from the basal plane; 3. Abaxial view; 4. Adaxial view showing the circular and wide foramina located on the basal edge of the rays. 5-7. Specimen USTL3162-12 from sample R21: 5. Adaxial view showing the foramina with raised rim surrounded by shallow depressions; 6-7. Lateral views. 8-10. Specimen USTL3163-11 from sample R21: 8, 10. Lateral views; 9. Adaxial view showing the circular and wide basally displaced foramina with raised rim and surrounding depression. Scale bars are all 200  $\mu$ m.

is necessary before definitely concluding on the assignment of the specimens from this and previous studies.

Genus ALLONNIA Doré and Reid, 1965

**Type species.** *Allonnia tripodophora* Doré and Reid, 1965, Cambrian stage 2, Carteret, Armorican Massif, France.

**Diagnosis.** See Moore et al. (2014, p. 850).

*Allonnia erromenosa* (Jiang in Luo et al., 1982)  
Figure 8.1-10

The list of synonymy of the species *Allonnia erromenosa* in Moore et al. (2014) is considered valid in addition to the following synonym:

2016 *Allonnia erromenosa* Jiang, in Luo et al.; Peel et al., p. 249, fig. 6l.

**Material.** 106 articulated sclerites including the three figured phosphatic internal moulds USTL3162-6, USTL3162-12 and USTL3163-11.

**Distribution.** Cerro Rajón section, samples R21 and R53 from units 1 and 2 of the Puerto Blanco Formation.

**Description.** The articulated sclerites are preserved as fragmented (tips of rays broken) internal phosphatic moulds (Figure 8.1-10). Sclerites are radially symmetrical with three equivalent marginal rays (3+0 form; Figure 8.3-5, 8.9) angled from the basal plane at 45° (Figure 8.8) to 65° (Figure 8.7). When preserved rays are relatively long, some recurve away relatively abruptly (Figure 8.1-2, 8.6). All rays taper distally from the basal plane, either abruptly after their basal part (Figure 8.1-2, 8.4-5) or gradually (Figure 8.7-10). Due to breakage of all recovered rays, it is not possible to measure their length. Size of sclerites is estimated from the diam-

eter of the basal plane and varies between 400 and 490  $\mu\text{m}$ . The three rays join in a Y-shaped junction marked by pronounced straight furrows between adjoining articulatory facets (Figure 8.2-3, 8.5, 8.7, 8.10). Angles between adjoining rays of the same sclerite are heterogeneous (varying between 100 and 150°). Foramina are located very close to the basal edge of the sclerites (Figure 8.4-8, 8.9). Foramina are circular and large (from 170 to 225  $\mu\text{m}$  in diameter) relatively to the size of the basal facets, so that they occupy most of their surfaces (Figure 8.4-5, 8.9). The rim of the foramen is raised and directly surrounded by a shallow, circular depression (Figure 8.4-5, 8.9).

**Comparisons.** As noted by Moore et al. (2014), most of the 3+0 disarticulated chancelloriid sclerites have been assigned to *Allonnia*. However, the characters that discriminate *Allonnia* sclerites from sclerites of other chancelloriid genera are not the number of rays, but the fact that no central rays are present, and all rays are angled or curved steeply abaxially away from the basal plane. This configuration occurs in the present specimens which are, therefore, assigned to *Allonnia*. The other species from the genus with three rays is *Allonnia tripodophora* Doré and Reid, 1965, which is differentiated from sclerites attributed to *A. erromenosa* in this study and by Moore et al. (2014) by an angle between rays and basal plane of less than 45°. However, such a variation might be intraspecific making *A. erromenosa* a synonym of *A. tripodophora*. 3+0 sclerites assigned to *Allonnia* have otherwise been described from articulated scleritomes and are, therefore, more difficult to compare. Generally, the number of rays in the sclerites of articulated scleritomes is easily observed, but little is known about their position relative to the basal plane. So far, scleritomes exclusively constituted of 3+0 sclerites have only been assigned to *Allonnia* (*A. phrixothrix* and *A. tintinopsis*, Bengtson and Collins, 2015, and *A. erjiensis* Yun et al., 2018) despite lack of knowledge on the configuration of the rays. However, Moore et al. (2014) suggested that *Allonnia phrixothrix* may instead belong to *Archiasterella*. Although Bengtson and Collins (2015) assigned their new species *A. tintinopsis* to *Allonnia*, they acknowledged the proposal of Moore et al. (2014) and suggested further study of the variability and distribution of sclerites in assemblages and full-body preservation to resolve the taxonomic issue. The same issue is raised for *A. erjiensis* Yun et al., 2018, newly described based on articulated scleritomes for which it is difficult to determine the angle

between the rays and the basal plane so the assignment to *Allonnia* or *Archiasterella*. 3+0 sclerites have otherwise been assigned to *Archiasterella* when one principal ray only is angled or recurved away from the basal plane (cf. *Archiasterella charma*). 3+0 sclerites have also been reported in *Chancelloria* by Bengtson and Collins (2015), but they are very rare and main sclerites are 5+1 to 8+1, the most common forms being 6-7+1. Additionally, the 3+0 sclerites described in *Chancelloria* from articulated scleritomes by Bengtson and Collins (2015) are flatter than *Allonnia* sclerites and star-shaped with rays not really angled or curved from the basal plane so correctly assigned to *Chancelloria*.

**Other occurrences.** Cambrian stage 2-3 (*Sinosachites flabelliformis* – *Tannuolina zhangwentangi* Assemblage Zone and *Rhombocorniculum cancellatum* Taxon Range Zone) of South China: Bad-aowan Member of the Dengying Formation and Qiongzhusian Member of the Yu'an-shan Formation, Dahai, Huize County (Luo et al., 1982; Qian and Bengtson, 1989) and Meishucun, Jinning County (Luo et al., 1984; Qian, 1989; Jiang, 1992; Parkhaev and Demidenko, 2010), Lower Chiungdulssu Formation, Kunyang, Jinning County (Qian, 1989), Shiyantou and Yu'an-shan formations, Xiaotan, Yongshan County (Li and Xiao, 2004; Moore et al., 2014), Yunnan Province; Xinji Formation, Tanbao, Xihaoping and middle member of the Chiulaotung Formation, Malinya (Qian, 1989), Sichuan Province; Dengying and Shuijingtuo Formation, Xiaoyang and Zengjiapo, Shaanxi Province (Li et al., 2004; Yang et al., 2015). Cambrian stage 2 (*Sinosachites flabelliformis* – *Tannuolina zhangwentangi* Assemblage Zone) of India: Tal Formation, Ganga Valley, Lesser Himalaya, Uttar Pradesh (Kumar et al., 1987; Bhatt, 1989).

*Allonnia tetrathallis* (Jiang, in Luo et al., 1982)  
Figure 9.1-12

The list of synonymy of the species *Allonnia tetrathallis* in Moore et al. (2014) is considered valid in addition to the following synonym:

2016 2016 *Allonnia tetrathallis* (Jiang, in Luo et al., 1982); Peel et al., p. 248, figs. 6E, G.

**Material.** 28 articulated sclerites including the four figured phosphatic internal moulds USTL3163-8, USTL3163-3, USTL3163-10 and USTL3162-4.

**Distribution.** Cerro Rajón section, sample R21 from unit 1 of the Puerto Blanco Formation.

**Description.** The articulated sclerites are preserved as fragmented (tips of rays broken) internal phosphatic moulds (Figure 9.1-12). Two sclerites correspond to the 4+0 form (Figure 9.1-5), one

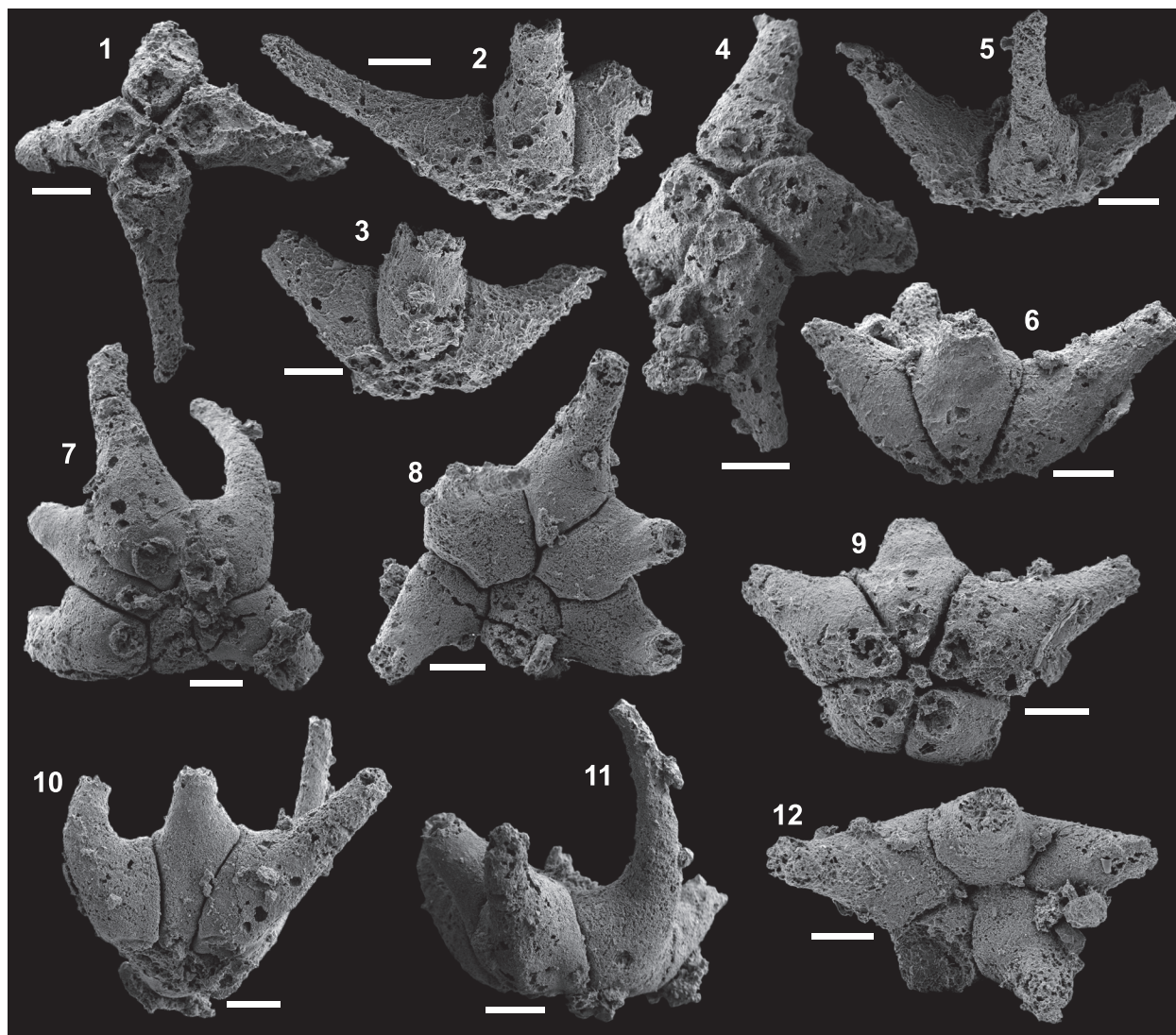


**FIGURE 9.** Articulated but broken internal moulds of sclerites of *Allonnia tetrathallis* from the Puerto Blanco Formation of Cerro Rajón, Sonora, Mexico. 1-3, 5. Specimen USTL3163-8 from sample R21 (4+0 form): 1. Adaxial view; 2-3, 5. Lateral views. 4. Specimen USTL3163-3 from sample R21 (4+0 form) in adaxial view. 6, 9, 12. Specimen USTL3163-10 from sample R21 (5+0 form): 6. Lateral view; 9. Adaxial view; 12. Abaxial view. 7-8, 10-11. Specimen USTL3162-4 from sample R21 (6+0 form): 7. Adaxial view; 8. Abaxial view; 10, 11. Lateral views. Scale bars are all 200  $\mu\text{m}$ .

sclerite to the 5+0 form (Figure 9.6, 9.9, 9.12) and one sclerite possibly corresponds to the 6+0 form and is only tentatively assigned to the species (Figure 9.7-8, 9.10-11).

The 4+0 sclerites exhibit four marginal rays, all angled from the basal plane with an angle varying between 30 and 50° (Figure 9.2-3, 9.5-6) with the longer broken rays showing a tendency to be recurved from the basal plane (Figure 9.2). Rays mainly taper gradually distally (Figure 9.1-4), but some exhibit an abrupt accentuation of tapering at the transition from the basal to the distal part of rays (Figure 9.5). Due to breakage of all recovered rays, it is not possible to give their length. Diameter

of the basal plane varies between 490 and 520  $\mu\text{m}$ . Two opposite rays meet in a central suture (Figure 9.1, 9.4). Those rays are also in contact with the two adjoining horizontal rays so that they exhibit three articular facets (Figure 9.1, 9.4). The lateral rays that do not meet at the centre of the sclerite have only two articular facets so that the four lateral rays do not meet at a single point (Figure 9.1, 9.4). The space between two adjoining rays is wide (Figure 9.1, 9.4). The angles between adjoining rays approach the right angle, slightly varying between 80 and 100°. Foramina are not well preserved and seem to be wide relative to the size of the basal plane (between 110 and 130 for

the maximum diameter), without other structure than a hole (Figure 9.1, 9.4), but one has a slightly smaller diameter and a raised rim (Figure 9.4).

In the 5+0 sclerite, the five lateral rays are similarly but slightly more strongly angled from the basal plane than in 4+0 forms (Figure 9.6). Two opposite rays also meet in a central suture and on one side, only one ray is intercalated between those rays centrally in contact while on the other side, two rays are intercalated, one being in contact with three rays so with three articulatory facets (Figure 9.9, 9.12). The angle between rays in basal view is constant, varying only between 60 and 85° (Figure 9.9, 9.12).

The 6+0 specimen is tentatively assigned to *Allonnia tetrathallis* as all six rays do not meet at a single point but a central articulatory between two opposite rays is present (Figure 9.7-8). On one side, only one ray is intercalated between those rays centrally in contact while on the other side, three rays are intercalated, the middle one being very slender and having four articulatory facets (Figure 9.7-8). The angle between rays is therefore highly variable (Figure 9.7-8). The angle between the rays and the basal plane and the curvature are more strongly expressed and the space between rays thinner (Figure 9.10-11). The preservation of the foramina is better and a raised rim is clearly visible (Figure 9.7).

**Comparisons.** The specimens described above recovered from sample R21 of the Puerto Blanco Formation are assigned to *Allonnia* as all the rays are angled and/or recurved away from the basal plane. Within the genus, the Mexican sclerites are assigned to *A. tetrathallis* due to the similarities between the 4+0 forms and the material already assigned to the species in the literature. The 5+0 forms are also assigned to the species by comparisons with the material described and illustrated by Moore et al. (2014). The 6+0 forms are tentatively assigned to *A. tetrathallis* for the first time.

**Other occurrences.** Cambrian stage 2-3 (*Sinosachites flabelliformis* – *Tannuolina zhangwentangi* Assemblage Zone and *Rhombocorniculum cancellatum* Taxon Range Zone or *Ninella tarimensis* – *Cambroclavus fangxianensis* Zone) of South China: Shuijingtuo Formation, Xiaoyang (Li et al., 2004), Xihaoping Member, Dengying Formation and Shuijingtuo Formation, Zengjiapo and Xiaoyangba, Zhenba County (Yang et al., 2015), Xihaoping Member, Dengying Formation, Xiaowan and Sanlangpu (Steiner et al., 2004), Shaanxi Province; Baodawan and Lower Yuanshan Member, Qiongzhusi Formation and Shiyantou Formation,

Dahai, Xiaotan, Huize and Meishucun (Luo et al., 1982, 1984; Qian and Bengtson, 1989; Li and Xiao, 2004; Moore et al., 2014), Yunnan Province; middle member of the Chiulaotung Formation, Malinya, Sichuan Province (Qian, 1989) and Lower Minghsinssu Formation, Yankong, Guizhou Province (Qian, 1989). Cambrian stage 3 of Germany: Upper Zwetau Carbonate Member, Doberlug-Torgau Synclinorium (Elicki, 1994). Cambrian stage 4 of Antarctica? Allochthonous boulders (Me33, 66), King George Island (Wrona, 2004). Cambrian of Pakistan: Hazira Formation (Fuchs and Mostler, 1972, Mostler, 1980).

Genus CHANCELLORIA Walcott, 1920

**Type species.** *Chancelloria eros* Walcott, 1920, Cambrian stage 5 (Great Phyllopod Bed, Walcott Quarry Member, Burgess Shale Formation), Ontario, Canada.

**Diagnosis.** See Kouchinsky et al. (2011, p. 146).

*Chancelloria* spp. Figure 10.1-29

**Material.** 35 articulated sclerites including the eight figured phosphatic internal moulds with partially preserved external coating USTL3189-4, USTL3168-5, USTL3168-10, USTL3169-3, USTL3170-2, USTL3170-6, USTL3178-4 and USTL3178-1.

**Distribution.** Cerro Rajón section, samples R21 from unit 1, R53, R54, R64 and R65 from unit 2 of the Puerto Blanco Formation.

**Description.** The articulated sclerites are preserved as fragmented (most rays broken), internal, phosphatic moulds with partial external coating (Figure 10.1-29). 5+1 (two sclerites, Figure 10.21-29), 6+1 (one poorly preserved sclerite), 7+1 (seven sclerites, Figure 10.1-9, 10.11-12, 10.15-17, 10.19-20), 8+1 (one specimen, Figure 7.18) and 9+1 (one specimen, Figure 10.10, 10.13-14) forms are present.

Sclerites 5+1 exhibit five marginal, gradually tapering rays that are all slightly angled from the basal plane (Figure 10.23, 10.26-29). One of the lateral rays (in the uppermost part of the sclerites in Figure 10.21-22, 10.24) is more massive than the others and exhibits the smallest angles with the neighbouring rays (~60°) and opposite is the largest angle between neighbouring rays (~100°; Figure 10.21-22, 10.24, 10.27). Other lateral rays are otherwise very similar to each other. The central ray is the most massive of all the rays (Figure 10.22-23, 10.26-29). The diameter of the basal plane varies between 650 and 1110 µm (Figure 10.21, 10.24). The central ray, in contact with all the other rays, exhibits five articulatory facets,

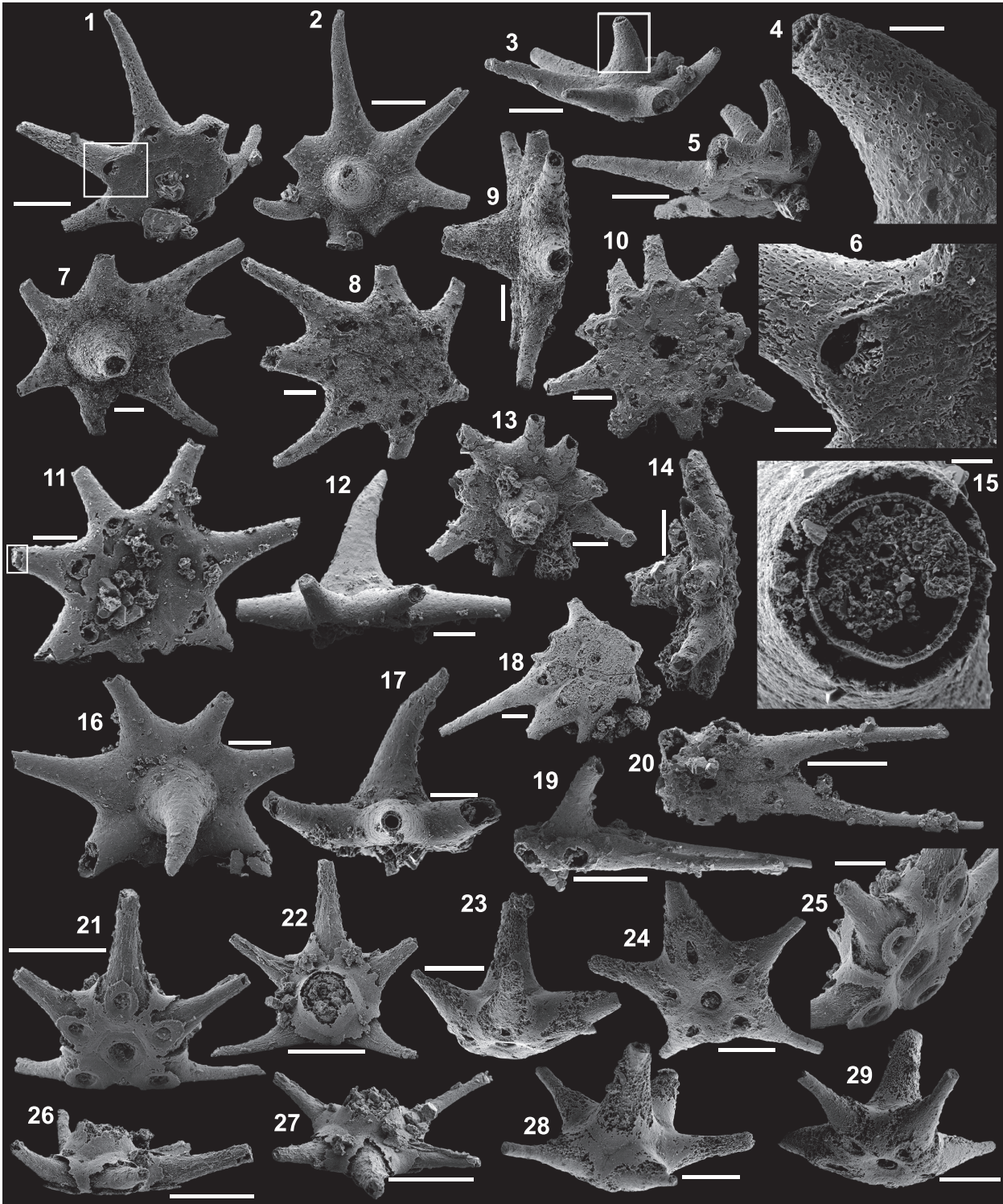


FIGURE 10. Caption on next page.

whereas each lateral ray is in contact with the central ray and two neighbouring lateral rays and so exhibit three articulatory facets (Figure 10.21, 10.24-25). Foramina are all circular in one specimen (Figure 10.21, 10.25) and in the other specimen only the foramen of the central ray is circular, whereas foramina of the lateral rays are tear drop in shape (Figure 10.24, 10.29). In both specimens, the foramen of the central ray is much wider than in lateral rays (Figure 10.22-23, 10.26-29). Numerous phosphatic filaments are present in the space between the external and internal coating (Figure 10.21, 10.22, 10.26-27), and the internal mould is composed of massive phosphate clusters (Figure 10.22, 10.27).

In the 6 to 9+1 forms, the central ray is very massive, strongly tapering and curved (Figure 10.2-3, 10.7, 10.12-14, 10.16-17, 10.19), whereas lateral rays are all slender, slightly tapering and straight (Figure 10.1-3, 10.7-8, 10.10-11, 10.13, 10.16, 10.18-20). Lateral rays are irregularly organized around the central ray (Figure 10.2, 10.7-8, 10.10-11, 10.13, 10.16, 10.18, 10.20) and not (Figure 10.9, 10.12, 10.19) to slightly angled from the basal plane (Figure 10.3, 10.14, 10.17). Diameter of the basal plane varies between 435 and 930  $\mu\text{m}$  (Figure 10.1, 10.8, 10.10-11, 10.18, 10.20). The central ray is in contact with all the other rays so exhibits six to nine articulatory facets whereas each lateral ray is in contact with the central ray and two neighbouring lateral rays so exhibit three articulatory facets (Figure 10.1-2, 10.7, 10.13, 10.16). When observable, the central foramen through the external coating is relatively wide and circular (Figure 10.10, 10.18, 10.20), whereas lateral foramina are visible as slits through the external coating in the distalmost part of the basal

planes of rays (Figure 10.1, 10.5-6, 10.8, 10.10, 10.18, 10.20), which seems to correspond to distal foramina themselves based on a specimen with broken external coating (Figure 10.11). The external coating is either smooth (Figure 10.11-12, 10.16-17) or porous (Figure 10.1-6). A thin layer of fibrous phosphate lines the internal coating (Figure 10.15). The void between the external coating and internal layer (thickness  $\sim 11\text{-}12\ \mu\text{m}$ ; Figure 10.15) corresponds to the dissolved calcareous shell.

**Remarks.** 5+1 sclerites have been described separately from the other forms because they all have been recovered from one single sample (R64), and they do not co-occur with other forms. They probably represent a separate species. It is otherwise not possible to determine if the 6 to 9+1 forms belong to the same or different species. The phosphatic filaments in the space between the external and internal coating and the massive phosphate clusters constituting the internal moulds are probably related to microbial activities.

**Comparisons.** Among disarticulated sclerites, the 5+1 forms described herein are comparable to the specimen ГИHN 3593/598 of Missarzhevsky (1989, pl. XXII, figure 9) assigned to *Ginospina araniformis* Missarzhevsky, 1989, which also exhibits one central and five lateral rays. However, the basal part of the rays is more rounded in the Siberian specimen (and should be assigned to *Chancelloriella* following Moore et al., 2014), and the basal plane of the Mexican specimens is more flattened. This difference may be related to the preservation of the Siberian specimen as an internal mould, whereas the Mexican specimens have an external coating that may obscure the possible rounded basal part of the rays and, therefore, its assignment to *Chancelloriella* instead. Comparison

**FIGURE 10** (figure on previous page). Internal moulds with external coatings of *Chancelloria* spp. from the Puerto Blanco Formation of Cerro Rajón, Sonora, Mexico. 1-6. Specimen USTL3189-4 from sample R53 (7+1 form): 1. Adaxial view, area in the square is magnified in 6; 2. Abaxial view showing the massive central ray; 3. Lateral view, area in the square is magnified in 4; 4. Detail of the curved and massive central ray with porous external coating; 5. Lateral view; 6. Detail of the slit-like lateral foramen running through the external coating. 7-9. Specimen USTL3168-5 from sample R54 (7+1 form): 7. Abaxial view; 8. Adaxial view; 9. Lateral view. 10, 13, 14. Specimen USTL3168-10 from sample R54 (8+1 form): 10. Adaxial view; 13. Abaxial view; 14. Lateral view. 11-12, 15-17. Specimen USTL3169-3 from sample R54 (7+1 form): 11. Adaxial view, area in the square is magnified in 15; 12. Lateral view showing the massive, recurved central ray; 15. Detail of the cross-section through a broken ray showing the external coating, the internal mould with the phosphatic internal layer and the void corresponding to dissolved shell material; 16. Abaxial view; 17. Lateral view. 18. Specimen USTL3170-2 from sample R54 (8+1 form). 19-20. Specimen USTL3170-6 from sample R54 (8+1 form): 19. Lateral view with long, slender lateral rays aligned with the basal plane; 20. Adaxial view. 21-22, 25-27. Specimen USTL3178-4 from sample R64 (5+1 form): 21. Adaxial view; 22. Abaxial view; 25. Detail of the basal plane; 26, 27. Lateral views. 23-24, 27-29. Specimen USTL3178-1 from sample R64 (5+1 form): 23, 28, 29. Lateral views; 24. Adaxial view. Scale bars are: 15, 20  $\mu\text{m}$ ; 4, 6, 50  $\mu\text{m}$ ; 1-3, 5, 7-14, 16-18, 25, 200  $\mu\text{m}$ ; 19-24, 26-29, 500  $\mu\text{m}$ .

with the specimen N°84898 of 5+1 form assigned to *Chancelloria irregularis* by Qian (1989) can also be made, although the central ray of this specimen is much smaller, relative to the basal plane size, than in the present material. One 5+1 disarticulated specimen similar to the Mexican material has been assigned to *Chancelloria eros* by Yang et al. (2014) and otherwise disarticulated 5+1 sclerites have been assigned to *Chancelloria maroccana* by Sdzuy, 1969. Other 5+1 forms have also been described in *Chancelloria eros* by Bengtson and Collins (2015) in articulated specimens.

Order HYOLITHELMINTHIDA Fischer, 1962  
Family HYOLITHELLIDAE Walcott, 1886  
Genus HYOLITHELLUS Billings, 1871

**Type species.** *Hyolithellus micans* Billings, 1871, Cambrian stage 3 (*Fallotaspis* Zone), Taconic allochthon, southern Québec.

**Diagnosis.** See Álvaro et al. (2002, p. 402).

*Hyolithellus* spp. Figure 11.1-23

**Material.** 1415 specimens including figured USTL3189-2, USTL3169-8, USTL3168-9, USTL3181-5, USTL3183-5, USTL3187-3, USTL3187-6, USTL3184-2, USTL3185-2, USTL3186-14, USTL3186-2, USTL3182-4 and USTL3188-5.

**Distribution.** Cerro Rajón section, sample R21, R53, R54, R55, R56, R60, R61, R62, R63, R64, R65, R66, R69, R71, R72, R75, R78, R83, R90, R92, R93 and R94 from unit 1 to 4 of the Puerto Blanco Formation.

**Description.** The phosphatic tube fragments are straight (Figure 11.1, 11.4, 11.7, 11.14, 11.18, 11.20, 11.23) to slightly undulating (Figure 11.3, 11.5, 11.10). Length is variable, ranging from 796 µm to 4957 µm. The tubes are slightly, but continuously tapering with a very low average angle of 3° (maximum value of 20° and minimum of 1°) and always open at both ends (Figure 11.2, 11.6, 11.8, 11.11-13). The cross-section is circular at both extremities (Figure 11.6, 11.8, 11.11-13) with a diameter reaching 128 µm at tapered end and 788 µm at opposite extremity. The internal cavity of the tube is either empty (Figure 11.2) or filled with phosphatized sediment (Figure 11.6, 11.8, 11.11-13) and the internal surface is completely smooth (Figure 11.2, 11.8, 11.14-15). The external surfaces exhibit various types of ornamentations. Some specimens have an almost smooth external surface, only with distantly separated and very low and faint transverse annulations (Figure 11.1, 11.3). Other specimens exhibit dense and irregular transverse striations to low ribs (Figure 11.4-5,

11.9). In most specimens, external ornamentation consists of ribs forming pronounced annulations (Figure 11.7-8, 11.10, 11.14, 11.16-23). The distance between the ribs is large compared to the tube diameter and either relatively regular (Figure 11.7, 11.14, 11.18-19, 11.23) or completely irregular (Figure 11.10, 11.17), even with sinusoidal to coalescent ribs (Figure 11.17, 11.22). The annulated ornamentation is sometimes covered by minerals (Figure 11.7-8). The surface between the ribs is either smooth (Figure 11.10, 11.17, 11.22) or with irregular and coarse longitudinally oriented striations forming a fasciculate pattern (Figure 11.14, 11.16, 11.18-21). In one specimen, different parts of the tube are smooth, others bear faint, transverse, dense striations or distant ribs associated with longitudinal fasciculations (Figure 11.20-21). The tube wall is composed of laminated (Figure 11.15) calcium phosphate. Its thickness is highly variable (Figure 11.2, 11.6, 11.8, 11.11-13, 11.15), ranging between 3 to 65 µm and the thickness increases towards the tapering end (Figure 11.2, 11.8).

**Remarks.** Variations in observed wall thickness is likely related to exfoliation of the laminated walls (Figure 11.2, 11.6, 11.8, 11.11-13), which is also responsible for the high variability in external ornamentation (Figure 11.17, 11.20-21).

**Comparisons.** All specimens are assigned to the genus *Hyolithellus* Billings, 1871, based on the low angle of divergence, circular cross-section and phosphatic laminated walls, but the species assignment is left open due to the poorly constrained taxonomy of *Hyolithellus* species. A revision of the genus, involving an effective consideration of the preservation, is necessary, but is out of the scope of this study. Pending revision of the genus, the specimens presented herein are attributed to various unidentified species due to the variability in their ornamentations. The longitudinal ornamentations in some of the present specimens enable comparisons with *Byronia*, but the latter differs by the presence of furrows on the internal surface of the tubes that correspond to the annulations and longitudinal ribs of the external surface as described by Matthew (1899). Several species of *Hyolithellus* also exhibit longitudinal ornamentation between the transverse annulations. The longitudinal ornamentation of *Hyolithellus grandis* Missarzhevsky in Rozanov et al., 1969, and *Hyolithellus irregularis* Qian, 1989, are much finer. The present longitudinal ornamentations are more comparable to those of *Hyolithellus insolitus*

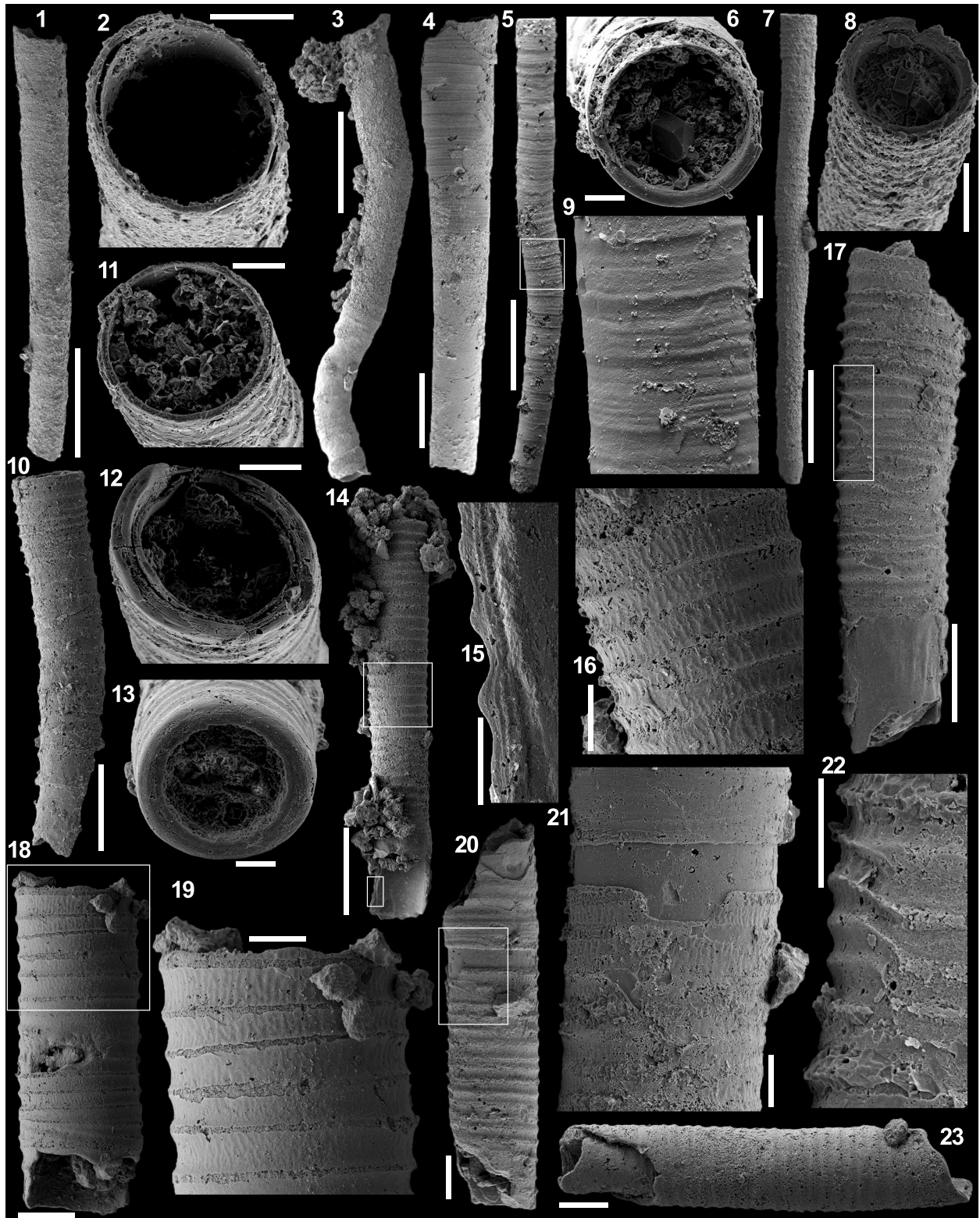


FIGURE 11. Caption on next page.

Voronin et al., 1982, which are quite coarse and irregular.

Class HYOLITHA Marek, 1963  
Order ORTHOTHECIDA Marek, 1966  
Family CUPITHECIDA Duan, 1984  
Genus CUPITHECA Duan, 1984

**Type species.** *Paragloborilus mirus* (He in Qian, 1977), Fortunian (*Paragloborilus subglobosus* – *Purella squamulosa* Zone), Maidiping, Emei County, Sichuan Province, South China.

**Diagnosis.** See Parkhaev and Demidenko (2010, p. 949).

*Cupithec* cf. *C. mira* Figure 12.1-14

**Material.** 21 specimens including the figured incomplete internal and external coating of conchs USTL3176-9 and USTL3176-3.

**Distribution.** Cerro Rajón section, sample R63, R75 and R83 from unit 2 to 4 of the Puerto Blanco Formation.

**Description.** The conchs are slowly and uniformly expanding throughout their length with a maximum angle of divergence varying between 9 and 11° in different specimens. Specimens are always broken so only a short, straight part, including the closed termination, is present (Figure 12.1-2, 12.6-7) with a measured length varying between 1360 and 1900 µm. Cross-sections are circular (Figure 12.8, 12.11) and maximum measured diameter varies between 545 and 595 µm. The closed termination exhibit two different organizations: (1) one is hemispherically bulbous with a shallow and relatively broad circular groove separating it from the rest of the conch (Figure 12.6, 12.12-13) and (2) the other is flat, makes a sharp angle with the lateral walls of the conch and seems to lack a circular groove but breakage prevents any definite conclusion on this character (Figure 12.1-3, 12.5). In two specimens, the internal cavity of the conch is subdivided into

two chambers separated by a transverse septum (Figure 12.1-4, 12.6-8, 12.10, 12.12). In those two specimens, the chambers are 710 to 1060 µm in length and partly filled with loose to dense phosphatic coccoidal pseudomorphs (Figure 12.1-4, 12.6-8, 12.10, 12.12). The shell walls are observed as a gap, sometimes with phosphatic filaments, between internal and external phosphatic coatings (Figure 12.1, 12.4, 12.6, 12.8, 12.11, 12.14). The wall constituting the septum is 30 to 45 µm in thickness and continuous with the lateral wall of the conch (Figure 12.4, 12.14). The septum is flat to very slightly apically convex, smooth and forms a sharp angle with the lateral walls (Figure 12.1, 12.4, 12.6, 12.12, 12.14). The surfaces of external and internal coatings are completely smooth (Figure 12.1-2, 12.6-7).

**Remarks.** The variation in the organization of the closed termination of the conchs has been interpreted to be related to their ontogenetical development (Bengtson et al., 1990). The conch has been interpreted to discard the apical region during the growth of the organism (Bengtson et al., 1990). Therefore, fragments of *Cupithec* corresponding to the discarded part are common, but more complete specimens (at least conch with embryonic part and internal septum preserved) are rare (Malinky and Skovsted, 2004). In the Mexican material, the hemispherical, bulbous apex (the embryonic shell) is exceptionally preserved in one specimen, along with a later internal septum. In a second specimen, the flat and angular closed termination corresponds to a later segment of the conch closed by a flat and angular septum as seen in the internal cavity of the specimen with the embryonic shell preserved. This specimen also has an exceptionally preserved later internal septum. The specimen USTL3176-3 is interpreted to include the embryonic shell, and a secondary

**FIGURE 11** (figure on previous page). Incomplete tubes of *Hyolithellus* spp. from the Puerto Blanco Formation of Cerro Rajón, Sonora, Mexico. 1-2. Specimen USTL3189-2 from sample R53: 1. Lateral view; 2. Detail of the large aperture. 3. Specimen USTL3182-4 from sample R66 in lateral view. 4. Specimen USTL3169-8 from sample R54 in lateral view. 5-6, 9. Specimen USTL3168-9 from sample R54: 5. Lateral view, area in the square is magnified in 9; 6. Narrow aperture; 9. Detail of the external surface ornamentation. 7-8. Specimen USTL3181-5 from sample R71: 7. Lateral view; 8. Apertural view. 10-11. Specimen USTL3183-5 from sample R83: 10. Lateral view; 11. Apertural view. 12. Aperture of specimen USTL3187-3 from sample R92. 13. Aperture of specimen USTL3187-6 from sample R92. 14-16. Specimen USTL3184-2 from sample R83: 14. Lateral view, area in the lower square is magnified in 15 and area in the upper square is magnified in 16; 15. Detail of the laminar wall structure; 16. Detail of the external surface ornamentation. 17, 22. Specimen USTL3185-2 from sample R92: 17. Lateral view, area in the square is magnified in 22; 22. Detail of the irregular transverse ribs. 18-19. Specimen USTL3186-14 from sample R92: 18. Lateral view, area in the square is magnified in 19; 19. Detail of the external surface ornamentation. 20-21. Specimen USTL3186-2 from sample R92: 20. Lateral view, area in the square is magnified in 21; 21. Detail of the external surface ornamentation et exfoliation. 23. Lateral view of Specimen USTL3188-5 from sample R93. Scale bars are: 6, 11, 13, 15, 22, 50 µm; 2, 8-9, 12, 16, 19, 21, 100 µm; 10, 17-18, 20, 23, 200 µm; 1, 4-5, 7, 14, 500 µm; 3, 1 mm.

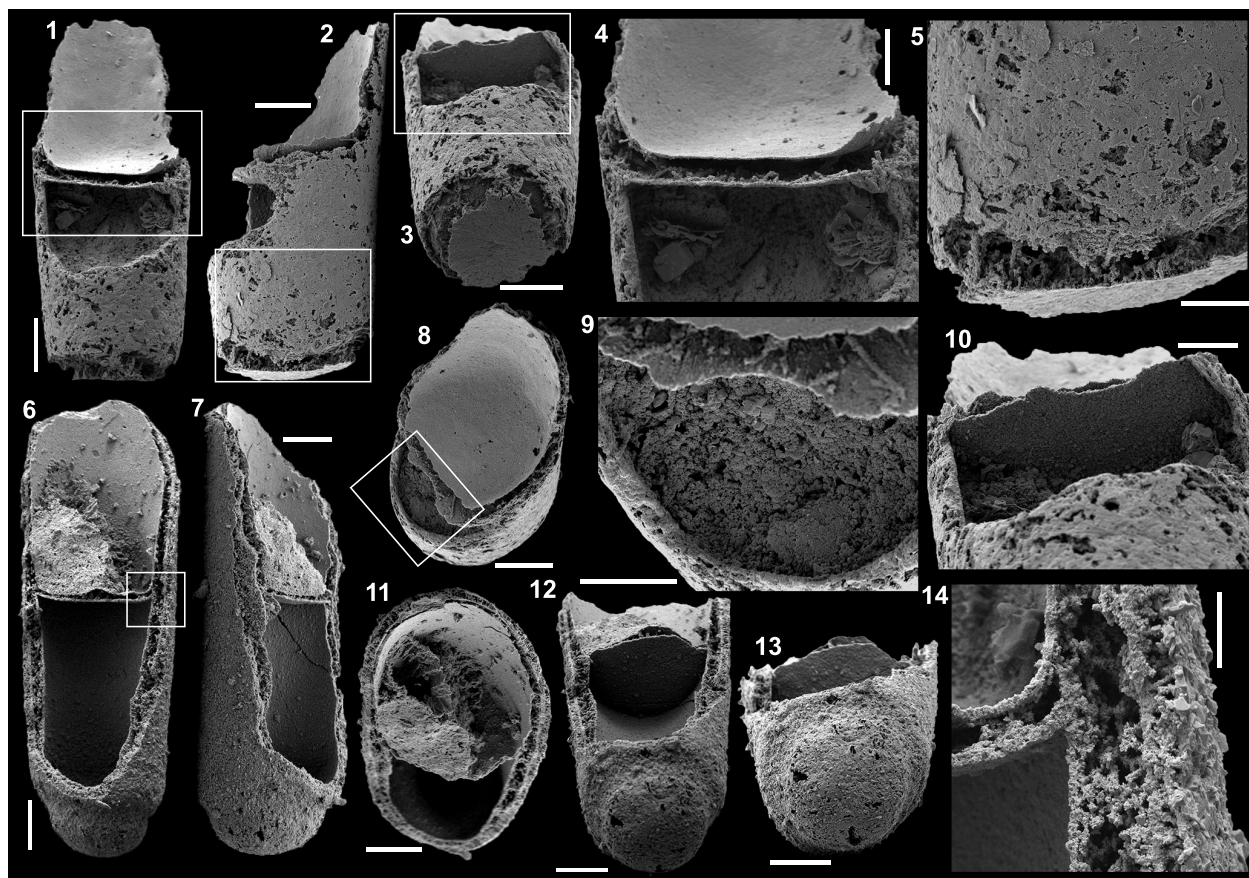


**FIGURE 12.** Incomplete conchs of *Cupitheca* cf. *C. mira* from the Puerto Blanco Formation of Cerro Rajón, Sonora, Mexico. 1-5, 8-10. Specimen USTL3176-9 from sample R63: 1. Lateral view, area in the square is magnified in 4; 2. Lateral view, area in the square is magnified in 5; 3. Apical view, area in the square is magnified in 10; 4. Detail of the septum; 5. Detail of the flat and angular closed termination; 8. Abapical view, area in the square is magnified in 9; 9. Detail of the filling of a chamber; 10. Detail of the smooth septum. 6-7, 11-14. Specimen USTL3176-3 from sample R63: 6. Lateral view, area in the square is magnified in 14; 7. Lateral view; 11. Abapical view; 12, 13. Apical view showing the hemispherical embryonic shell; 14. Detail of the relation between the septum and the lateral wall. Scale bars are: 14, 50  $\mu\text{m}$ ; 4-5, 9-10, 100  $\mu\text{m}$ ; 1-3, 6-8, 11-13, 200  $\mu\text{m}$ .

chamber isolated from the embryonic shell by a flat and angular septum (Figure 13). Specimen USTL3176-9 preserves only later ontogenetical stages with secondary segments as attested by the flat and angular closed termination, which corresponds to a septum and not to the embryonic, bulbous, original apex (Figure 13). The occurrence of two joined segments in the Mexican specimens is rather exceptional compared to typical *Cupitheca* material.

**Comparisons.** The present specimens are assigned to *Cupitheca* cf. *C. mira* as specimens described by McMenemy (1984), which possess a similar apex. However, they differ in the preservation, the present specimens being phosphatic coatings of conchs, whereas the specimens in McMenemy (1984) are preserved as internal moulds. Therefore, the former exhibits preserved

septation and two chambers, whereas the latter corresponds to discarded parts of the conch. The specimens recovered in this study can also be compared to *Cupitheca mira* as they exhibit similar apices and absence of ornamentations (smooth conchs). However, the preservation is also different between the present specimens and other specimens of this species, which is why the specimens are only tentatively assigned to this species as *Cupitheca* cf. *C. mira*. They differ from all the other species of *Cupitheca* by the total absence of ornamentation (smooth internal and external coatings).

Order ORTHOTHECIDA Marek, 1966  
 Family CIRCOTHECIDAE Missarzhevsky in  
 Rozanov et al., 1969  
 Genus PETASOTHECA Landing and Bartowski,  
 1996

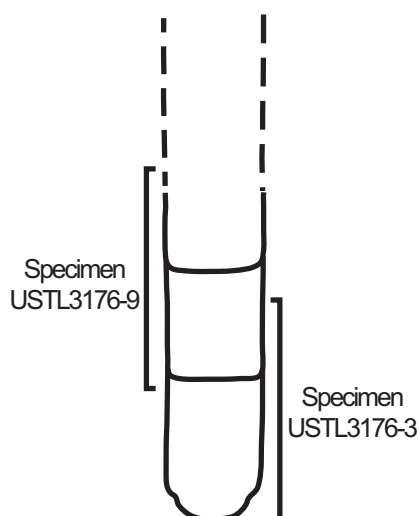


**FIGURE 13.** Reconstruction of a complete conch of *Cupitheca* cf. *C. mira* with delimited parts corresponding to the various parts that were preserved. The dashed lines represent material which was not preserved in the Mexican material, but which are inferred from the data of Bengtson et al. (1990).

**Type species.** *Petasotheca minuta* Landing and Bartowski, 1996, Cambrian stage 3-4 (middle *Olenellus* zone), Claverack village, New York State, USA.

**Diagnosis.** See Landing and Bartowski (1996, p. 757).

*Petasotheca* sp. Figure 14.1-19

**Material.** 21 specimens including the four figured phosphatic incomplete conchs USTL3174-1, USTL3175-7, USTL3175-10, USTL3166-5 and the four figured phosphatic external coatings of opercula USTL3177-13, USTL3174-2, USTL3174-5, USTL3177-5.

**Distribution.** Cerro Rajón section, samples R53, R56 and R63 from unit 2 of the Puerto Blanco Formation.

**Description.** The conchs are rapidly and uniformly expanding with a maximum angle of divergence varying between 12 and 18° in different specimens. The conchs are slightly curved (Figure 14.1, 14.4, 14.7), with a measureable length (not real length as all the specimen tips are broken) varying between 1030 and 1975 µm. Cross-sections are circular (Figure 14.5) to slightly subcircular (Figure 14.2) and the apertural diameter varies between 355 and 650 µm. The apertural margin is straight in lateral view and perpendicular to the longitudinal axis (Figure 14.1, 14.4, 14.7). The apex is unknown due to breakage of the conch's tip (Figure

14.3, 14.6-7). The external surface exhibits fine comarginal growth lines (Figure 14.1, 14.4, 14.7-8).

The concavo-convex opercula are preserved as external phosphatic coatings disarticulated from the conchs even if they co-occur in the same samples. Opercula are circular in outline with slightly elevated central round apex (Figure 14.9, 14.14, 14.18). The external surface of the operculum is convex with fine concentric growth lines (Figure 14.9, 14.14, 14.16, 14.18). In external lateral view, opercula are low conical (Figure 14.15-16). The internal surface is concave, very depressed at growth centre (internal equivalent of the apical zone) and is surrounded by a concentric ridge separated from the margin by a narrow surface (Figure 14.11, 14.13, 14.17). Polygonal imprints ranging from 4 to 7 µm are observed on this narrow surface and on the ridge (Figure 14.16-17, 14.19). The concentric ridge exhibits a variable height around the operculum: the ridge has a medium height on one side (located in the upper part of Figure 14.11, 14.13, 14.17), a maximum height laterally (of up to 75 µm), where clavicle-like structures (possibly up to 5 in number) are difficult to see (Figure 14.11-12) and a minimum height on the last side (lower part of opercula in Figure 14.11, 14.13, 14.17).

**Comparisons.** The Mexican conchs are simple, conoidal with a round cross-section typical of *Petasotheca* (Landing and Bartowski, 1996). Such conchs have few diagnostic characters, therefore, they are also comparable with those of *Conotheca*, especially *Conotheca brevica* Missarzhevsky in Rozanov et al., 1969 or *C. australiensis* Bengtson in Bengtson et al., 1990. Differentiation is mainly based on the opercula. The opercula of the Mexican specimens can be compared with several specimens, which exhibit only clavicle-like structures and lack cardinal processes. They belong to *Allatheca* Missarzhevsky in Rozanov et al., 1969 or *Majatheca* Missarzhevsky in Rozanov et al., 1969. However, *Allatheca* sp. (Missarzhevsky in Rozanov et al., 1969; plate XI, figures 4, 8) differs from the Mexican specimens by the triangular cross-section typical of the Allathecidae. An operculum referred as allathecid by Matthews and Missarzhevsky (1975; plate 2, figures 17, 20) is very similar to the Mexican material but assignment to allathecids is doubtful due to the circular cross-section. It could instead belong to the same species as the present specimens. Specimens of *Majatheca tumefacta* Missarzhevsky in Rozanov et al., 1969, figured by Kouchinsky et al. (2015) differ by the restriction of the more strongly marked internal concentric (with the apertural margin) ridge to a much more central

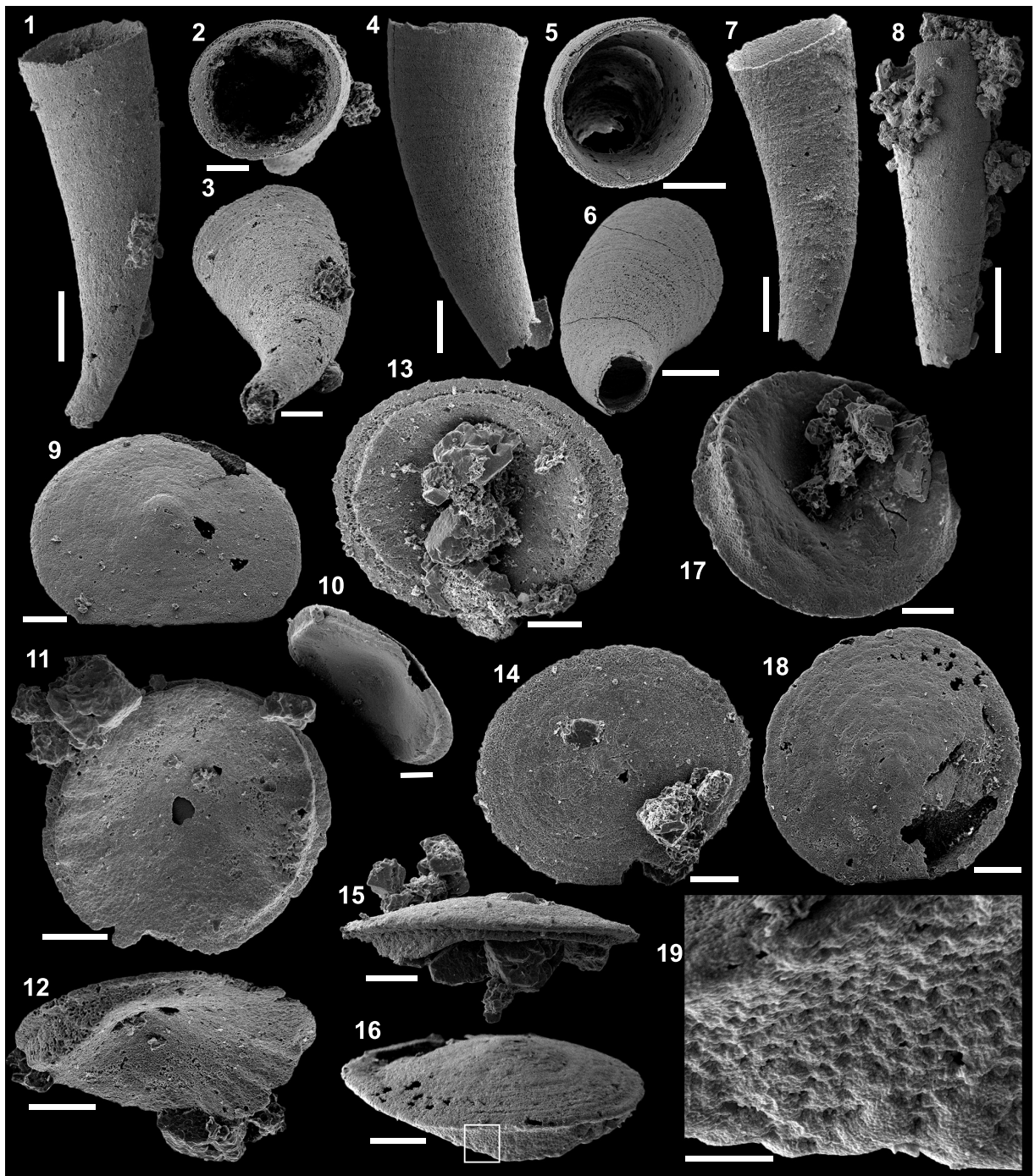


**FIGURE 14.** Conchs and opercula of *Petasotheca* sp. from the Puerto Blanco Formation of Cerro Rajón, Sonora, Mexico. 1-3. Specimen USTL3174-1 from sample R56: 1. Lateral view of the conch; 2. Apertural view; 3. Apical view. 4-6. Specimen USTL3175-7 from sample R63: 4. Lateral view of the conch; 5. Apertural view; 6. Apical view. 7. Specimen USTL3175-10 from sample R63, lateral view of the conch. 8. Specimen USTL3166-5 from sample R53, lateral view of the conch. 9-10. Specimen USTL3177-13 from sample R63: 9. External surface; 10. Lateral view of internal surface. 11-12. Specimen USTL3174-2 from sample R56: 11. Internal surface; 12. Lateral view of internal surface showing the organization of the raised concentric ridge and the clavicle-like structures. 13-15. Specimen USTL3174-5 from sample R56: 13. Internal surface; 14. External surface with fine concentric growth lines; 15. Lateral view. 16-19. Specimen USTL3177-5 from sample R63: 16. Lateral view, area in the square is magnified in 19; 17. Internal surface; 18. External surface with rounded subcentral apex and fine concentric growth lines; 19. Detail of the polygonal imprints on the internal concentric ridge. Scale bars are: 19, 20  $\mu\text{m}$ ; 2-3, 9-18, 100  $\mu\text{m}$ ; 1, 4-7, 200  $\mu\text{m}$ ; 8, 500  $\mu\text{m}$ .

position (figure 24 in Kouchinsky et al., 2015). Kouchinsky et al. (2015; figure 28D) also report, from the Cambrian stage 3 of the Emyaksin Formation at Bol'shaya, Kuonamka, an operculum with weakly developed cardinal processes and radially oriented lateral folds of the circular distal ridge that is similar to the specimens presently described except that the apex is largely excentric in the Siberian specimen. Cardinal processes are also absent from *Ladatheca* Sysoev, 1968, but the organization of the internal concentric (with the apertural margin) ridge is different (different variations of the height) and they also lack the clavicle-like structures observed in the Mexican specimens. A similar comparison can be made with *Conothecha subcurvata* Yu, 1974 (emended by Devaere et al., 2014) and opercula referred to as orthothecid operculum A in Peel et al. (2016). In both, the opercula lack cardinal processes as well as clavicle-like structures and have a large eccentric apex (Devaere et al., 2014; Peel et al., 2016). The opercula-like objects reported by Bengtson et al. (1990; figure 138) have, like the Mexican specimens, a central apex and an internal concentric ridge without cardinal processes, but lack the clavicle-like structures, which are observed herein. Those operculum-like objects have tentatively been assigned to *Cupitheca* Duan in Xing et al. (1984), but a recent study by Skovsted et al. (2016) provided data on the opercula of *Cupitheca* which are very different from these objects and from the present specimens. The Mexican specimens, especially the opercula, are more similar to *Petasotheca minuta* Landing and Bartowski, 1996, but are not assigned to this species due to their differences in number and organization of the clavicles. The Mexican specimens may represent a new species, but the preservation prevents erection of a new species so it is left with open nomenclature.

Order HYOLITHIDA Sysoev, 1957  
Family and genus uncertain  
Hyalolithid sp. Figure 15.1-6

**Material.** 41 specimens including the two figured phosphatic internal moulds USTL3169-5 and USTL3169-1.

**Distribution.** Cerro Rajón section, sample R53, R54 and R63 from unit 2 of the Puerto Blanco Formation.

**Description.** The conchs are rapidly expanding (maximum angle of divergence varying between 12 and 16°), straight and incompletely preserved (apical part broken, maximum preserved length varying between 1920 and 3870 µm; Figure 15.1-2, 15.4-5). The transverse cross-section is subtriangular

(Figure 15.3, 15.6). The ventral side is flat (Figure 15.6) to concave (Figure 15.3), and the lateral sides and dorsal side are slightly convex (Figure 15.3, 15.6). The ligula is semi-elliptical, about three times wider than long (Figure 15.1-2). The surface of internal mould (Figure 15.4-5) and shell replacement (?) are smooth (Figure 15.1-2).

**Comparisons.** The conchs are assigned to hyolithid sp. because no associated opercula have been recovered and, therefore, an insufficient number of characters is available for more detailed assignment.

Genus PARKULA Bengtson in Bengtson et al., 1990

**Type species.** *Parkula bounites* Bengtson in Bengtson et al., 1990, Cambrian stage 3 (*Abadiella huoi* Zone), Kulpara, Yorke Peninsula, Australia.

**Diagnosis.** See Skovsted (2006b, p. 492).

*Parkula bounites* (Bengtson in Bengtson et al., 1990) Figure 15.7-20

- 1990 *Parkula bounites* n. sp.; Bengtson in Bengtson et al., p. 223-228, figs. 149-151.  
2001 *Parkula bounites* Bengtson in Bengtson et al.; Parkhaev in Gravestock et al., p. 101-102, pl. IX, figs. 12-13.  
2003 *Parkula bounites* Bengtson in Bengtson et al.; Wrona, p. 197, fig. 5F.  
2004 *Parkula bounites* Bengtson in Bengtson et al.; Malinky and Skovsted, p. 559, figs. 3G, 4A, B, 5.

**Material.** Four specimens including the two figured phosphatic internal and external coatings of opercula USTL3175-9 and USTL3176-1.

**Distribution.** Cerro Rajón section, sample R63 from unit 2 of the Puerto Blanco Formation.

**Description.** Opercula have a wedge shape in apical view, with a semi-circular outline of the conical shield and an angular outline of the cardinal shield and a mean diameter varying between 1050 and 1270 µm (Figure 15.7, 15.13). The conical shield is more developed than the cardinal shield (Figure 15.7, 15.13). The apex is located on the conical shield at the angle of junction with the cardinal shield, has an elliptical shape, is smooth and slightly raised from the conical shield, with a maximum diameter of about 200 µm (Figure 15.13, 15.19). The tectula (or rooflets) are poorly defined (Figure 15.7, 15.13). The external surface of the opercula exhibits comarginal (faint on the conical shield but stronger on the cardinal shield; Figure 15.13, 15.19) and radial ridges (Figure 15.7, 15.10, 15.13). In lateral view, the conical shield is strongly convex (Figure 15.9, 15.17). The cardinal shield is

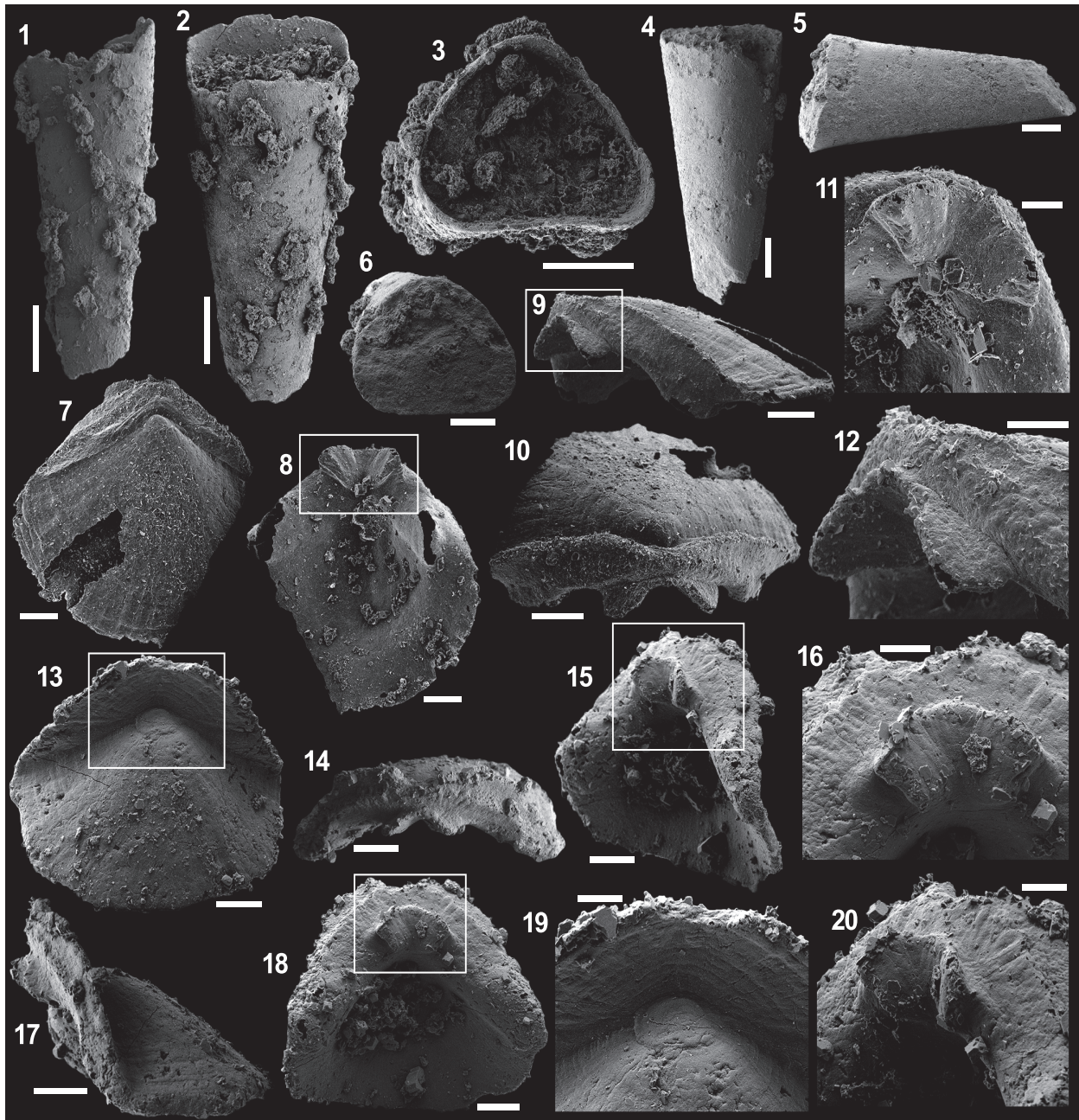


**FIGURE 15.** Conchs of hyolithid sp. and opercula of *Parkula bounites* Bengtson in Bengtson et al., 1990 from the Puerto Blanco Formation of Cerro Rajón, Sonora, Mexico. 1-3. Specimen USTL3169-5 of hyolithid sp. from sample R54: 1. Lateral view; 2. Dorsal view; 3. Apertural view. 4-6. Specimen USTL3169-1 of hyolithid sp. from sample R54: 4. Dorsal view; 5. Lateral view; 6. Apertural view. 7-12. Specimen USTL3175-9 of *Parkula bounites* Bengtson in Bengtson et al., 1990, from sample R63: 7. External view; 8. Internal view, area in the square is magnified in 11; 9. Lateral view, area in the square is magnified in 12; 10. Dorsal view; 11-12. Details of the cardinal processes. 13-20. Specimen USTL3176-1 of *Parkula bounites* Bengtson in Bengtson et al., 1990 from sample R63: 7. External view, area in the square is magnified in 19; 14. Dorsal view; 15. Lateral internal view, area in the square is magnified in 20; 16, 20. Details of the cardinal processes; 17. Lateral view; 18. Internal view, area in the square is magnified in 16; 19. Detail of apical area. Scale bars are: 11-12, 16, 19-20, 100  $\mu\text{m}$ ; 7-10, 13-15, 17-18, 200  $\mu\text{m}$ ; 1-6, 500  $\mu\text{m}$ .

inclined at an angle of 55 to 65° from the plane of the apertural margin of the conical shield (Figure 15.9, 15.17). A comarginal ridge lines the junction between the cardinal and conical shield on the internal surface of the cardinal shield (Figure 15.9-10, 15.12, 15.14, 15.17). The cardinal processes are located on the internal surface of the cardinal shield, at the junction between the cardinal and conical shields (Figure 15.9-10, 15.12, 15.14-15, 15.20). They are short and diverging at ~90° (Figure 15.8, 15.11, 15.16, 15.18). On the internal surface of the opercula, below the tectula, a pair of clavicles is located at the junction between the cardinal and conical shields and ends in blade-like projections (Figure 15.9, 15.17). On internal views, the conical shields are deep (Figure 15.8, 15.15, 15.18).

**Comparisons.** The opercula are assigned to the genus *Parkula* as they exhibit the characteristic conical shield, the short cardinal processes and the pair of clavicles ending in blade-like projections included in the diagnosis emended by Skovsted (2006b). They differ from the opercula of *Parkula esmeraldina* Skovsted, 2006, by the less developed ornamentation of transverse striations and by the cardinal processes that do not project well beyond the cardinal shield.

**Other occurrences.** Cambrian stages 3-4 (*Micrina etheridgei* SSF Zone of Betts et al. (2016) and *Abadiella huoi*, *Pararaia tatei* and *P. bunyerooensis* trilobite zones) of Australia: Parara Limestone, Kulpara (Bengtson et al., 1990); Kulpara Formation and Parara Limestone, Horse Gully, Curramulka Quarry, CD-2, SYC-101 and Cur-D1B (Gravestock et al., 2001), Yorke Peninsula, Stansbury Basin; Sellick Hill Formation, Myponga Beach, Fleurieu Peninsula (Gravestock et al., 2001). Cambrian stage 3 (*P. tatei* Zone) of Antarctica: erratic boulder Me66, King George Island (Wrona, 2003). Cambrian stages 3-4 (*Bonnina* – *Olenellus* Zone) of northeast Greenland: Upper Bastion Formation at Albert Heim Bjerger and Ostenfeld Nunatak (Malinky and Skovsted, 2004).

Phylum MOLLUSCA Cuvier, 1797  
Class HELCIONELLOIDA Peel, 1991  
Order and Family uncertain  
Genus MACKINNONIA Runnegar  
In Bengtson et al., 1990

**Type species.** *Mackinnonia davidi* Runnegar in Bengtson et al., 1990, Cambrian stage 3 (*Abadiella huoi* Zone), Horse Gully, Yorke Peninsula, Australia.

**Diagnosis.** See Bengtson et al. (1990, p. 233).

*Mackinnonia corrugata* (Runnegar in Bengtson et al., 1990)

Figure 16.1-18

- ?1988 *Helcionella abrupta* (Shaler and Foerste, 1888); Landing, p. 684, fig. 5.14.  
1990 *Leptostega? corrugata* n. sp.; Runnegar in Bengtson et al., p. 234, fig. 160A-G  
2001 *Mackinnonia plicata* (Missarzhevsky, 1989); Parkhaev in Gravestock et al., p. 178-179, pl. XXXVIII, figs 6-12, pl. XXXIX, figs 1-10.  
2009 *Mackinnonia corrugata* (Runnegar in Bengtson et al., 1990); Topper et al., p. 225-227.

**Material.** 202 specimens including the six figured phosphatic internal moulds USTL3189-5, USTL3189-3, USTL3165-1, USTL3166-1, USTL3166-8 and USTL3172-8.

**Distribution.** Cerro Rajón section, samples R53, R55 and possibly R56 from unit 2 of the Puerto Blanco Formation.

**Description.** The internal moulds of the univalve conchs are cap-shaped and bilaterally symmetrical (Figure 16.6, 16.8, 16.12, 16.16-17). Strong lateral compression is observed (mean width/length of 0.50 with a maximum width of 785 µm and a maximum length of 1520 µm), whereas the height (1435 µm at maximum) is comparable to the length (mean height/length of 0.99). The apex is blunt, rounded, shifted posteriorly (arbitrarily defined as in Devaere et al., 2013) and slightly overhangs the subapical apertural margin (Figure 16.1-2, 16.6-7, 16.10-12, 16.15, 16.18). As the apex is shifted posteriorly, the conch is loosely coiled into one-third of a whorl (Figure 16.1, 16.7, 16.10-11, 16.15, 16.18). In lateral view, the anterior field (from the apex to the anterior margin) is convex and the subapical field is concave (Figure 16.1, 16.7, 16.10-11, 16.15, 16.18). In posterior/anterior view, the lateral fields are straight but crossed by ornamentations (Figure 16.4, 16.8, 16.16). The aperture is strongly elliptically elongate with the maximum width at the anterior part and the minimum width below the apex (Figure 16.2, 16.17). The external surface of internal moulds displays about five (but from two to seven depending on the preservation) strongly expressed, continuous, comarginal corrugations. In profile, corrugations have a rounded shape on the lateral fields (Figure 16.3-5, 16.8, 16.16), a relatively flattened shape on the anterior field (Figure 16.1, 16.7, 16.10-11, 16.15, 16.18) and a rounded triangular shape on the posterior subapical field (Figure 16.1, 16.7, 16.10-11, 16.15, 16.18). The posterior parts of the corrugations become higher towards the aperture and almost form a platform at the apertural margin (Figure 16.13). Polygonal

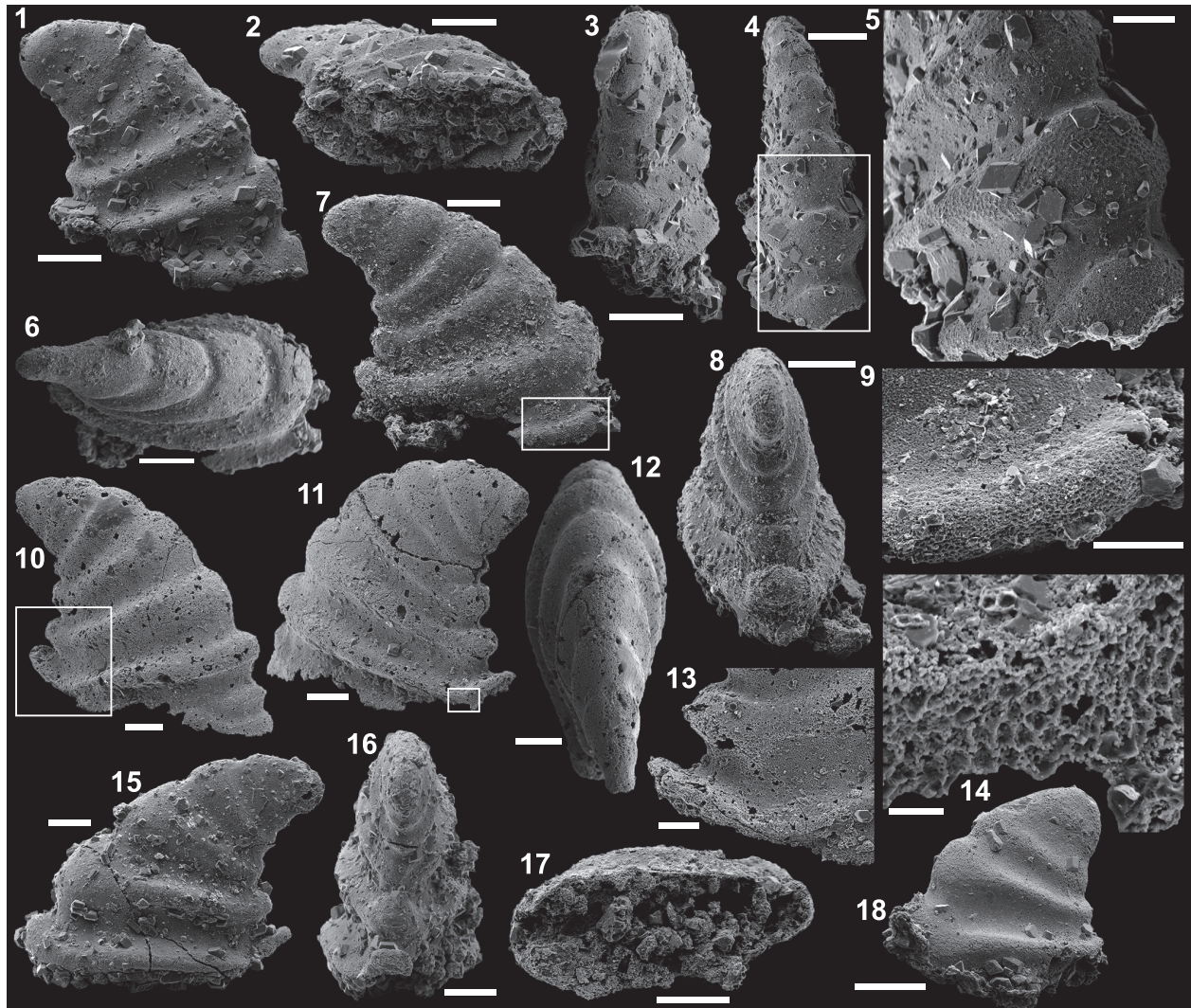


**FIGURE 16.** Internal moulds of *Mackinnonia corrugata* Runnegar in Bengtson et al., 1990 from the Puerto Blanco Formation of Cerro Rajón, Sonora, Mexico. 1-5. Specimen USTL3189-5 from sample R53: 1. Lateral view; 2. Apertural view; 3. Posterior view; 4. Anterior view, area in the square is magnified in 5; 5. Detail of the anterior field showing the polygonal imprints restricted to the summit of the comarginal corrugations. 6-9. Specimen USTL3189-3 from sample R53: 6. Upper view; 7. Lateral view, area in the square is magnified in 9; 8. Posterior view; 9. Detail of the polygonal imprints lining the apertural margin. 10-14. Specimen USTL3165-1 from sample R53: 10. Antero-lateral view, area in the square is magnified in 13; 11. Postero-lateral view, area in the square is magnified in 14; 12. Posterior view; 13. Detail of the high, sharp posterior part of the comarginal corrugations; 14. Detail of the polygonal imprints lining the apertural margin. 15-16. Specimen USTL3166-1 from sample R53: 15. Lateral view; 16. Posterior view. 17. Specimen USTL3172-8 from sample R55 in apertural view. 18. Specimen USTL3166-8 from sample R53 in lateral view. Scale bars are: 14, 20  $\mu\text{m}$ ; 5, 9, 13, 100  $\mu\text{m}$ ; 1-4, 6-8, 10-12, 15-18, 200  $\mu\text{m}$ .

imprints (about 8  $\mu\text{m}$  in average diameter) are present on the internal moulds, particularly on the summit of the comarginal corrugations (Figure 16.3-5) and lining the apertural margin (Figure 16.9, 16.14).

**Comparisons.** The Mexican specimens exhibit the typical ornamentations (similar comarginal corrugation alternating with furrows and polygonal imprints) of *Mackinnonia*. The Mexican material

has a wider shell and less posteriorly inclined apex than reported in specimens from Australia by Runnegar in Bengtson et al. (1990) as *Leptostega? corrugata*, by Topper et al. (2009) as *Mackinnonia corrugata* and by Parkhaev in Gravestock et al. (2001) as *Mackinnonia plicata*. The specimens described by McMenamin (1984) as *Bemella pauper* (p. 48-50), but figured as *Bemella mexicana* sp. nov. (plate 13, figures 3-5), are most probably

equivalent to the present specimens. The specimens are also relatively similar to *Mackinnonia rostrata* Zhou and Xiao 1984 except for the posterior apertural margin which marks a strong backward extension in *Mackinnonia rostrata*, but which just almost forms a small platform as the posterior corrugations become higher in *M. corrugata*. The Mexican specimens completely differ from *M. anabarica* Parkhaev, 2005 by the absence of the typical strong apertural fold that is continuous with the subapical train.

**Other occurrences.** Cambrian stages 3-4 (*Abadiella huoi*, *Pararaia tatei*, *P. bunyerooensis* and *P. janea* trilobites zones) of Australia (Bengtson et al., 1990; Gravestock et al., 2001): Parara Limestone, Curramulka, CD-2 (drill core, east of the Curramulka Quarry), SYC-101 (drill core southwest of the town of Curramulka and 6 km northeast of the town of Minlaton in central Yorke Peninsula), Cur-D1B (drill core, 2.8 km east of Minlaton 2 in central Yorke Peninsula) and Horse Gully (Gravestock et al., 2001); Ajax Limestone, Mount Scott Range (Bengtson et al., 1990); Oraparinna Shale, Bunyeroo Gorge; Mernmerna Formation, Mulyungarie-2 and Yalkalpo-2, Arrowie Basin (Gravestock et al., 2001) and MMF section, Angorichina Station, Flinders Ranges (Topper et al., 2009).

Genus XIANFENGELLA He and Yang, 1982

**Type species.** *Xianfengella prima* He and Yang, 1982, Cambrian stage 2 (*Watsonella crosbyi* Zone), Meishucun, South China.

**Diagnosis.** See Devaere et al. (2013, p. 42).

*Xianfengella* sp. Figure 17.1-17

**Material.** Ten specimens including the five figured phosphatic internal moulds USTL3163-6, USTL3162-5, USTL3163-12, USTL3162-10 and USTL3162-3.

**Distribution.** Cerro Rajón section, sample R21 from unit 1 of the Puerto Blanco Formation.

**Description.** The internal moulds of the univalve conchs are cap-shaped and almost bilaterally symmetrical (Figure 17.3, 17.6, 17.9, 17.11). Conchs are longitudinally elongate (mean width/length of 0.58 with a maximum width of 415  $\mu\text{m}$ ) and low (mean height/length of 0.49 with a maximum length of 1025  $\mu\text{m}$  and height of 380  $\mu\text{m}$ ). The rounded (Figure 17.3, 17.6, 17.9, 17.11) to slightly angular apex (Figure 17.10-13, 17.16-17) is shifted toward the posterior side of the conch, curved downward up to half a whorl (Figure 17.2, 17.5, 17.10, 17.13) and stops slightly before the posterior apertural margin in one specimen (Figure 17.1-2), otherwise it overhangs it (Figure 17.5, 17.10, 17.13). In lateral

view, the anterior field (from the apex to the anterior margin) is moderately (Figure 17.2, 17.13) to strongly (Figure 17.5, 17.10) convex. The restricted posterior part (from the apex to the posterior margin) of the internal mould is preserved in two ways: either a wedge of phosphatic material fills the deeply concave, posterior, subapical field (Figure 17.1-8) or this part of the internal mould is broken (Figure 17.9-17). In the first case, a subapical notch, which length can be estimated at maximum 1/4 of the conch length, is present between the main part and the subapical part of the internal mould (Figure 17.1-8). This notch corresponds to a shell thickening/projection or fold, which subdivides the internal cavity into a subapical chamber and main chamber. In posterior or anterior view, the lateral fields are straight to slightly convex (Figure 17.3-4, 17.6, 17.11, 17.15-16). The aperture is regularly elliptically elongate (Figure 17.1, 17.6, 17.14), but posterolateral angularities are sometimes present (Figure 17.9-10). The apertural margin is planar (Figure 17.2, 17.10, 17.13) to slightly convex (Figure 17.5). The external surface of the internal mould is generally smooth, but polygonal imprints can rarely be observed (arrowed in Figure 17.14, 17.16).

**Comparisons.** The Mexican specimens are assigned to the genus *Xianfengella* because some specimens exhibit the typical notch of the internal mould corresponding to an internal projection of the shell. Such internal projection of the shell in a cap-shaped mollusc has also been described in *Merismoconcha* Yu, 1979. In *Merismoconcha*, the notch is narrow, transverse and located anteriorly to the apex (see figure 16.7-12 in Devaere et al., 2013). In the Mexican specimens, the notch is deep and posterior to the apex, a characteristic of *Xianfengella*. The Mexican specimens are not assigned to either *Xianfengella prima* He and Yang, 1982, from the Cambrian stage 2 or *Xianfengella yatesi* Parkhaev in Gravestock et al., 2001, from the late Cambrian stage 3 to 4, the supposedly valid species of *Xianfengella*, because the distinction between the two species is questionable given the material available. Parkhaev (in Gravestock et al., 2001, p. 181) argues that *Xianfengella yatesi* “differs from the type one by more gentle transition of the posterior field into lateral fields and by more rounded outlines of the aperture, without posterolateral angularities.” The Mexican material assigned to *Xianfengella*, which was recovered from a single bed, displays specimens with either sharp transition of the posterior field into lateral fields and posterolateral angularities of the aper-

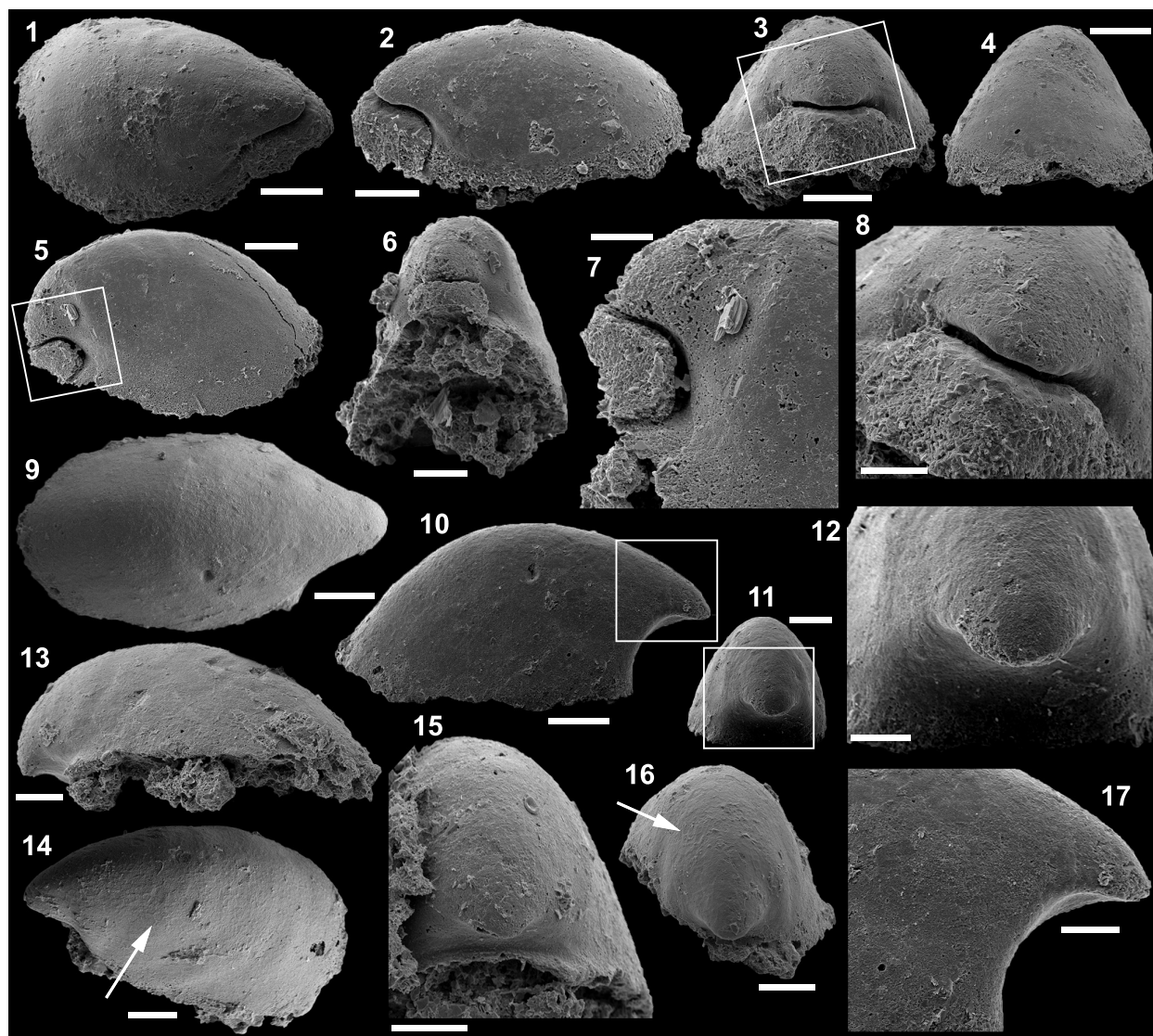


**FIGURE 17.** Internal moulds and coatings of *Xianfengella* sp. from the Puerto Blanco Formation of Cerro Rajón, Sonora, Mexico. 1-4, 8. Specimen USTL3163-6 from sample R21: 1. Upper view; 2. Lateral view; 3. Posterior view, area in the square is magnified in 8; 4. Anterior view; 8. Detail of the subapical notch in the internal mould. 5-7. Specimen USTL3162-5 from sample R21: 5. Lateral view, area in the square is magnified in 7; 6. Subapical view; 7. Detail of the subapical notch and wedge. 9-12, 17. Specimen USTL3163-12 from sample R21: 9. Upper view; 10. Lateral view, area in the square is magnified in 17; 11. Posterior view, area in the square is magnified in 12; 12, 17. Details of the apical region. 13, 15. Specimen USTL3162-10 from sample R21: 13. Lateral view; 15. Posterior view. 14, 16. Specimen USTL3162-3 from sample R21: 14. Upper lateral view, arrow pointing polygonal imprints on the internal mould; 16. Posterior view, arrow pointing polygonal imprints on the internal mould. Scale bars are: 7-8, 12, 17, 50  $\mu\text{m}$ ; 1-6, 9-11, 13-16 100  $\mu\text{m}$ .

ture outlines (Figure 17.9-12) or gentle transition of the posterior field into lateral fields and rounded outlines of the aperture (Figure 17.6, 17.13-16).

Order PELAGIELLIDA MacKinnon, 1985  
 Family PELAGIELLIDAE Knight, 1956  
 Genus PELAGIELLA Matthew, 1895

**Type species.** *Cyrtolites atlantoides* Matthew, 1894, Cambrian stage 3?, New Brunswick, Canada.

**Diagnosis.** See Kouchinsky et al. (2011, p. 135).

*Pelagiella* sp.  
 Figure 18.1-27

**Material.** Twenty-five specimens including figured USTL3168-2, USTL3175-1, USTL3177-6,

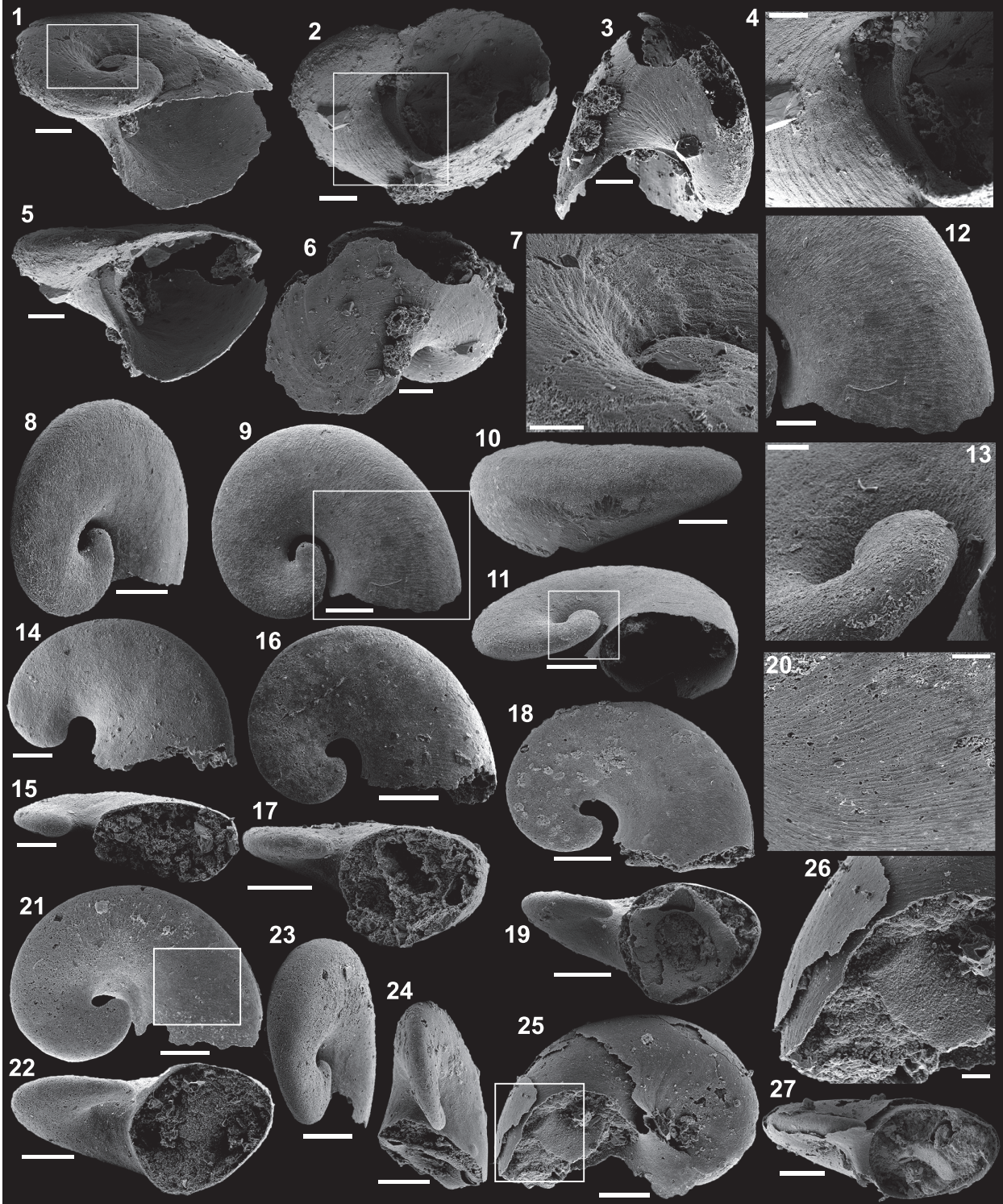


FIGURE 18. Caption on next page.

USTL3175-6, USTL3177-10, USTL3175-3 and USTL3177-8.

**Distribution.** Cerro Rajón section, samples R53, R54, R63 and R64 from unit 2 of the Puerto Blanco Formation.

**Description.** The univalve conchs (preserved as phosphatic replaced shell, Figure 18.1-7, or as phosphatic internal moulds and coatings, Figure 18.8-24, with phosphatic external coating, Figure 18.25-27) are rapidly expanding, dextrally coiled (Figure 18.1, 18.11, 18.15, 18.17, 18.19, 18.22-24, 18.27) with 0.5 to 2 whorls (mean whorl numbers 1.3; Figure 18.1, 18.9, 18.14, 18.16, 18.18, 18.21). On the adapical side, the spire is flat and aligned with the adapical apertural margin, whereas the abapical parts of the whorls are strongly convex (Figure 18.5, 18.10-11, 18.15, 18.17, 18.19, 18.22, 18.27). Conchs are elongated in the plane of the flat adapical surface (at 0.49 on average) and relatively low (at 0.71 on average). The whorls cross-section, best observed at the flared aperture, is elliptical (Figure 18.15) to subtriangular with a slight angle in the abapical apertural margin (Figure 18.5) depending on the size of the conch. The apex is bulbous (Figure 18.9, 18.13-14, 18.16, 18.18, 18.21, 18.24). In the specimen preserved as shell replacement, the subumbilical apertural margin exhibits a comarginal furrow which starts at the umbilicus and ends at the angle of the abapical apertural margin (Figure 18.2, 18.4-5). In this specimen, the internal and external surfaces of the shell are covered with striations perpendicular to the apertural margin (Figure 18.1-4, 18.7). The external surfaces of internal moulds have faint, transverse (i.e., parallel to the apertural margin) striations (Figure 18.9, 18.12, 18.16, 18.20).

**Comparisons.** The specimens referred herein to *Pelagiella* sp. are most probably equivalent to the

specimens described and figured by McMenamin (1984), although the preservation of the figured specimens is very poor. The specimen USTL3168-2 (Figure 18.1-7) is similar to *Pelagiella subangulata* (Tate, 1982) because it exhibits a comparable size, cross-section of the aperture (with a small angle) and a furrow parallel to the apertural margin below the umbilicus (as seen in specimens assigned to *P. subangulata* in figures 168A, B from Bengtson et al., 1990 and plate XLV, figures 1-2 from Gravestock et al., 2001 and figure 8G from Skovsted, 2004). It is not possible to confidently assign the specimen to this species because such comparable characters have been reported by Kouchinsky et al. (2011) in *Pelagiella* sp. cf. *Cambretina mareki* Horný, 1964, and *Pelagiella* sp. cf. *Costipelagiella zazvorkai* Horný, 1964 (although the angle of the apertural margin forms a very long auricle in *Pelagiella* sp. cf. *C. mareki* that is not seen in the Mexican specimens). The differentiation of the specimens described by Kouchinsky et al. (2011) is mainly based on “the reticulate ornamentation of the shell exterior” and “comarginal costae,” which both contrast with the “closely spaced rounded costae that meet at an acute angle on the whorl periphery [...] and which may interfere with the growth lines to produce a series of regularly arranged nodes on some parts of the shell” of *P. subangulata* (Bengtson et al., 1990). The ornamentation of the external surface of the shell is different in the Mexican specimens. The shells preserved by calcium phosphate replacement possess only the outer shell layer. This outer shell layer is composed of fibrous crystals arranged perpendicular to the growth lines (Bengtson et al., 1990).

The other specimens are preserved as phosphatic internal moulds in which comarginal lines

**FIGURE 18** (figure on previous page). *Pelagiella* sp. from the Puerto Blanco Formation of Cerro Rajón, Sonora, Mexico. 1-7. Specimen USTL3168-2 (shell replacement) from sample R54: 1. Oblique apertural view, area in the square is magnified in 7; 2. Apertural view, area in the square is magnified in 4; 3. Abapical view; 4. Detail of the subumbilical furrow and of the radial shell striations; 5. Apertural view showing the triangular apertural cross-section; 6. Abapical view with radial striations visible; 7. Detail of the apex and umbilicus. 8-13. Specimen USTL3175-1 (internal coating) from sample R63: 8. Oblique apical view; 9. Apical view, area in the square is magnified in 12; 10. Abapertural view; 11. Apertural view, area in the square is magnified in 13; 12. Detail of the surface of the internal coating with comarginal striations; 13. Detail of the bulbous apex. 14-15. Specimen USTL3177-6 (internal mould and coating) from sample R63: 14. Apical view; 15. Apertural view. 16-17. Specimen USTL3175-6 (internal mould and coating) from sample R63: 16. Apical view; 17. Apertural view. 18-19, 24. Specimen USTL3177-10 (internal mould and coating) from sample R63: 18. Apical view; 19. Apertural view; 24. Lateral view. 20-23. Specimen USTL3175-3 (internal mould and coating) from sample R63: 20. Detail of the internal coating with comarginal striations; 21. Apical view, area in the square is magnified in 20; 22. Apertural view; 23. Lateral view. 25-27. Specimen USTL3177-8 (internal mould and coating, partial external coating) from sample R63: 25. Abapical view, area in the square is magnified in 24; 26. Detail of the external coating and internal mould and coating; 27. Apertural view. Scale bars are: 13, 20, 26, 50  $\mu\text{m}$ ; 4, 7, 12, 14-15, 100  $\mu\text{m}$ ; 1-3, 5-6, 8-11, 16-19, 21-25, 27, 200  $\mu\text{m}$ .

reproduce the inner layer of the shell; these are interpreted as comarginally arranged fibrous crystals (Bengtson et al., 1990). One specimen (USTL3177-8; Figure 18.25-27) also preserved a phosphatic, smooth, external coating of the shell. It is difficult to compare the Mexican specimens to other *Pelagiella* species because (1) the systematics of the genus is poorly defined (see Parkhaev, 2004 for a list of included species; it should be noted that most of those species have been poorly figured and described and they could probably be greatly reduced) and (2) they do not exhibit many discriminating characters (e.g., variable cross-section, number of whorls). The number of whorls and cross-sections are probably related to the size of the specimens. The first specimen (USTL3168-2; Figure 18.1-7), most comparable to *Pelagiella subangulata*, is much larger than the other specimens (from 1.4 to 2.5 larger); the smaller specimens may represent earlier ontogenetic stages.

Class BIVALVIA Linnaeus, 1758

Order uncertain

Family FORDILLIDAE Pojeta, 1975

Genus POJETAIA Jell, 1980

**Type species.** *Pojetaia runnegari* Jell, 1980, Cambrian stage 4, Horse Gully, South Australia.

**Diagnosis.** See Elicki and Gürsu (2009, p. 281).

*Pojetaia* sp. Figure 19.1-18

**Material.** Nine specimens including the figured phosphatic internal mould USTL3171-4 and the two figured phosphatic internal and external coatings of disarticulated valves USTL3175-2, USTL3176-7 and USTL3176-5.

**Distribution.** Cerro Rajón section, samples R54 and R63 from unit 2 of the Puerto Blanco Formation.

**Description.** The internal moulds of the conch correspond to the infill of two equal valves, which are subovate (mean height/length of 0.73 with a maximum length of 2180 µm and a maximum height of 1680 µm), slightly elongate anteriorly, in outline (Figure 19.1-3). Similar observations are made on disarticulated valves although their frequent breakage makes the identification of the exact outline difficult (Figure 19.5-6, 19.11, 19.16). The conch is slightly higher in the posterior part and the posterior margin is largely convex, whereas the anterior margin is more angular (Figure 19.3). A structure comparable to an auricle is observed on the posterior part of the conch (only visible in Figure 19.3 otherwise broken in disarticulated valves). The umbones are prosogyre (Figure 19.5) and located

approximately in the medial area of the dorsum (at ~53% of the total length to the anterior margin in Figure 19.3). In dorsal view, the dorsal margin is straight and the conch has an egg-shape (Figure 19.3), the maximum width being located slightly posteriorly to the umbo (of 970 µm, mean width/length of 0.60). The hinge has only one tooth in each valve and corresponding socket (Figure 19.3-4, 19.11, 19.17). The disarticulated valves are preserved as empty, thin coatings of the shell (internal and external; Figure 19.5-18). The void between the external and internal coatings corresponds to the dissolved shell, which was ~25 µm in thickness (Figure 19.5, 19.7) and perforated by microbes as attested by the presence of branching phosphatic filaments (Figure 19.16, 19.18). The external coating replicates the ornaments of the shell, which correspond to fine, dense, comarginal growth lines (Figure 19.6, 19.10, 19.12-13); low, radial, antero-dorsal ribs are also present (Figure 19.1-3). Muscle scars and traces of the ligament are not observed.

**Comparisons.** The Mexican specimens are assigned to *Pojetaia* as they exhibit most of the typical features of this genus (size, height/length, position and characters of the umbo, general shape, outline and outer ornamentation). However, the preservation and number of specimens is too poor to conclude on the species assignment. The Mexican specimens also exhibit a feature, which is generally observed in the other fordillid genus *Fordilla* Barrande, 1881: the hinge contains only two teeth, one on each valve, although specimens of *Pojetaia* with only two teeth have also been reported (e.g., specimen PIN no. 4664/0473 in figure 3.4.C of Parkhaev, 2008).

Phylum ARTHROPODA Siebold and Stannius, 1845

Class uncertain

Order BRADORIIDA Raymond, 1935

Family and genus uncertain

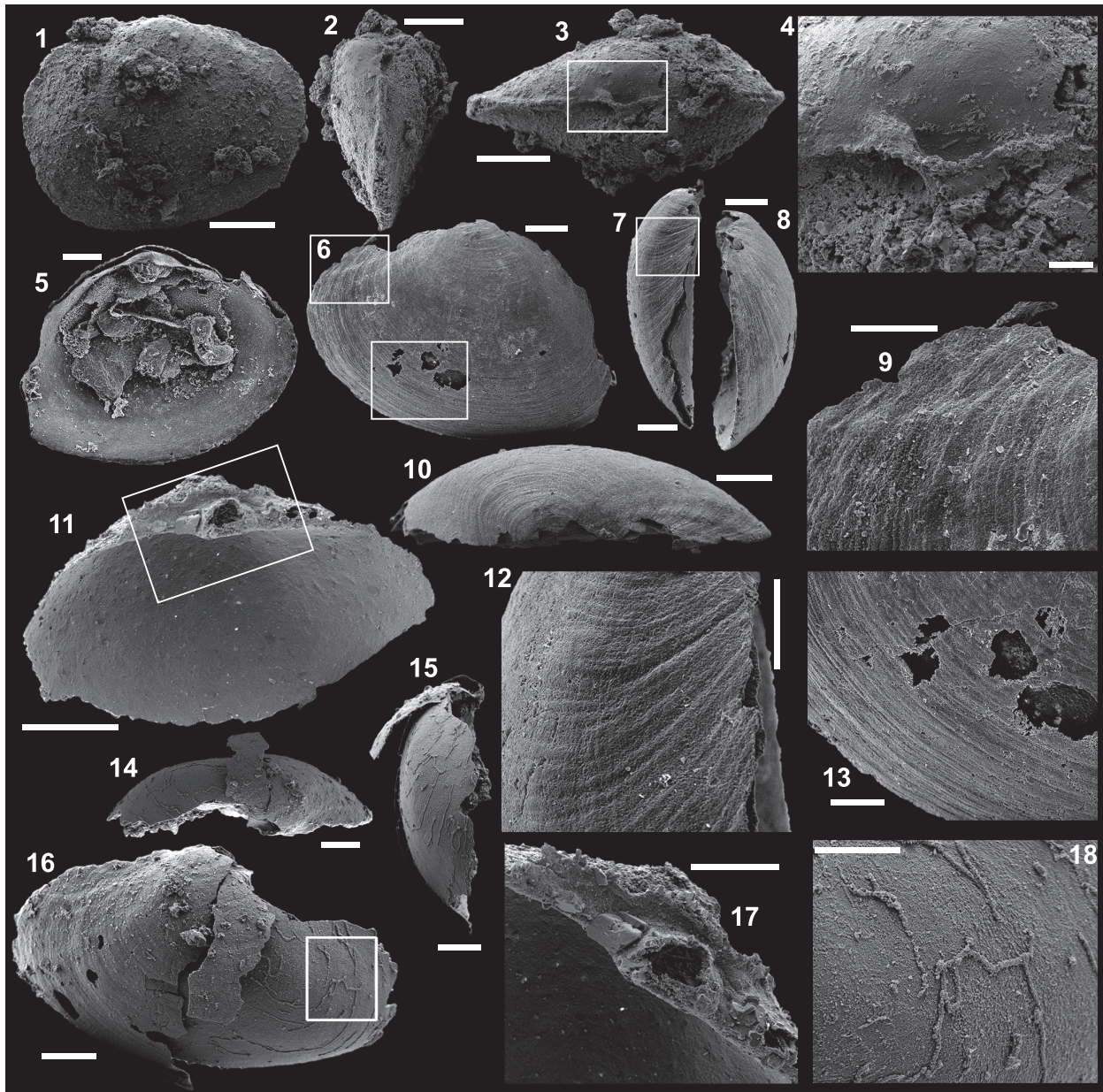
Bradoriid sp.

Figure 20.1-9

**Material.** One disarticulated figured valve USTL3182-4.

**Distribution.** Cerro Rajón section, sample R66 from unit 2 of the Puerto Blanco Formation.

**Description.** The valve is hemispherical in outline (Figure 20.1) and moderately inflated (Figure 20.2, 20.5-7). The hinge line is only partially preserved and the preserved part is straight (Figure 20.1). The free margin is strongly curved with a well-developed rim covered by a polygonal pattern (Fig-



**FIGURE 19.** *Pojetaia* sp. from the Puerto Blanco Formation of Cerro Rajón, Sonora, Mexico. 1-4. Specimen USTL3171-4 (internal mould) from sample R54: 1. Right lateral view; 2. Anterior view; 3. Dorsal view, area in the square is magnified in 4; 4. Detail of the hinge showing the two teeth and associated sockets (one on each valve). 5-10, 12-13. Specimen USTL3175-2 (coating of disarticulated left valve) from sample R63: 5. Internal view, note the prosogyre umbo; 6. External view with the fine, dense comarginal, growth lines, area in the upper left square is magnified in 9 and area in the lower right square is magnified in 13; 7. Posterior view, area in the square is magnified in 12; 8. Anterior view; 9. Detail of the growth lines and the radial ribs of the anterior area; 10. Dorsal view; 12, 13. Details of the growth lines. 11, 17. Specimen USTL3176-7 from sample R63 (coating): 11. Internal view, area in the square is magnified in 17; 17. Detail of the hinge with the tooth. 14-16, 18. Specimen USTL3176-5 from sample R63 (coating): 14. Dorsal view; 15. Posterior view; 16. External view with external coating preserved in the anterior area (commarginal growth lines and radial ribs) and internal coating in the posterior area with branching microbial filaments, area in the square is magnified in 18; 18. Details of the microbial filaments. Scale bars are: 4, 9, 12-13, 17-18, 100 µm; 5-8, 10-11, 14-16, 200 µm; 1-3, 500 µm.

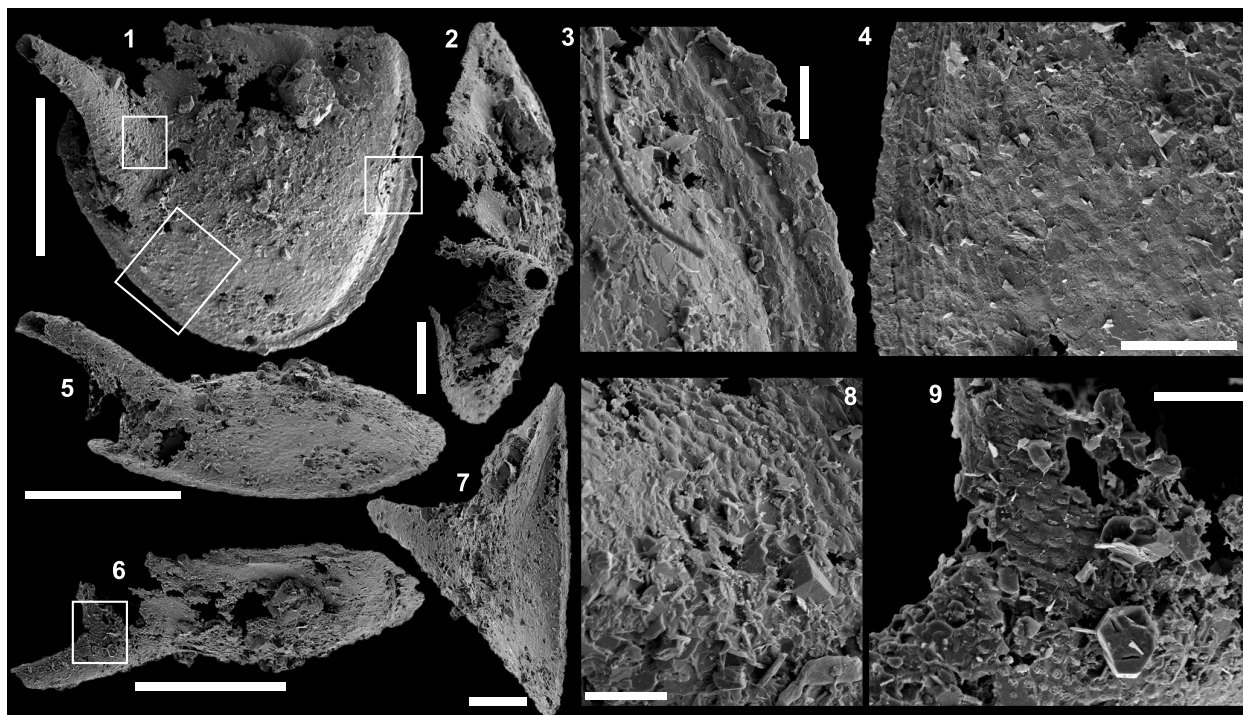


**FIGURE 20.** Valve of Bradoriid sp. from the Puerto Blanco Formation of Cerro Rajón, Sonora, Mexico. 1-9. Specimen USTL3182-4 from sample R66: 1. External view, area in the right square is magnified in 3, area in the lower left square is magnified in 4 and area in the upper left square is magnified in 8; 2. Dorso-lateral view; 3-4. Details of the rim; 5. Ventral view; 6. Dorsal view, area in the square is magnified in 9; 7. Lateral view; 8-9. Details of the pustulose ornamentation. Scale bars are: 3, 8-9, 50  $\mu\text{m}$ ; 4, 100  $\mu\text{m}$ ; 2, 7, 200  $\mu\text{m}$ ; 1, 5-6, 500  $\mu\text{m}$ .

ure 20.1, 20.3-4). A long spine is present near the margin of one side of the valve (Figure 20.1, 20.5-7). The surface of the valve around the spine bears a pustulose ornamentation (Figure 20.8-9).

**Remarks.** Due to the incomplete preservation of the hinge line, it is not possible to suggest any assignment within the order Bradoriida.

Phylum LOBOPODIA Snodgrass, 1938  
Class XENUSIA Dzik and Krumbiegel, 1989  
Order SCLERONYCHOPHORA Hou and Bergström, 1995

Family EOCONCHARIIDAE Hao and Shu, 1987  
Genus MICRODICTYON Bengtson, Matthews and Missarzhevsky in Missarzhevsky and Mambetov, 1981

**Type species.** *Microdictyon effusum* Bengtson, Matthews and Missarzhevsky in Missarzhevsky and Mambetov, 1981, Cambrian stage 3 (*Rhombocorniculum cancellatum* Zone), Maly Karatau, Kazakhstan.

**Diagnosis.** See Zhang and Aldridge (2007, p. 403) for the complete organism and Bengtson et al. (1990, p. 333) for the sclerites.

*Microdictyon multicavus* (McMenamin, 1984)  
Figure 21.1-20

1984 *Microdictyon multicavus* n. sp.; McMenamin, p. 80, pl. 13, figs. 1, 2, 4.

1986 *Microdictyon* cf. *rhomboidale*; Bengtson et al., p. 102, 104, fig. 7.

**Material.** Eight specimens including the complete figured sclerite USTL3180-2 and the three incomplete figured phosphatic sclerites USTL3176-4, USTL3177-3 and USTL3179-2.

**Distribution.** Cerro Rajón section, samples R60, R63, R65, R69 and R71 from units 2 and 3 of the Puerto Blanco Formation.

**Description.** The complete sclerite measures up to 2320  $\mu\text{m}$  and is bilaterally symmetrical with a complexly subtriangular outline (Figure 21.1, 21.6). A reentrant of 1/8 of the maximum size of the sclerite is observed, which is opposite to an acute protrusion (Figure 21.1, 21.6). From the reentrant to the protrusion, the outline draws three small angular (of  $\sim 90^\circ$ ) protrusions separated by two curvatures (convex toward the centre of the sclerite; Figure 21.1, 21.6). The edge of the sclerite exhibits a peripheral girdle, which corresponds to a flat (Figure 21.2, 21.7) or laminated surface (Figure

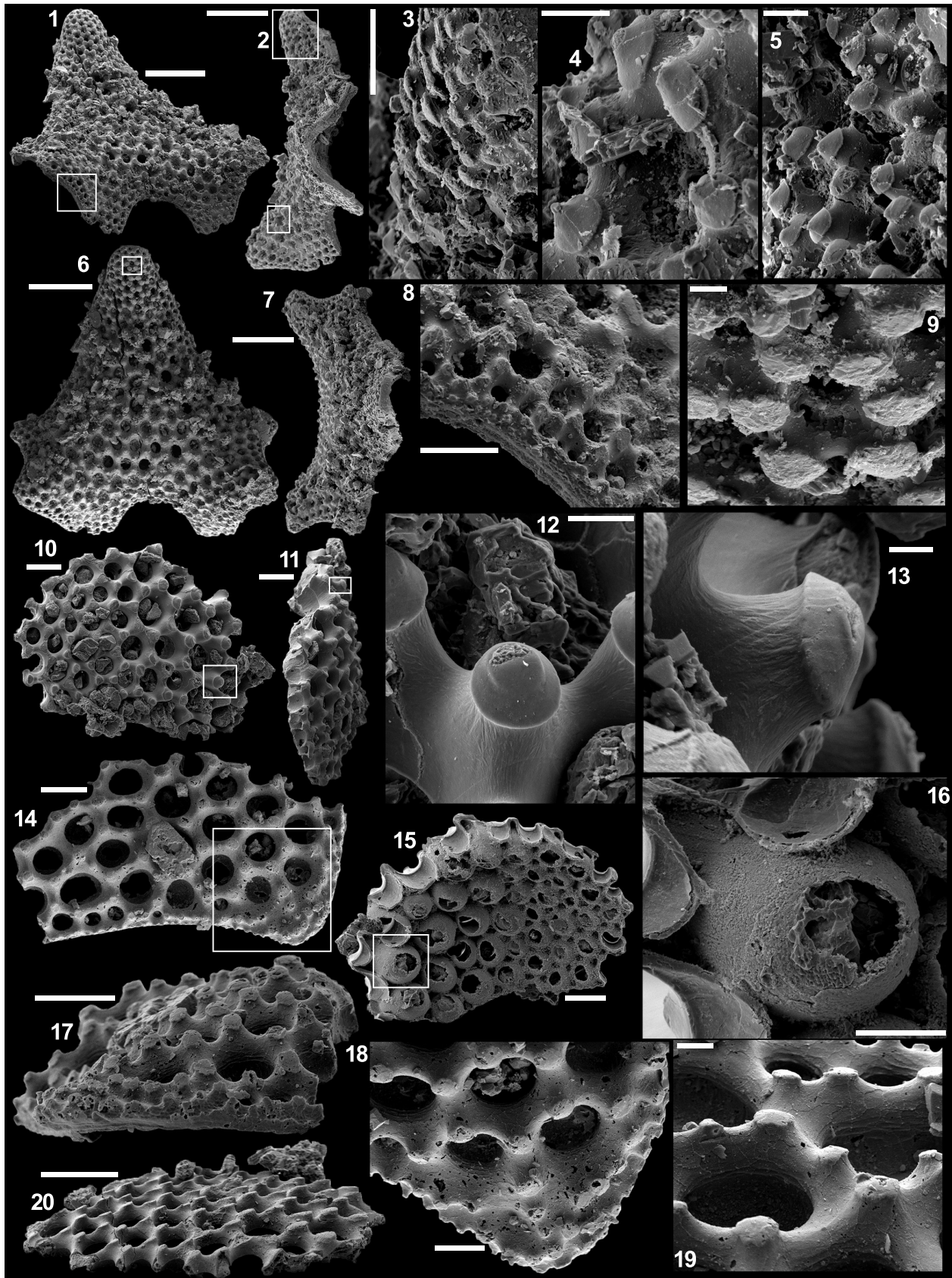


FIGURE 21. Caption on next page.

21.8, 21.17). A small protrusion and the girdle are observed in one incomplete specimen, which preserves the edge of the sclerite (Figure 21.14, 21.17-18), whereas the other incomplete specimens correspond to more central pieces of the sclerite, without the edge (Figure 21.10-11, 21.15, 21.20). In lateral view, the complete sclerite is undulated (Figure 21.2, 21.7), whereas the incomplete specimens are flat (Figure 21.11, 21.20) to concavo-convex (Figure 21.17). The sclerites themselves consist of a meshwork of holes or depressions surrounded by shell material. The holes/depressions are circular to ovate in external view (Figure 21.6, 21.10, 21.14) and range in diameter from 13 to 187  $\mu\text{m}$ , with a decrease of diameter from the centre to the periphery of the sclerite (Figure 21.6, 21.14). Holes extend as bulbous structures below the external surface of the sclerite (Figure 21.11, 21.15-16). The basal part of holes is partially closed by a hemispherical structure with an opening, which corresponds to the continuation of the phosphatic layer constituting the sclerite (Figure 21.15-16). The opening in the hemispherical basal structure is narrow to wide (Figure 21.15). Each hole/depression is surrounded by five to seven nodes (Figure 21.4-5, 21.8-9, 21.18-19). The diameter of the nodes increases from the edge to the centre of the sclerite and varies from 6 to 75  $\mu\text{m}$  (Figure 21.1, 21.6, 21.8, 21.14, 21.17-48). Smaller nodes line the peripheral girdle (Figure 21.1, 21.8, 21.14, 21.18). The extremity of the nodes sometimes exhibits a cap with a subcentral apex (Figure 21.4-5, 21.12-13) or a flat cap (Figure 21.9, 21.17-19), also called short, wedge-shaped nodes by Wotte and Sundberg (2017) or no cap and just a flat surface (Figure 21.11, 21.20) also called simple, smooth nodes by Wotte and Sundberg (2017). In the complete specimen, the nodes with a flat top are the most peripheral and, towards

the centre of the sclerite, the nodes first exhibit a flat cap and then a pointed cap (Figure 21.3).

**Comparisons.** We agree with Topper et al. (2011) that intraspecific and ontogenetic variation have to be considered for formal taxonomic identification within the group. Such information is not accessible from the Mexican material. However, the morphology of the disarticulated sclerites recovered from the Puerto Blanco Formation is so unique that assignment to the species newly defined by McMenamin (1984) *Microdictyon multicavus* and referred to as *Microdictyon cf. rhomboidale* in Bengtson et al. (1986) based on disarticulated sclerites is proposed here. All the specimens recovered in the Cerro Rajón are attributed to *M. multicavus*, although they may exhibit different nodes. The specimens with flat top nodes (Figure 21.14-20) are interpreted to correspond to peripheral-most parts of the sclerites, which exhibit also flat top nodes in the complete specimen (Figure 21.4, 21.8-9).

Various similarities between *M. multicavus* and *M. rhomboidale* (or referred to as *Microdictyon aff. rhomboidale* as in Zhang and Aldridge, 2007 and *Microdictyon cf. M. rhomboidale* in Kouchinsky et al., 2015) are observed: in both species, the nodes have a subcentral apex, the outer girdle is covered with reduced nodes, and the outline is rhombic with a reentrant at one of the sides between two protrusions. However, they also differ. The basal terminations of the holes differ: they are wide opened in *M. rhomboidale*, *M. aff. rhomboidale* and *Microdictyon cf. M. rhomboidale* and almost closed by a hemispherical, pierced structure in *M. multicavus* and completely closed in *M. cf. rhomboidale*. This difference is most probably related to variation in preservation (complete breakage of the basal closure in *M. rhomboidale* and *M. aff. rhomboidale* and partial breakage in *M. multicavus*). In addition, *M. rhomboidale* and *M. aff.*

**FIGURE 21** (figure on previous page). *Microdictyon multicavus* McMenamin, 1984, from the Puerto Blanco Formation of Cerro Rajón, Sonora, Mexico. 1-9. Specimen USTL3180-2 from sample R69: 1. Oblique view, area in the square is magnified in 8; 2. Lateral view, upper lower area in the square is magnified in 3 and lower area in the square is magnified in 4; 3. Detail of the node extremities from the edge to the centre of the sclerite (flat, flat cap, cap with subcentral apex); 4, 5. Detail of the caped-nodes with a subcentral apex; 6. External view, area in the square is magnified in 9; 7. Lateral view; 8. Detail of the peripheral girdle; 9. Detail of the nodes with a flat cap. 10-13, 15-16. Specimen USTL3179-2 from sample R65: 10. External view, area in the square is magnified in 13; 11. Lateral view, area in the square is magnified in 12; 12, 13. Detail of a caped-node with a subcentral apex; 15. Internal view, area in the square is magnified in 16; 16. Detail of the basal termination of a hole/depression. 14, 17-19. Specimen USTL3177-3 from sample R63: 14. External view, area in the square is magnified in 18; 17. Oblique view; 18. Detail of the peripheral girdle; 19. Detail of the holes and surrounding nodes. 20. Lateral view of specimen USTL3176-4 from sample R63. Scale bars are: 9, 13, 19, 20  $\mu\text{m}$ ; 4-5, 12, 18, 50  $\mu\text{m}$ ; 3, 8, 14, 16-17, 100  $\mu\text{m}$ ; 10-11, 15, 200  $\mu\text{m}$ ; 1-2, 6-7, 500  $\mu\text{m}$ .

*rhomboidale* lack the large protrusion described in *M. multicavus* and *M. cf. rhomboidale*. However, the former taxa mainly correspond to specimens of relatively small size compared to the size of the specimens attributed to the latter. Therefore, it is possible that the specimens described as *M. rhomboidale* and *M. aff. rhomboidale* represent early ontogenetic stages of the sclerites attributed to *M. multicavus* and *M. cf. rhomboidale* in which the protrusion is not yet grown, as already suggested in Bengtson et al. (1986). It should be noted also that specimens attributed to *M. cf. rhomboidale* by Bengtson et al. (1986) exhibit other, complex morphologies. Therefore, *M. rhomboidale*, *M. aff. rhomboidale* and *M. cf. rhomboidale* are most probably junior synonyms of *M. multicavus*, but we lack sufficient material from Mexico and a revision of previously published specimens is required prior definite conclusion on the synonymy. Recently, Wotte and Sundberg (2017) described various small and poorly preserved fragments of sclerites that they assign to *Microdictyon*. The definition of the two new species *M. montezumaensis* Wotte and Sundberg, 2017, and *M. cuneum* Wotte and Sundberg, 2017, is based on the ornamentation of the nodes. However, the new species are defined based only on the study of fragments which have proven to be of limited use. The complete sclerite of *M. multicavus* from Cerro Rajón described herein exhibits variable node ornamentations. The complete sclerite includes the “simple, smooth nodes” of *M. montezumaensis* and the “short, wedge-shaped nodes” of *M. cuneum*. The fragments assigned to *M. rhomboidale* Bengtson et al., 1986, by Wotte and Sundberg (2017) bear the “mushroom-shaped with distinct brim” nodes with a subcentral apex also observed in *M. multicavus*. All the fragments only differ in the basal terminations of the holes, probably for the same reasons as *M. rhomboidale* and *M. aff. rhomboidale*. So, the two new species and the fragments assigned to *M. rhomboidale* by Wotte and Sundberg (2017) are most probably synonyms of *M. multicavus*. All the fragments described by Wotte and Sundberg come from the same sample (M5), supporting their assignment to the same species. With this example, the use of fragments of sclerites for the definition of new species of *Microdictyon* is strongly questioned. We consider that the specimens they describe as *Microdictyon* sp. should not be assigned to *Microdictyon*, but instead considered as an indeterminate fossil, probably of archaeocyathans or other sponges. Such fragments have also been recovered from the Cerro Rajón section and

are described later. Fragments of sclerites assigned to *Microdictyon cf. depressum* Bengtson in Bengtson et al. (1990) by Skovsted (2006) exhibit nodes with an inclined flat surface that are also observed in the specimens of *M. multicavus* presently described. This observation suggests that the specimens of Skovsted (2006) might represent synonyms of *M. multicavus* although complete sclerites are required to finally conclude on this synonymy. Finally, no sclerites with the complex outline of *M. multicavus* have been recovered in articulated specimens.

**Other occurrences.** For *Microdictyon cf. rhomboidale*: Cambrian stage 3 (*Fallotaspis* and *Nevadella* zones) of Canada, Sekwi Formation, Mackenzie Mountains, British Columbia (Bengtson et al., 1986). For *M. rhomboidale*: Cambrian stage 3 (*Rhombicorniculum cancellatum* Zone or *Ushbaspis limbata* and *Hebediscus orientalis* zones) of Kazakhstan, Shabakty Formation, River Uchbas, Maly Karatau and of Siberia, Bograd, Bateny Hills, Kuznetskij Alatau Range (Bengtson et al., 1986). For *M. aff. rhomboidale*: Cambrian stage 3 (*Eoredlichia* – *Wittungaspis* trilobite Zone) of South China, Zhongbao, Zhenping County, Shaanxi Province (Zhang and Aldridge, 2007). For *Microdictyon cf. M. rhomboidale*: Cambrian stage 3 (middle *Judomia* trilobite Zone) of Siberia, Emyaksin Formation, Bol’shaya Kuonamka River (Kouchinsky et al., 2015).

Phylum BRACHIOPODA Duméril, 1806

Subphylum LINGULIFORMEA Williams, Carlson, Brunton, Holmer and Popov, 1996

Class PATERINATA Williams, Carlson, Brunton, Holmer, and Popov, 1996

Order PATERINIDA Rowell, 1965

Superfamily PATERINOIDEA Schuchert, 1893

Family uncertain

Genus RAJONIA McMenamin, 1984

**Type species.** *Rajonia ornata* McMenamin, 1984, Cambrian stage 3, Sonora, Mexico.

**Diagnosis.** See McMenamin (1984, p. 53).

**Remarks.** Unlike McMenamin (1984), we herein formally assign *Rajonia* to the class Paterinata, the order Paterinida and the superfamily Paterinoidea based on the new data on the posterior margin. However, the classification of the Paterinoidea at the family level requires a revision, more particularly for the Cryptotretidae as suggested by Topper et al. (2013). Therefore, the assignment of *Rajonia* is left open at the family level.

*Rajonia ornata* (McMenamin, 1984) Figure 22.1-12

1984 *Rajonia ornata* n. sp.; McMenamin, p. 54, pl. 16, figs. 1-4, pl. 18, fig. 5.

**Material.** Six specimens including the figured ventral valve USTL3179-1 and the two figured fragments of valves USTL3179-5 and USTL3179-3.

**Distribution.** Cerro Rajón section, sample R65 from unit 2 of the Puerto Blanco Formation.

**Description.** The ventral valve is bilaterally symmetrical, semi-circular (maximum observed width 2400  $\mu\text{m}$ , maximum length 1190  $\mu\text{m}$ ) in outline (Figure 22.1, 22.5). The valve is moderately convex in lateral view, the maximum convexity is at the umbo and the post-larval shell tends to be flat towards the commissure (Figure 22.5). The larval shell is subcircular (mean diameter of 270  $\mu\text{m}$ ), bulbous and smooth (Figure 22.1, 22.4). The post larval shell external ornament is constituted of high and coarse, concentric filae with variable width and separated by variable distance (Figure 22.1, 22.3, 22.8-14). The concentric filae are subcircular in cross-section (Figure 22.9-10). The interval between successive filae is low, concave and covered by poorly defined, radial ribs (Figure 22.1, 22.3, 22.9, 22.12). The hinge line is straight (Figure 22.5). The ventral interarea is catacline (Figure 22.2, 22.5-7) and the triangular delthyrium is wide (Figure 22.6-7). A laminar homeodelthyidium (?) or part of the dorsal valve is present (Figure 22.6-7). No muscle and mantle canal scars can be observed as the internal surface of the valve is covered with phosphatic grains and spheres (~10  $\mu\text{m}$  in diameter) either isolated or organized in clusters (Figure 22.5). The shell is constituted of a single, relatively thick (~40  $\mu\text{m}$ ) phosphatic layer (Figure 22.5) although laminations are possibly present below the umbo (Figure 22.7).

**Comparisons.** See McMenamin (1984).

Class LINGULATA Gorjansky and Popov, 1985

Order LINGULIDA Waagen, 1885

Family ZHANATELLIDAE Koneva, 1986

Genus EOBOLUS Matthew, 1902

**Type species.** *Obolus triparilis* Matthew, 1902, Drumian (*eteminicus* Zone), Cape Breton, Canada.

**Diagnosis.** See Balthasar (2009, p. 416-417).

*Eoobolus* sp. Figure 22.13-16

**Material.** One ventral valve USTL3182-3.

**Distribution.** Cerro Rajón section, sample R66 from unit 3 of the Puerto Blanco Formation.

**Description.** The ventral valve is evenly convex (Figure 22.14, 22.16) and teardrop shaped in outline with an apical angle of 75° (Figure 22.13-14). The pseudointerarea is constituted of a prominent triangular duplicature and is orthocline (Figure

22.13). The duplicature is composed of a median, deep, wide, funnel-shaped pedicle groove flanked by two raised propareas with marked flexure lines (Figure 22.13). No muscle and mantle canal scars can be observed on the internal surface of the valve (Figure 22.13). The external surface exhibits comarginal growth lines and small, irregular pustules (Figure 22.16).

Fossil indet. Figure 23.1-10

**Material.** Tens of fragments including the figured specimens USTL3174-12, USTLUSTL3174-13, USTL3174-11, USTL3176-11.

**Distribution.** Cerro Rajón section, samples R56 and R63 from unit 2 of the Puerto Blanco Formation.

**Description.** These indeterminate fossils consist of a relatively flat, but slightly undulating, meshwork of phosphatic, interconnected rods (Figure 23.1-2, 23.5, 23.9) that is, in some specimens, surrounded by a thin phosphatic layer (Figure 23.3-4, 23.6-8, 23.10). The meshwork consists of coarsely phosphatic rods (Figure 23.9-10) interconnected around circular holes of variable diameter. In some specimens, large holes alternate relatively regularly with smaller ones (Figure 23.1, 23.5), whereas in others, large holes are dominant and smaller ones are only rarely intercalated (Figure 23.3, 23.6). The phosphatic outer layer is very thin and the surface is smooth to slightly granular (Figure 23.3, 23.8). In some areas, the meshwork is fused to the outer layer (Figure 23.4, 23.10).

**Comparisons.** Fragments of plates belonging to the same indeterminate species were also reported from unit 2 of the Puerto Blanco and identified as genus and species indeterminate D by McMenamin (1984). Wotte and Sundberg (2017) report similar fossils in the Montenegro Member of the Campito Formation, Montezuma Range, Nevada. They figured three fragments of the meshwork with holes of variable diameter. They assigned the specimens to *Microdictyon* sp. However, neighbouring holes of the plates of *Microdictyon* have a similar diameter, and the diameter of the holes only varies on a gradient, increasing from the rim toward the centre of the sclerite, which is not the case in the plates described herein and in Wotte and Sundberg (2017). These plates are also completely devoided of the nodes found in *Microdictyon*. Finally, the specimens from the Puerto Blanco Formation also exhibit an outer layer, which is absent from *Microdictyon* sclerites. Therefore, these plates should not be assigned to *Microdictyon* sp., but are considered here as indeterminate

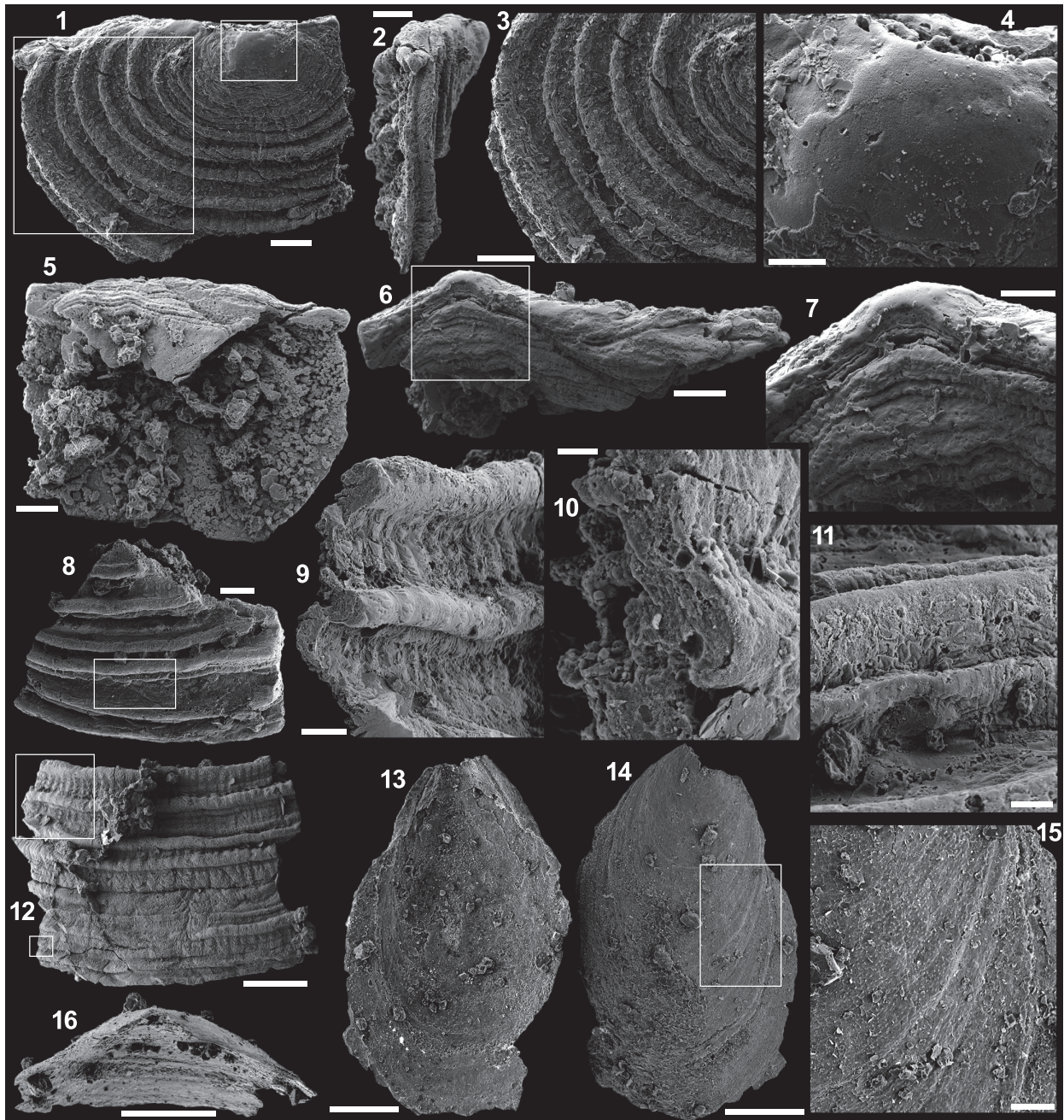


**FIGURE 22.** Brachiopods from the Puerto Blanco Formation of Cerro Rajón, Sonora, Mexico. 1-14. *Rajonia ornata*. 1-7. Specimen USTL3179-1 from sample R65: 1. External view, area in the lower square is magnified in 3 and area in the upper square is magnified in 4; 2. Lateral view; 3. Detail of the shell ornamentation; 4. Detail of the larval shell; 5. Internal view; 6. Subapical view, area in the square is magnified in 7; 7. Detail of the articulation. 8, 11. Specimen USTL3179-5 from sample R65: 8. External view; 11. Detail of the concentric filia. 9, 10, 12. Specimen USTL3179-3 from sample R65: 12. External view, area in the upper square is magnified in 9, area in the lower square is magnified in 10; 9-10. Details of the shell structure. 13-16. Specimen USTL3182-3 of a ventral valve of *Eoobolus* sp. from sample R66. Scale bars are: 10, 20  $\mu\text{m}$ ; 4, 11, 50  $\mu\text{m}$ ; 7, 9, 15, 100  $\mu\text{m}$ ; 1-3, 5-6, 8, 200  $\mu\text{m}$ ; 12-14, 16, 500  $\mu\text{m}$ .

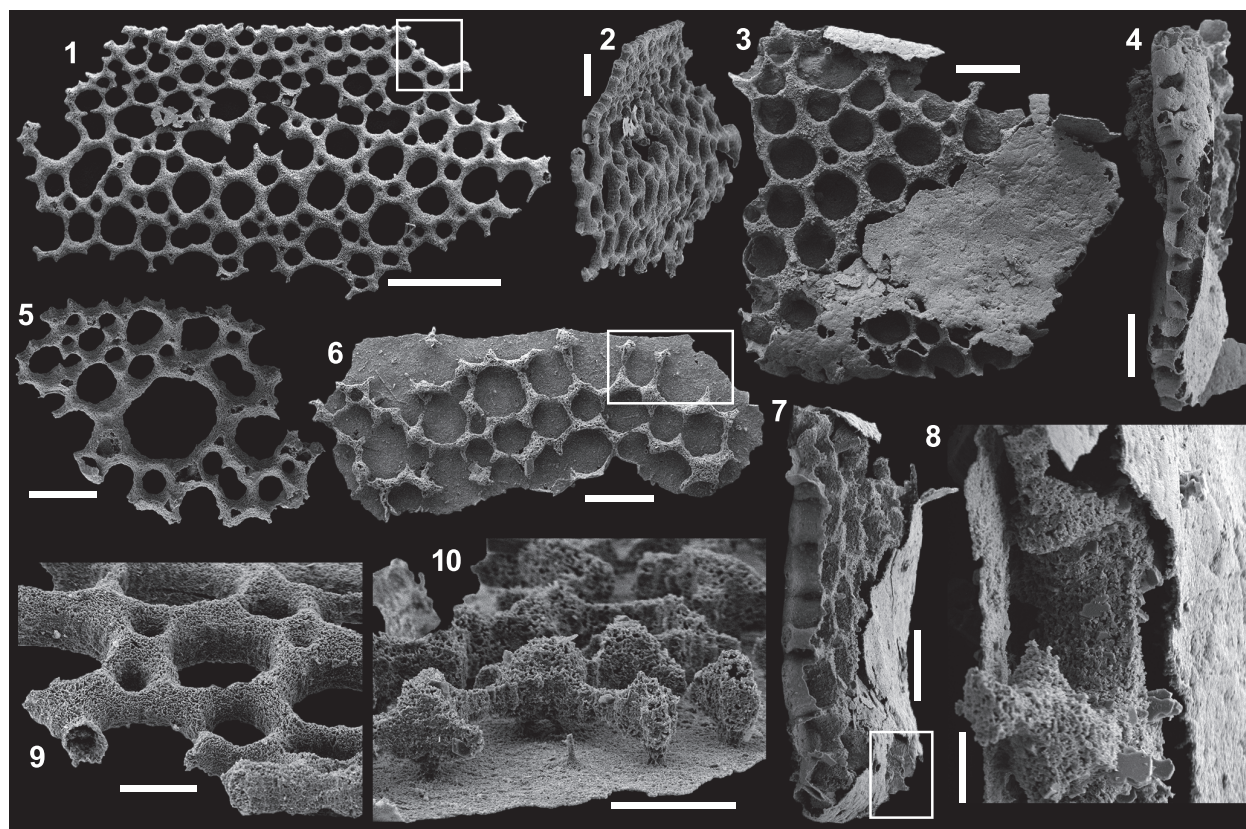


**FIGURE 23.** Indeterminate fossil from the Puerto Blanco Formation of Cerro Rajón, Sonora, Mexico. 1-2, 9. Specimen USTL3174-12. 3-4, 7-8. Specimen USTL3176-11. 5. Specimen USTL3174-13. 6, 10. Specimen USTL3174-11. Scale bars are: 8, 50 µm; 9, 10, 100 µm; 2-7 200 µm; 1, 500 µm.

fossils, probably of archaeocyathan or other sponges.

#### ACKNOWLEDGEMENTS

The authors are grateful to Dr. G.I. Espinoza from the University of Sonora for leading the authors to the location of the studied section. E. Locatelli and P. Recourt from the University of Lille are thanked for their valuable technical support. LD benefited from fundings from the Alexander von

Humboldt Foundation and SC from grant from Spanish Ministry of Economics, Finance and Competitiveness CGL2017-87631-P. The study was supported by projects UNAM-DGAPA-PAPIIT No. IN105012, CONACyT No. 165826 and ECOS-France-Mexico No. M13U01. The authors acknowledge the four anonymous reviewers for their constructive comments that greatly improved the manuscript.

#### REFERENCES

- Álvaro, J.J., Ahlberg, P., Babcock, L.E., Bordonaro, O.L., Choi, D.K., Cooper, R.A., Ergaliev, G.K., Gapp, I.W., Ghobadi Pour, M., Hughes, N.C., Jago, J.B., Korovnikov, I., Laurie, J.R., Lieberman, B.S., Paterson, J.R., Pegel, T.V., Popov, L.E., Rushton, A.W.A., Sukhov, S.S., Tortello, M.F., Zhou, Z.Y., and Żylińska, A. 2013. Global Cambrian trilobite palaeobiogeography assessed using parsimony analysis of endemism, p. 273-296. In Harper, D.A.T. and Servais, T. (eds.), *Early Palaeozoic Biogeography and Palaeogeography*. Geological Society, London. <https://doi.org/10.1144/M38.19>

- Álvaro, J.J., Elicki, O., Debrenne, F., and Vizcaïno, D. 2002. Small shelly fossils from the Lower Cambrian Lastours Formation, southern Montagne Noire, France. *Géobios*, 35:397-409. [https://doi.org/10.1016/S0016-6995\(02\)00036-0](https://doi.org/10.1016/S0016-6995(02)00036-0)
- Amato, J.M., Lawton, T.F., Manuel, D.J., Leggett, W.J., González-León, C.M., Farmer, G.L., and Wooden, J.L. 2009. Testing the Mojave-Sonora megashear hypothesis: evidence from Paleoproterozoic igneous rocks and deformed Mesozoic strata in Sonora, Mexico. *Geology*, 37:75-78. <https://doi.org/10.1130/G25240A.1>
- Anderson, T.H. and Schmidt, V.A. 1983. The evolution of Middle America and the Gulf of Mexico-Caribbean Sea region during Mesozoic time. *Geological Society of America Bulletin*, 94:941-966. [https://doi.org/10.1130/0016-7606\(1983\)94<941:TEOMAA>2.0.CO;2](https://doi.org/10.1130/0016-7606(1983)94<941:TEOMAA>2.0.CO;2)
- Anderson, T.H. and Silver, L.T. 2005. The Mojave-Sonora megashear—Field and analytical studies leading to the conception and evolution of the hypothesis, p. 1-50. In Anderson, T.H., Nourse, J.A., McKee, J.W. and Steiner, M.B. (eds.), *The Mojave-Sonora Megashear Hypothesis: Development, Assessment, and Alternatives*. Geological Society of America, Boulder. <https://doi.org/10.1130/0-8137-2393-0.1>
- Arellano, A.R.V. 1956. Relaciones del Cambrico de Caborca, especialmente con la base del Paleozoico. *Congreso Geológico Internacional, 20th, Mexico; el Sistema Cambrico, su paleogeografía y el problema de su base symposium*, 2:509-527.
- Babcock, L.E., Peng, S.C., Zhu, M.Y., Xiao, S.H., and Ahlberg, P. 2014. Proposed reassessment of the Cambrian GSSP. *Journal of African Earth Sciences*, 98:3-10. <https://doi.org/10.1016%2Fj.jafrearsci.2014.06.023>
- Babcock, L.E., Robison, R.A., and Peng, S.C. 2011. Cambrian stage and series nomenclature of Laurentia and the developing global chronostratigraphic scale. *Museum of Northern Arizona Bulletin*, 67:12-26.
- Balthasar, U. 2009. The brachiopod *Eoobolus* from the Early Cambrian Mural Formation (Canadian Rocky Mountains). *Paläontologische Zeitschrift*, 83:407-418. <https://doi.org/10.1007%2Fs12542-009-0026-4>
- Barrande, J. 1881. *Système Silurien du Centre de la Bohême. Volume VI: Acéphales. Système Silurien du Centre de la Bohême*. Prague, 342 pp. <https://doi.org/10.5962%2Fbhl.title.82327>
- Bengtson, S. and Collins, D. 2015. Chancelloriids of the Cambrian Burgess Shale. *Palaeontologia Electronica*, 18.1.6A:1-67. <https://doi.org/10.26879%2F498>  
<http://palaeo-electronica.org/content/2015/1031-chancelloriids>
- Bengtson, S., Conway Morris, S., Cooper, B.J., Jell, P.A., and Runnegar, B.N. 1990. Early Cambrian fossils from south Australia. *Memoirs of the Association of Australasian Palaeontologists*, 9:1-364.
- Bengtson, S., Matthews, S.C., and Missarzhevsky, V.V. 1986. The Cambrian netlike fossil *Microdictyon*, p. 97-115. In Hoffman, A. and Nitecki, M.H. (eds.), *Problematic Fossil Taxa*. Oxford University Press, Oxford.
- Betts, M.J., Paterson, J.R., Jago, J.B., Jacquet, S.M., Skovsted, C.B., Topper, T.P., and Brock, G.A. 2016. A new lower Cambrian shelly fossil biostratigraphy for South Australia. *Gondwana Research*, 36:176-208. <https://doi.org/10.1016%2Fj.gr.2016.05.005>
- Bhatt, D.K. 1989. Small shelly fossils, Tommotian and Meishucunian stages and the Precambrian-Cambrian boundary – Implications of the recent studies in the Himalayan sequences. *Journal of the Palaeontological Society of India*, 34:55-68.
- Billings, E. 1871. On some new species of Palaeozoic fossils. *Canadian Naturalist*, 6:213-233, 240. <https://doi.org/10.2475/ajs.s3-3.17.352>
- Bond, G.C., Nickeson, P.A., and Kominz, M.A. 1984. Breakup of a supercontinent between 625 Ma and 555 Ma: New evidence and implications for continental histories. *Earth and Planetary Science Letters*, 70:325-345. <https://doi.org/10.1016%2F0012-821x%2884%2990017-7>
- Brasier, M.D., Cowie, J., and Taylor, M. 1994. Decision on the Precambrian-Cambrian boundary stratotype. *Episodes*, 17:3-8.
- Budd, G.E. and Jackson, I.S.C. 2016. Ecological innovations in the Cambrian and the origins of the crown group phyla. *Philosophical Transactions of the Royal Society B*, 371:20150287. <https://doi.org/10.1098%2Frstb.2015.0287>
- Buffler, R.T. and Thomas, W.A. 1994. Crustal structure and evolution of the southeastern margin of North America and the Gulf of Mexico basin, p. 219-264. In Speed, R.C. (ed.), *Phanerozoic Evolution of North American Continent-Ocean Transitions, Geology of North America Continent-Ocean Transects*. Geological Society of America, Boulder. <https://doi.org/10.1130%2Fdnag-cot-pen.219>

- Campa, M.F. and Coney, P.J. 1983. Tectonostratigraphic terrains and mineral resource distributions in Mexico. *Canadian Journal of Earth Sciences*, 20:1040-1051. <https://doi.org/10.1139%2F39-094>
- Clausen, S., Álvaro, J.J., Devaere, L., Ahlberg, P., and Babcock, L.E. 2015. The Cambrian explosion: Its timing and stratigraphic setting. *Annales de Paléontologie*, 101:153-160. <https://doi.org/10.1016%2Fj.annpal.2015.07.001>
- Conway-Morris, S. and Fritz, W. H. 1984. *Lapworthella filigrana* n. sp. (incertae sedis) from the Lower Cambrian of the Cassiar Mountains, northern British Columbia, Canada, with comments on possible levels of competition in the early Cambrian. *Paläontologische Zeitschrift*, 58:197-209. <https://doi.org/10.1007%2F39-094>
- Cooper, G.A. and Arellano, A.R.V. 1946. Stratigraphy near Caborca, northwest Sonora, Mexico. *Bulletin of the American Association of Petroleum Geologists*, 30:606-610. <https://doi.org/10.1306%2F39-094>
- Cooper, G.A. and Arellano, A.R.V. 1952. Introduction and stratigraphy, p. 1-18. In Cooper, G.A., Arellano, A.R.V., Johnson, J.H., Okulitch, V.J., Stoyanow, A., and Lochman, C. (eds.), *Cambrian Stratigraphy and Paleontology Near Caborca, Northwest Sonora, Mexico*. Smithsonian Institution, Washington, D.C.
- Cuen-Romero, F.J., Valdez-Holguín, J.E., Buitrón-Sánchez, B.E., Monreal, R., Enríquez-Ocaña, L.F., Aguirre-Hinojosa, E., Ochoa-Granillo, J.A., and Palafox-Reyes, J.J. 2018. Trilobite-based biostratigraphy (Arthropoda-Trilobita) and related faunas of the Cambrian from Sonora, Mexico. *Journal of South American Earth Sciences*, 83:227-236. <https://doi.org/10.1016/j.jsames.2018.03.002>
- Cuvier, G. 1797. *Tableau élémentaire de l'histoire naturelle des animaux*. Baudouin, Paris.
- Debrenne, F. 1987. Archaeocyatha from Mexico in the Smithsonian Institution. New data from recent collectings. *Geobios*, 20(2):267-273. <https://doi.org/10.1016%2F39-094>
- Debrenne, F., Gandin, A., and Rowland, S.M. 1989. Lower Cambrian bioconstructions in northwestern México (Sonora). Depositional setting, paleoecology and systematics of Archaeocyaths. *Geobios*, 22(2):137-195. <https://doi.org/10.1016%2F39-094>
- Devaere, L., Clausen, S., Álvaro, J.J., Peel, J.S. and Vachard, D. 2014. Terreneuvian orthothecid (Hyalolitha) digestive tracts from northern Montagne Noire, France: Taphonomic, ontogenetic and phylogenetic implications. *PLoS ONE*, 9(2):e88583. <https://doi.org/10.1371%2Fjournal.pone.0088583>
- Devaere, L., Clausen, S., Steiner, M., Álvaro, J.J., and Vachard, D. 2013. Chronostratigraphic and palaeogeographic significance of an early Cambrian microfauna from the Heraultia Limestone, northern Montagne Noire, France. *Palaeontologia Electronica*, 16.2.17A:1-91. <https://doi.org/10.26879%2F366>  
<http://palaeo-electronica.org/content/in-press/298-french-cambrian-microfauna>
- Dickinson, W.R. 1981. Plate tectonic evolution of the southern Cordillera, p. 113-135. In Dickinson, W.R. and Payne, W.D. (eds.), *Relations of Tectonics to Ore Deposits in the Southern Cordillera*. Arizona Geological Society, Tucson.
- Doré, F. and Reid, R.E. 1965. *Allonia tripodophora* nov. gen., nov. sp., nouvelle éponge du Cambrien inférieur du Carteret (Manche). *Comptes Rendus Sommaires des Séances de la Société Géologique de France*, 1:20-21.
- Duan, C. 1984. Small shelly fossils from the Lower Cambrian Xihaoping Formation I the Shennongjia district, Hubei province – hyoliths and fossil skeletons of unknown affinities. *Bulletin of the Tianjin Institute of Geology and Mineral Resources*, 7:141-188. (In Chinese with English abstract)
- Duméril, A.M.C. 1806. *Zoologie analytique ou méthode naturelle de classification des animaux*. Allais, Paris. <https://doi.org/10.5962/bhl.title.44835>
- Dzik, J. and Krumbiegel, G. 1989. The oldest 'onychophoran' *Xenusion*: a link connecting phyla? *Lethaia*, 22:169-181. <https://doi.org/10.1111%2Fj.1502-3931.1989.tb01679.x>
- Eardley, A.J. 1951. *Structural Geology of North America*. Harper and Brothers, New York. <https://doi.org/10.5962%2Fbhl.title.62079>
- Eells, J.L. 1972. *Geology of the Sierra de la Berruga, Northwestern Sonora, Mexico*. Unpublished MSc thesis, California State University, San Diego, USA.
- Elicki, O. 1994. Lower Cambrian carbonates from eastern Germany: Palaeontology, stratigraphy and palaeogeography. *Neues Jahrbuch für Geologie und Paläontologie*, 191:69-93.

- Elicki, O. 2011. First skeletal microfauna from the Cambrian Series 3 of the Jordan Rift Valley (Middle East). *Memoirs of the Association of Australasian Palaeontologists*, 42:153-173.
- Elicki, O. and Gürsu, S. 2009. First record of *Pojetaia runnegari* Jell, 1980 and *Fordilla* Barrande, 1881 from the Middle East (Taurus Mountains, Turkey) and critical review of Cambrian bivalves. *Paläontologische Zeitschrift*, 83:267-291. <https://doi.org/10.1007%2Fs12542-009-0021-9>
- Farmer, G.L., Bowring, S.A., Matzel, J., Espinosa Maldonado, G., Fedo, C., and Wooden, J. 2005. Paleoproterozoic Mojave province in northwestern Mexico? Isotopic and U-Pb zircon geochronologic studies of Precambrian and Cambrian crystalline and sedimentary rocks, Caborca, Sonora, p. 183-198. In Anderson, T.H., Nourse, J.A., McKee, J.W., and Steiner, M.B. (eds.), *The Mojave-Sonora Megashear Hypothesis: Development, Assessment, and Alternatives*. Geological Society of America, Boulder. <https://doi.org/10.1130%2F0-8137-2393-0.183>
- Fernández-Remolar, D.C. 2001. Chancelloriidae del Ovetiense Inferior de la Sierra de Córdoba, España. *Revista Española de Paleontología*, 16:39-61.
- Fritz, W.H. 1972. Lower Cambrian trilobites from the Sekwi Formation type section, Mackenzie Mountains, northwestern Canada. *Geological Survey of Canada Bulletin*, 212:1-90. <https://doi.org/10.4095%2F100784>
- Fritz, W.H. 1975. Broad correlations of some Lower and Middle Cambrian strata in the North America Cordillera. *Geological Survey of Canada Paper*, 75:533-540. <https://doi.org/10.4095%2F104639>
- Fuchs, G. and Mostler, H. 1972. Der erste Nachweis von Fossilien (kambrischen Alters) in der Hazira-Formation, Hazara, Pakistan. *Geologisch-Paläontologische Mitteilungen Innsbruck*, 3:1-12.
- Gorjansky, V.I. and Popov, L.E. 1985. Morfologiya, systematicheskoe polozhenie i proiskhozhdenie bezzamkovykh brachiopods karbonatnoi rakovinoi. [Morphology, systematic position and origin of the inarticulate brachiopods with calcareous shells]. *Paleontologicheskii Zhurnal*, 3:3-14. (In Russian)
- Grant, S.W. 1990. Shell structure and distribution of *Cloudina*, a potential index fossil for the terminal Proterozoic. *American Journal of Science*, 290:261-294.
- Gravestock, I., Alexander, E.M., Demidenko, Y.E., Esakova, N.V., Holmer, L.E., Jago, J.B., Lin, T.M., Melnikova, L., Parkhaev, P.Y., Rozanov, A.Y., Ushatinskaya, G.T., Zang, W.I., Zhegallo E.A., and Zhuravlev, A.Y. 2001. The Cambrian biostratigraphy of the Stansbury basin, south Australia. *Russian Academy of Sciences, Transactions of the Palaeontological Institute*, 282:1-344.
- Hao, Y.C. and Shu, D.G. 1987. The oldest known well-preserved *Phaeodaria* (Radiolaria) from southern Shaanxi. *Geoscience*, 1:301-310. (In Chinese with English abstract)
- He, T.G. and Yang, X.H. 1982. Lower Cambrian Meishucun Stage of the western Yangtze stratigraphic region and its Small Shelly Fossils. *Bulletin of the Chengdu Institute of Geological and Mineral Research*, 3:69-95. (In Chinese with English abstract)
- Hollingsworth, J.S. 2005. The earliest occurrence of trilobites and brachiopods in the Cambrian of Laurentia. *Palaeogeography, Palaeoclimatology, Palaeoecology*, 220:153-165. <https://doi.org/10.1016%2Fj.palaeo.2004.08.008>
- Hollingsworth, J.S. 2007. Fallotaspidoid trilobite assemblage from the Esmeralda Basin (western Nevada, USA). *Memoirs of the Australasian Association of Palaeontologists*, 32:123-140.
- Hollingsworth, J.S. 2011. Lithostratigraphy and biostratigraphy of Cambrian Stage 3 in western Nevada and eastern California, p. 26-42. In Hollingsworth, J.S., Sundberg, F.A., and Foster, J.R. (eds.), *Cambrian Stratigraphy and Paleontology of Northern Arizona and Southern Nevada*. Museum of Northern Arizona, Flagstaff.
- Horný, R.J. 1964. The Middle Cambrian Pelagiellacea of Bohemia (Mollusca). *Sborník Národního Muzea v Praze*, 20:133-140.
- Hou, X.G. and Bergström, J. 1995. Cambrian lobopodians—ancestors of extant onychophorans? *Zoological Journal of the Linnean Society*, 114:3-19. <https://doi.org/10.1111%2Fj.1096-3642.1995.tb00110.x>
- Iriondo, A., Martínez-Torres, L.M., Kunk, M.J., Atkinson, W.W., Premo, W.R., and McIntosh, W.C. 2005. Northward Laramide thrusting in the Quitovac region, northwestern Sonora, Mexico: Implications for the juxtaposition of Paleoproterozoic basement blocks and the Mojave-Sonora megashear hypothesis, p. 631-669. In Anderson, T.H., Nourse, J.A., McKee, J.W., and Steiner, M.B. (eds.), *The Mojave-Sonora Megashear Hypothesis: Development,*

- Assessment, and Alternatives*. Geological Society of America, Boulder. <https://doi.org/10.1130%2F0-8137-2393-0.631>
- Jell, P.A. 1980. Earliest known pelecypod on Earth – a new Early Cambrian genus from Australia. *Alcheringa*, 4:233-239. <https://doi.org/10.1080%2F03115518008618934>
- Jiang, Z.W. 1992. The Lower Cambrian fossil record of China, p. 311-333. In Lipps, J.H. and Signor, P.W. (eds.), *Origin and Early Evolution of the Metazoa*. Plenum Press, New York. [https://doi.org/10.1007/978-1-4899-2427-8\\_9](https://doi.org/10.1007/978-1-4899-2427-8_9)
- Knight, J.B. 1956. New families of gastropods. *Journal of the Washington Academy of Sciences*, 46:241-242.
- Koneva, S.P. 1986. A new family of the Cambrian inarticulate brachiopods. *Paleontologicheskii Zhurnal*, 1:49-55. (In Russian)
- Kouchinsky, A., Bengtson, S., Clausen, S., Gubanov, A., Malinky, J.M., and Peel, J.S. 2011. A middle Cambrian fauna of skeletal fossils from the Kuonamka Formation, northern Siberia. *Alcheringa*, 35:123-189. <https://doi.org/10.1080%2F03115518.2010.496529>
- Kouchinsky, A., Bengtson, S., Clausen, S., and Vendrasco, M.J. 2015. An early Cambrian fauna of skeletal fossils from the Emyaksin Formation, northern Siberia. *Acta Palaeontologica Polonica*, 60:421-512. <https://doi.org/10.4202%2Fapp.2012.0004>
- Kumar, G., Bhatt, D.K., and Raina, B.K. 1987. Skeletal microfauna of Meishucunian and Qiongzhusian (Precambrian-Cambrian boundary) age from the Ganga Valley, Lesser Himalaya, India. *Geological Magazine*, 124:167-171. <https://doi.org/10.1017%2Fs0016756800015995>
- Landing, E. 1988. Lower Cambrian of eastern Massachusetts: stratigraphy and small shelly fossils. *Journal of Paleontology*, 62:661-695.
- Landing, E. and Bartowski, K.E. 1996. Oldest shelly fossils from the Taconic allochthon and late Early Cambrian sea-levels in eastern Laurentia. *Journal of Paleontology*, 70:741-761. <https://doi.org/10.1017%2Fs0022336000023799>
- Landing, E., Geyer, G., and Bartowski, K.E. 2002. Latest early Cambrian small shelly fossils, trilobites, and Hatch Hill dysaerobic interval on the Québec continental slope. *Journal of Paleontology*, 76:287-305. <https://doi.org/10.1017%2Fs0022336000041718>
- Li, G. and Xiao S. 2004. *Tannuolina* and *Micrina* (Tannuolinidae) from the Lower Cambrian of eastern Yunnan, south China, and their scleritome reconstruction. *Journal of Paleontology*, 78:900-913. [https://doi.org/10.1666/0022-3360\(2004\)078<0900:TAMTFT>2.0.CO;2](https://doi.org/10.1666/0022-3360(2004)078<0900:TAMTFT>2.0.CO;2)
- Li, G., Zhu, M., Steiner, M., and Qian, Y. 2004. Skeletal faunas from the Qiongzhusian of southern Shaanxi: Biodiversity and lithofacies-biofacies links in the Lower Cambrian carbonate settings. *Progress in Natural Science*, 14:91-96. <https://doi.org/10.1080%2F10020070412331343201>
- Linnaeus, C. 1758. *Systema Naturae per Regna Tria Naturae, Secundum Classes, Ordines, Genera, Species, cum Characteribus, Differentiis, Synonymis, Locis. Editio Decima*, 1:1-824. <https://doi.org/10.5962%2Fbhl.title.542>
- Lochman, C. 1948. New Cambrian trilobite genera from northwest Sonora, Mexico. *Journal of Paleontology*, 22:451-464.
- Lochman, C. 1952. Trilobites, p. 60-61. In Cooper, G.A., Arellano, A.R.V., Johnson, J.H., Okulitch, V.J., Stoyanow, A., and Lochman, C. (eds.), *Cambrian Stratigraphy and Paleontology Near Caborca, Northwestern Sonora, Mexico*. Smithsonian Institution, Washington D.C.
- Longoria, J.F. 1981. Geologic features of northwest Sonora, p. 1-48. In Longoria, J.F. (ed.), *Regional Geology of Northwest Sonora*. Geological Society of America, Boulder.
- Loyd, S.J., Marenco, P.J., Hagadorn, J.W., Lyons, T.W., Kaufman, A.J., Sour-Tovar, F., and Corsetti, F.A. 2012. Sustained low marine sulfate concentrations from the Neoproterozoic to the Cambrian: insights from carbonates of northwestern Mexico and eastern California. *Earth and Planetary Science Letters*, 339-340:79-94. <https://doi.org/10.1016%2Fj.epsl.2012.05.032>
- Luo, H., Jiang, Z., Wu, X., Song, X. and Ouyang, L. 1982. *The Sinian-Cambrian boundary in eastern Yunnan, China*. Yunnan Institute of Geological Sciences. (In Chinese with English abstract).
- Luo, H., Jiang, Z., Wu, X., Song, X., Ouyang, L., Xing, Y., Liu, G., Zhang, S., and Tao, Y. 1984. *Sinian-Cambrian Boundary stratotype section at Meishucun, Jinning, Yunnan, China*. Peoples Publishing House, Yunnan. (In Chinese with English abstract)

- MacKinnon, D.I. 1985. New Zealand late Middle Cambrian molluscs and the origin of Rostroconchia and Bivalvia. *Alcheringa*, 9:65-fvrgtgMalinky, J.M. and Skovsted, C.B. 2004. Hyoliths and small shelly fossils from the Lower Cambrian of north-east Greenland. *Acta Palaeontologica Polonica*, 49:551-578.
- Marek, L. 1963. New knowledge on the morphology of *Hyalolithes*. *Sbornik Geologických Fed, Paleontologie*, 1:53-74.
- Marek, L. 1966. New hyolithid genera from the Ordovician of Bohemia. *Casopis Naradního Muzea*, 135:89-92.
- Matthew, G.F. 1894. Illustrations of the fauna of the St. John Group. *Transactions of the Royal Society of Canada*, 11:85-129. <https://doi.org/10.5962%2Fbhl.title.41116>
- Matthew, G.F. 1895. The *Protolenus* fauna. *Transactions of the New York Academy of Sciences*, 14:101-153. <https://doi.org/10.1126%2Fscience.1.17.452>
- Matthew, G.F. 1899. Studies on Cambrian faunas, No. 3 - Upper Cambrian Fauna of Mount Stephen, British Columbia - The Trilobites and Worms. *Transactions, Royal Society of Canada, 2nd series*, 5(4):39-123. <https://doi.org/10.1017%2Fs001675680018183x>
- Matthew, G.F. 1902. Notes on Cambrian faunas. *Transactions of the Royal Society of Canada*, 2(4):18, 93-112. <https://doi.org/10.5962%2Fbhl.title.63589>
- Matthews, S.C. and Missarzhevsky, V.V. 1975. Small Shelly Fossils of late Precambrian and early Cambrian age: A review of recent work. *Journal of the geological Society of London*, 131:289-304. <https://doi.org/10.1144%2Fgsjgs.131.3.0289>
- McMenamin, M.A.S. 1984. *Paleontology and Stratigraphy of Lower Cambrian and Upper Proterozoic Sediments, Caborca Region, Northwestern Sonora, Mexico*. Unpublished PhD thesis, University of California, Santa Barbara, USA.
- McMenamin, M.A.S. 1985. Basal Cambrian Small Shelly Fossils from the La Cienega Formation, Northwestern Sonora, Mexico. *Journal of Paleontology*, 59:1414-1425.
- McMenamin, M.A.S. 1987. Lower Cambrian trilobites, zonation and correlation of the Puerto Blanco Formation, Sonora, Mexico. *Journal of Paleontology*, 61:738-749. <https://doi.org/10.1017%2Fs0022336000029097>
- McMenamin, M.A.S. 1992. Two new species of the Cambrian genus *Mickwitzia*. *Journal of Paleontology*, 66:173-182. <https://doi.org/10.1017%2Fs0022336000033680>
- McMenamin, M.A.S. 1996. Ediacaran biota from Sonora, Mexico. *Proceedings of the National Academy of Sciences*, 93:4990-4993. <https://doi.org/10.1073%2Fpnas.93.10.4990>
- McMenamin, M.A.S. 2008. Early Cambrian sponge spicules from the Cerro Clemente and Cerro Rajón, Sonora, México. *Geologica Acta*, 6:363-367. <https://doi.org/10.1344/105.000000263>
- McMenamin, M.A.S., Awramik, S.M., and Stewart, J.H. 1983. Precambrian-Cambrian transition problem in western North America: Part II. Early Cambrian skeletonized fauna and associated fossils from Sonora, Mexico. *Geology*, 11:227-230. [https://doi.org/10.1130/0091-7613\(1983\)11<227:PTPIWN>2.0.CO;2](https://doi.org/10.1130/0091-7613(1983)11<227:PTPIWN>2.0.CO;2)
- McMenamin, M.A.S., Pittenger, S.L., Carson, M.R., and Larrabee, E.M. 1994. Upper Precambrian-Cambrian faunal sequence, Sonora, México and Lower Cambrian Fossils from New Jersey, United States, p. 213-227. In Landing, E. (ed.), *Festschrift Honouring Donald W. Fisher*. New York State Museum, Albany.
- Meert, J.G. and Torsvik, T.H. 2003. The making and unmaking of a supercontinent: Rodinia revisited. *Tectonophysics*, 375:261-288. <https://doi.org/10.1016%2Fs0040-1951%2803%2900342-1>
- Missarzhevsky, V.V. 1989. Oldest skeletal fossils of Late Precambrian and Early Cambrian age: a review of recent work. *Trudy Geologicheskogo Instituta AN SSSR*, 443:1-231. (In Russian)
- Missarzhevsky, V.V. and Mambetov, A.M. 1981. Stratigrafiya i fauna pograničnykh sloyev Kembriya i Dokembriya Malogo Karatau. [Stratigraphy and fauna of the Precambrian-Cambrian boundary beds of the Malyy Karatau]. *Trudy Ordena Trudovogo Krasnogo Znameni Geologicheskij Institut Akademiyi Nauka SSSR*, 326:1-90. (In Russian)
- Molina-Garza, R.S. and Iriondo, A. 2007. The Mojave-Sonora megashear: The hypothesis, the controversy, and the current state of knowledge, p. 233-259. In Alaniz-Álvarez, S.A. and Nieto-Samaniego, Á.F. (eds.), *Geology of México: Celebrating the Centenary of the Geological Society of México*. Geological Society of America, Boulder. <https://doi.org/10.1130%2F2007.2422%2807%29>
- Moore, J.L, Li, G., and Porter, S.M. 2014. Chancelloriid sclerites from the Lower Cambrian (Meishucunian) of eastern Yunnan, China, and the early history of the group. *Palaeontology*, 57:833-878. <https://doi.org/10.1111%2Fpala.12090>

- Moore, J.L., Porter, S.M., Steiner, M., and Li, G. 2010. *Cambrothyra ampulliformis*, an unusual coeloscleritophoran from the Lower Cambrian of Shaanxi Province, China. *Journal of Paleontology*, 84:1040-1060. <https://doi.org/10.1666/2F09-091.1>
- Mostler, H. 1980. Zur Mikrofauna des Unterkambriums in der Haziraformation - Hazara, Pakistan. *Annalen des Naturhistorisches Museum in Wien*, 83:245-257.
- Nourse, J.A., Premo, W.R., Iriondo, A., and Stahl, E.R. 2005. Contrasting Proterozoic basement complexes near the truncated margin of Laurentia, northwestern Sonora-Arizona international border region, p. 123-182. In Anderson, T.H., Nourse, J.A., McKee, J.W., and Steiner, M.B. (eds.), *The Mojave-Sonora Megashear Hypothesis: Development, Assessment, and Alternatives*. Geological Society of America, Boulder. <https://doi.org/10.1130/2F0-8137-2393-0.123>
- Nowlan, G.S., Narbonne, G.M., and Fritz, W.H. 1985. Small shelly fossils and trace fossils near the Precambrian-Cambrian boundary in the Yukon Territory, Canada. *Lethaia*, 18:233-256. <https://doi.org/10.1111/2Fj.1502-3931.1985.tb00701.x>
- Palmer, A.R. and Halley, R.B. 1979. Physical stratigraphy and trilobite biostratigraphy of the Carrara Formation (Lower and Middle Cambrian) in the southern Great Basin. *United States Geological Survey Professional Paper*, 1047:1-131.
- Parkhaev, P.Y. 2004. Malacofauna of the Lower Cambrian Bystraya Formation of Eastern Transbaikalia. *Paleontological Journal*, 38:590-608.
- Parkhaev, P.Y. 2005. Two new species of the Cambrian helcionelloid mollusks from the northern part of the Siberian Platform. *Paleontological Journal*, 39:615-619.
- Parkhaev, P.Y. 2008. The Early Cambrian radiation of Mollusca, p. 33-69. In Ponder, W. and Lindberg, D.R.R. (eds.), *Phylogeny and Evolution of the Mollusca*. University of California Press, Berkeley. <https://doi.org/10.1525/2Fcalifornia%2F9780520250925.003.0003>
- Parkhaev, P.Y. and Demidenko, Y.E. 2010. Zooproblematica and Mollusca from the Lower Cambrian Meishucun section (Yunnan, China) and taxonomy and systematics of the Cambrian Small Shelly Fossils of China. *Paleontological Journal*, 44:883-1161. <https://doi.org/10.1134/2Fs0031030110080010>
- Peel, J.S. 1991. The Classes Tergomya and Helcionelloida, and early molluscan evolution. *Grønlands Geologiske Undersøgelse, Bulletin* 161:11-65.
- Peel, J.S. and Skovsted, C.B. 2005. Problematic molluscs from the Bastion Formation of North-East Greenland. *Paläontologische Zeitschrift*, 79:461-470. <https://doi.org/10.1007/2Fb02988372>
- Peel, J.S., Streng, M., Geyer, G., Kouchinsky, A., and Skovsted, C.B. 2016. *Ovatoryctocara granulata* assemblage (Cambrian Series 2-Series 3 boundary) of Løndal, North Greenland. *Australasian Palaeontological Memoirs*, 49:241-282.
- Peiffer-Rangin, F. 1979. Les zones isopiques du Paleozoïque inferieur du nord-ouest mexicain, temoins du relais entre les Appalaches et la cordillere ouest-americaine. *Comptes Rendus Hebdomadaires des Séances de l'Académie des Sciences de Paris, série D*, 288:1517-1519.
- Peng, S., Babcock, L.E., and Cooper, R.A. 2012. The Cambrian Period, p. 437-488. In Gradstein, F.M., Ogg, J.G., Schmitz, M., and Ogg, G. (eds.), *The Geological Time Scale 2012 - 2<sup>nd</sup> Volume set*. Elsevier, Boston. <https://doi.org/10.1016/B978-0-444-59425-9.00019-6>
- Pojeta, J. 1975. *Fordilla troyensis* Barrande and early pelecypod phylogeny. *Bulletins of American Paleontology*, 67(287):363-384.
- Poole, F.G., Perry, W.J., Jr., Madrid, R.J., and Amaya-Martinez, R. 2005. Tectonic synthesis of the Ouachita-Marathon-Sonora orogenic margin of southern Laurentia: Stratigraphic and structural implications for timing of deformational events and plate-tectonic model, p. 543-596. In Anderson, T.H., Nourse, J.A., McKee, J.W., and Steiner, M.B. (eds.), *The Mojave-Sonora Megashear Hypothesis: Development, Assessment, and Alternatives*. Geological Society of America, Boulder. <https://doi.org/10.1130/2F0-8137-2393-0.543>
- Porter, S.M. 2008. Skeletal microstructure indicates cancelloriids and halkieriids are closely related. *Palaeontology*, 51:865-879. <https://doi.org/10.1111/2Fj.1475-4983.2008.00792.x>
- Qian, Y. 1977. Hyolitha and some problematica from the Lower Cambrian Meishucun Stage in central and SW China. *Acta Palaeontologica Sinica*, 16(2):255-278. (In Chinese with English abstract)
- Qian, Y. 1989. Early Cambrian Small Shelly Fossils of China with special reference to the Precambrian-Cambrian boundary. In *Stratigraphy and Palaeontology of Systemic Boundaries in China: Precambrian-Cambrian Boundary*. Nanjing University Publishing House, Nanjing.

- Qian, Y. and Bengtson, S. 1989. Palaeontology and biostratigraphy of the early Cambrian Meishucunian Stage in Yunnan province, south China. *Fossils and Strata*, 24:1-156.
- Raymond, P.E. 1935. *Leancoilia* and other mid-Cambrian Arthropoda. *Bulletin of the Museum of Comparative Zoology*, 76:205-230.
- Rowell, A.J. 1965. Inarticulata, p. 260-296. In Moore, R.C. (ed.), *Treatise on Invertebrate Paleontology, Part H. Brachiopoda*. Geological Society of America and University of Kansas Press, Boulder, Lawrence.
- Rožanov, A.Y., Missarzhevsky, V.V., Volkova, N.A., Voronova, L.G., Krylov, I.N., Keller, B.M., Korolyuk, I.K., Lenzion, K., Mikhnyar, R., Pykhova, N.G., and Sidorov A.D. 1969. Tommotskiu yarus i problema nizhney granisty Kembriya. *Trudy Geologiske Institut Leningrad*, 206:1-379. (In Russian)
- Sarmiento, G.N., Fernández-Remolar, D., and Göncüoğlu, M.C. 2001. Cambrian small shelly fossils from the Çal Tepe Formation, Taurus Mountains, Turkey. *Coloquios de Paleontología*, 52:117-134.
- Schuchert, C. 1893. A classification of the Brachiopoda. *American Geologist*, 11:141-167.
- Sdzuy, K. 1969. Unter- und mittelkambrische Porifera (Chancelloriida und Hexactinellida). *Paläontologische Zeitschrift*, 43:115-147. <https://doi.org/10.1007%2Fbf02987647>
- Seilacher, A. 1955. Spuren und Fazies in Unterkambrium, p. 11-143. In Schindewolf, O.H. and Seilacher, A. (eds.), *Beiträge zur Kenntnis des Kambriums in der Salt Range (Pakistan)*. Akademie der Wissenschaften und der Literatur zu Mainz, Mathematisch-naturwissenschaftliche Klasse, Abhandlungen.
- Shaler, N.S. and Foerste, A.F. 1888. Preliminary description of north Attleboro fossils. *Harvard Museum of Comparative Zoology Bulletin*, 16:27-41.
- Shu, D., Isozaki, Y., Zhang, X., Han, J., and Maruyama, S. 2014. Birth and early evolution of metazoans. *Gondwana Research*, 25(3):884-895. <https://doi.org/10.1016%2Fj.gr.2013.09.001>
- Siebold, C.T.E. and Stannius, H. 1845. *Lehrbuch der Vergleichenden Anatomie der Wirbellosen Thiere*. Con Veit, Berlin, Germany. <https://doi.org/10.5962%2Fbhl.title.1236>
- Signor, P.W. 1991. Early Cambrian biogeography of western North America, p. 427-447. In Hall, C.A. Jr., Doyle Jones, V., and Widawski B. (eds.), *Natural History of Eastern California and High-Altitude Research*. University of California, Los Angeles.
- Signor, P.W., McMenamin, M.A.S., Gevirtzman, D.A., and Mount, J.F. 1983. Two new pre-trilobite faunas from western North America. *Nature*, 303:415-418. <https://doi.org/10.1038%2F303415a0>
- Signor, P.W. and Mount, J.F. 1986. Lower Cambrian stratigraphic paleontology of the White-Inyo Mountains of eastern California and of Esmeralda County, Nevada. *White Mountain Research Station Symposium Volume*, 1:6-15.
- Signor, P.W., Mount, J.F., and Onken, B.R. 1987. A pre-trilobite shelly fauna from the White-Inyo region of eastern California and western Nevada. *Journal of Paleontology*, 61:425-438. <https://doi.org/10.1017%2Fs0022336000028614>
- Silver, L.T. and Anderson, T.H. 1974. Possible left-lateral early to middle Mesozoic disruption of the southwestern North America craton margin. *Geological Society of America Abstracts with Programs*, 6:955-956.
- Skovsted, C.B. 2003a. *The Early Cambrian Fauna of North-East Greenland*. Unpublished PhD Thesis, Uppsala Universitet, Uppsala, Sweden.
- Skovsted, C.B. 2003b. Unusually preserved *Salterella* from the Lower Cambrian Forteau Formation of Newfoundland. *GFF*, 125:17-22. <https://doi.org/10.1080%2F11035890301251017>
- Skovsted, C.B. 2004. Mollusc fauna of the Early Cambrian Bastion Formation of North-East Greenland. *Bulletin of the Geological Society of Denmark*, 51:11-37.
- Skovsted, C.B. 2005. A carapace of the bradoriid arthropod *Mongolitubulus* from the Early Cambrian of Greenland. *GFF*, 127:217-220. <https://doi.org/10.1080%2F11035890501273217>
- Skovsted, C.B. 2006a. Small shelly fauna from the upper Lower Cambrian Bastion and Ella Island formations, north-east Greenland. *Journal of Paleontology*, 80:1087-1112.
- Skovsted, C.B. 2006b. Small shelly fossils from the basal Emigrant Formation (Cambrian, uppermost Dyeran Stage) of Split Mountain, Nevada. *Canadian Journal of Earth Sciences*, 43:487-496. <https://doi.org/10.1139%2F05-119>
- Skovsted, C.B. 2016. A silicified tommotiid from the lower Cambrian of Greenland. *Bulletin of Geosciences*, 91(3):553-559. <https://doi.org/10.3140%2Fbull.geosci.1609>

- Skovsted, C.B. and Holmer, L.E. 2003. The Early Cambrian stem group brachiopod *Mickwitzia* from Northeast Greenland. *Acta Palaeontologica Polonica*, 48:11-30.
- Skovsted, C.B. and Holmer, L.E. 2005. Early Cambrian brachiopods from Northeast Greenland. *Palaeontology*, 48:325-345. <https://doi.org/10.1111%2Fj.1475-4983.2005.00450.x>
- Skovsted, C.B. and Holmer, L.E. 2006. The Lower Cambrian brachiopod *Kyrshabaktella* and associated shelly fossils from the Harkless Formation, southern Nevada. *GFF*, 128:327-337. <https://doi.org/10.1080%2F11035890601284327>
- Skovsted, C.B., Knight, I., Balthasar, U., and Boyce, W.D. 2017. Depth related brachiopod faunas from the lower Cambrian Forteau Formation of southern Labrador and western Newfoundland, Canada. *Palaeontologia Electronica*, 20.3.54A:1-52. <https://doi.org/10.26879/775>  
<https://paleo-electronica.org/content/2017/2048-brachiopods-of-the-forteau-formation>
- Skovsted, C.B., Pan, B., Topper, T.P., Betts, M.J., Li, G., and Brock, G.A. 2016. The operculum and mode of life of the lower Cambrian hyolith *Cupithea* from South Australia and North China. *Palaeogeography, Palaeoclimatology, Palaeoecology*, 443:123-130. <https://doi.org/10.1016%2Fj.palaeo.2015.11.042>
- Skovsted, C.B. and Peel, J.S. 2001. The problematic fossil *Mongolitubulus* from the lower Cambrian of Greenland. *Bulletin of the Geological Society of Denmark*, 48:135-147.
- Skovsted, C.B. and Peel, J.S. 2007. Small shelly fossils from the argillaceous facies of the Lower Cambrian Forteau Formation of Western Newfoundland. *Acta Palaeontologica Polonica*, 52:729-748.
- Skovsted, C.B. and Peel, J.S. 2010. Early Cambrian brachiopods and other shelly fossils from the basal Kinzers Formation of Pennsylvania. *Journal of Paleontology*, 84(4):754-762. <https://doi.org/10.1017%2Fs0022336000058467>
- Skovsted, C.B., Streng, M., Knight, I., and Holmer, L.E. 2010. *Setatella significans*, a new name for mickwitziid stem group brachiopods from the lower Cambrian of Greenland and Labrador. *GFF*, 132(2):117-122. <https://doi.org/10.1080%2F11035897.2010.490878>
- Snodgrass, R.E. 1938. Evolution of the Annelida, Onychophora, and Arthropoda. *Smithsonian Miscellaneous Collections*, 97(6):1-159.
- Solari, L.A., González-León, C.M., Ortega-Obregón, C., Valencia-Moreno, M., and Rascón-Heimpel, M.A. 2018. The Proterozoic of NW Mexico revisited: U-Pb geochronology and Hf isotopes of Sonoran rocks and their tectonic implications. *International Journal of Earth Sciences*, 107:845-861. <https://doi.org/10.1007%2Fs00531-017-1517-2>
- Sour-Tovar, F., Hagadorn, J. W., and Huitrón-Rubio, T. 2007. Ediacaran and Cambrian index fossils from Sonora, Mexico. *Palaeontology*, 50:169-175. <https://doi.org/10.1111%2Fj.1475-4983.2006.00619.x>
- Spencer, L. M. 1980. *Paleoecology of a Lower Cambrian Archaeocyathid Interreef Fauna from Southern Labrador*. Unpublished MSc thesis, State University of New York at Stony Brook, New York, USA.
- Steiner, M., Li, G., Qian Y., and Zhu, M. 2004. Lower Cambrian Small Shelly Fossils of northern Sichuan and southern Shaanxi (China), and their biostratigraphic importance. *Geobios*, 37:259-275. <https://doi.org/10.1016%2Fj.geobios.2003.08.001>
- Stevens, C.H., Stone, P., and Miller, J.S. 2005. A new reconstruction of the Paleozoic continental margin of southwestern North America: Implications for the nature and timing of continental truncation and the possible role of the Mojave-Sonora megashear, p. 597-618. In Anderson, T.H., Nourse, J.A., McKee, J.W., and Steiner, M.B. (eds.), *The Mojave-Sonora Megashear Hypothesis: Development, Assessment, and Alternatives*. Geological Society of America, Boulder. <https://doi.org/10.1130%2F0-8137-2393-0.597>
- Stewart, J.H. 1970. Upper Precambrian and Lower Cambrian strata in the southern Great Basin, California and Nevada. *U.S. Geological Survey Professional Paper*, 620:1-206.
- Stewart, J.H. 1982. Regional relations of Proterozoic and Lower Cambrian rocks in the western United States and northern Mexico, p. 171-186. In Cooper, J.D. Troxel, B., and Wright, L.A. (eds.), *Geology of Selected Areas in the San Bernardino Mountains, Western Mojave Desert, and South Great Basin, California*. Geological Society of America, Anaheim.
- Stewart, J.H. 1984. *Stratigraphic Sections of Lower Cambrian and Upper Proterozoic Rocks in Nye, Lander, and Lincoln Counties, Nevada, and Sonora, Mexico*. U.S. Geological Survey Open-File Report, 84-691.
- Stewart, J.H. 2005. Evidence for Mojave-Sonora megashear – Systematic left-lateral offset of Neoproterozoic to Lower Jurassic strata and facies, western United States and northwestern

- Mexico, p. 209-231. In Anderson, T.H., Nourse, J.A., McKee, J.W., and Steiner, M.B. (eds.), *The Mojave-Sonora Megashear Hypothesis: Development, Assessment, and Alternatives*. Geological Society of America, Boulder. <https://doi.org/10.1130%2F0-8137-2393-0.209>
- Stewart, J.H., Amaya-Martinez, R., and Palmer, A.R. 2002. Neoproterozoic and Cambrian strata of Sonora, Mexico: Rodinian supercontinent to Laurentian Cordilleran margin, p. 5-47. In Barth, A. (ed.), *Contributions to Crustal Evolution of the Southwestern United States*. Geological Society of America, Boulder. <https://doi.org/10.1130%2F0-8137-2365-5.5>
- Stewart, J.H., McMenamin, M.A.S., and Morales-Ramirez, J.M. 1984. Upper Proterozoic and Cambrian rocks in the Caborca region, Sonora, Mexico – Physical stratigraphy, biostratigraphy, paleocurrent studies, and regional relations. *U.S. Geological Survey Professional Paper*, 1309:1-36.
- Stewart, J.H. and Poole, F.G. 1975. Extension of the Cordilleran miogeosynclinal belt to the San Andreas fault, southern California. *Geological Society of America Bulletin*, 86:205-212. [https://doi.org/10.1130/0016-7606\(1975\)86<205:EOTCMB>2.0.CO;2](https://doi.org/10.1130/0016-7606(1975)86<205:EOTCMB>2.0.CO;2)
- Stewart, J.H. and Poole, F.G. 2002. *Inventory of Neoproterozoic and Paleozoic Strata in Sonora, Mexico*. U.S. Geological Survey Open-File Report, 02-97.
- Streng, M., Babcock, L.E., and Hollingsworth, J.S. 2005. Agglutinated protists from the lower Cambrian of Nevada. *Journal of Paleontology*, 79:1214-1218.
- Sysoev, V.A. 1957. K morfologii, sistematischeskomupolozhennyy i sistematike kholitov. [To the morphology, systematics and systematic position of the hyoliths]. *Proceedings of the USSR Academy of Science, Leningrad*, 116:304-307 (in Russian).
- Sysoev, V.A. 1968. Stratigrafiâ i hiolity drevnejših sloevnižnego kembriâ Sibirskoj platformy. *Âkutskij filial' Sibirskogo tdeleniâ Instituta Geologii AN SSSR, Âkutsk*, 1-67. (In Russian)
- Tate, R. 1892. The Cambrian fossils of South Australia. *Transactions of the Royal Society of Southern Australia*, 15:183-189.
- Topper, T.P., Brock, G.A., Skovsted, C.B., and Paterson, J.R. 2009. Shelly fossils from the lower Cambrian *Pararaia bunyerooensis* Zone, Flinders Ranges, South Australia. *Memoirs of the Association of Australasian Palaeontologists*, 37:199-246.
- Topper, T.P., Brock, G.A., Skovsted, C.B., and Paterson, J.R. 2011. *Microdictyon* plates from the lower Cambrian Ajax Limestone of South Australia: Implications for species taxonomy and diversity. *Alcheringa*, 35:427-443. <https://doi.org/10.1080%2F03115518.2011.533972>
- Topper, T.P., Holmer, L.E., Skovsted, C.B., Brock, G.A., Balthasar, U., Larsson, C.M., Petterson Stolk, S., and Harper, D.A.T. 2013. The oldest brachiopods from the lower Cambrian of South Australia. *Acta Palaeontologica Polonica*, 58:93-109. <https://doi.org/10.4202%2Fapp.2011.0146>
- Tynan, H.C. 1980. A probable new phylum and associated microfauna from the Lower Cambrian, White and Inyo Mountains, California. *Geological Society of America Abstracts with Programs*, 12:539.
- Tynan, H.C. 1981a. *A New Group of Corals and Other Microfossils (Echinoderms, Sponges, Crustaceans, Foraminifers, Molluscs, Brachiopods, Problematica) from the Early Cambrian Deep Spring, Campito, and Poleta Formations, White-Inyo Mountains, California*. Unpublished PhD thesis, the University of Iowa, Iowa City, USA.
- Tynan, H.C. 1981b. Microfossils from the Lower Cambrian Campito and Poleta Formations, White-Inyo Mountains, California, p. 231. In Taylor, H.E. (ed.), *Short Papers for the Second International Symposium on the Cambrian System*. U.S. Geological Survey Open-File Report, 81-743.
- Tynan, H.C. 1983. Coral-like microfossils from the Lower Cambrian of California. *Journal of Paleontology*, 57:1188-1211.
- Vachard, D., Clausen, S., Palafox-Reyes, J.J., Buitron-Sanchez, B.E., Devaere, L., Hayart, V. And Régnier, S. 2017. Lower Ordovician microfacies and microfossils from Cerro San Pedro (San Pedro de la Cueva, Sonora, Mexico), as a westernmost outcrop of the newly defined Nuia Province. *Facies*, 63(3):1-37. <https://doi.org/10.1007%2Fs10347-017-0497-9>
- Vassiljeva, N.I. 1998. Melkaya rakovinnaya fauna i biostratigrafiya nizhnego kembriya Sibirskoi platformy. [Small shelly fauna and biostratigraphy of the Lower Cambrian of the Siberian platform]. Vseross. Nauchno-Issled. Geologorazved. Inst. (VNIGRI), St. Petersburg. (In Russian)
- Vassiljeva, N.I. and Sayutina, T.A. 1988. Morfologicheskie raznoobrazie skleritov khantsellorij. [The morphological diversity of chancelloriid sclerites]. *Trudy Instituta Geologii i Geofiziki, Sibirskoe Otdelenie*, 720:190-198. (In Russian)

- Voronin, Y.I., Voronova, L.G., Grigorjeva, N.V., Drozdova, N.A., Zhegallo, E.A., Zhuravlev, A.Y., Ragozina, A.L., Rozanov, A.Y., Sayutina, T.A., Sysoev, V.A., and Fonin, V.D. 1982. Granitsa dokem briya i kembriya v geosinklinal'nykh oblastiakh (opornyj razrez Salany-Gol, MNR). [The Precambrian-Cambrian boundary in the geosynclinal areas (the reference section of Salany-Gol, MPR)]. *Sovmestnaya Sovetsko-Mongol'skaya Paleontologicheskaya Ekspeditsiya Trudy, Nauka, Moscow*, 18:1-150. (In Russian)
- Voronova, L.G., Drozdova, N.A., Esakova, N.V., Zhegallo, E.A., Zhuravlev, A.Y., Rozanov, A.Y., Sayutina, T.A., and Ushatinskaya, G.T. 1987. Iskopaemye nizhnego kembriya gor Makkenzi (Kanada). *Trudy Paleontologicheskogo Instituta, Akademiya Nauk SSSR*, 224:1-88. (In Russian)
- Waagen, W. 1885. Salt Range fossils, Vol. 1, Part 4. *Productus* Limestone fossils, Brachiopoda. *Memoirs of the Geological Survey of India, Palaeontologia Indica*, 13:729-770.
- Walcott, C.D. 1886. Second contribution to the studies on the Cambrian faunas of North America. *U.S. Geological Survey Bulletin*, 30:1-225. <https://doi.org/10.5962%2Fbhl.title.38399>
- Walcott, C.D. 1920. Middle Cambrian Spongiae. *Smithsonian Miscellaneous Collections*, 67:261-364.
- Webster, M. 2011. Trilobite biostratigraphy and sequence stratigraphy of the upper Dyeran (traditional Laurentian "Lower Cambrian") in the southern great basin, U.S.A, p. 121-153. In Hollingsworth, J.S., Sundberg, F.A., and Foster, J.R. (eds.), *Cambrian Stratigraphy and Paleontology of Northern Arizona and Southern Nevada*. Museum of Northern Arizona, Flagstaff.
- Webster, M. and Bohach, L.L. 2014 Systematic revision of the trilobite genera *Laudonia* and *Lochmanolenellus* (Olenelloidea) from the lower Dyeran (Cambrian Series 2) of western Laurentia. *Zootaxa*, 3824(1):001-066. <https://doi.org/10.11646/zootaxa.3824.1.1>
- Williams, A., Carlson, S.J., Brunton, C.H.C., Holmer, L.E., and Popov, L.E. 1996. A supra-ordinal classification of the Brachiopoda. *Philosophical Transactions of the Royal Society of London B*, 351:1117-1193. <https://doi.org/10.1098%2Frstb.1996.0101>
- Wotte, T. and Sundberg, F.A. 2017. Small shelly fossils from the Montezuman-Delamaran of the Great Basin in Nevada and California. *Journal of Paleontology*, 91:883-901. <https://doi.org/10.1017%2Fjpa.2017.8>
- Wrona, R. 2003. Early Cambrian molluscs from glacial erratics of King George Island, West Antarctica. *Polish Polar Research*, 24:181-216.
- Wrona, R. 2004. Cambrian microfossils from glacial erratics of King George Island, Antarctica. *Acta Palaeontologica Polonica*, 49:13-56.
- Xing, Y., Ding, Q., Luo, H., He, T., and Wang, Y. 1984. The Sinian-Cambrian boundary of China and its related problems. *Geological Magazine*, 121:155-170. (In Chinese with English abstract) <https://doi.org/10.1017%2Fs001675680002820x>
- Yang, B., Steiner, M., and Keupp, H. 2015. Early Cambrian palaeobiogeography of the Zhenba-Fangxian Block (South China): Independent terrane or part of the Yangtze Platform. *Gondwana Research*, 28:1543-1565. <https://doi.org/10.1016%2Fj.gr.2014.09.020>
- Yang, B., Steiner, M., Li, G., and Keupp, H. 2014. Terreneuvian small shelly faunas of East Yunnan (South China) and their biostratigraphic implications. *Palaeogeography, Palaeoclimatology, Palaeoecology*, 398:28-58. <https://doi.org/10.1016%2Fj.palaeo.2013.07.003>
- Yu, W. 1974. Cambrian hyoliths, p. 111-113. In *Handbook of the Stratigraphy and Paleontology of Southwest China*. Science Press, Beijing. (In Chinese)
- Yu, W. 1979. Earliest Cambrian monoplacophorans and gastropods from western Hubei with their biostratigraphical significance. *Acta Palaeontologica Sinica*, 18:233-270 (In Chinese with English abstract)
- Yun, H., Zhang, X., and Li, L. 2018. Chancelloriid *Allonnia erjiensis* sp. nov. from the Chengjiang Lagerstätte of South China, *Journal of Systematic Palaeontology*, 16(5):435-444. <https://doi.org/10.1080/14772019.2017.1311380>
- Zhang, X.G. and Aldridge, R.J., 2007. Development and diversification of trunk plates of the Lower Cambrian lobopodians. *Palaeontology*, 50:401-415. <https://doi.org/10.1111%2Fj.1475-4983.2006.00634.x>
- Zhang, X., Ahlberg, P., Babcock, L.E., Choi, D.K., Geyer, G., Gozalo, R., Hollingsworth, J.S., Li, G., Naimark, E.B., Pegel, T., Steiner, M., Wotte, T., and Zhang, Z. 2017. Challenges in defining the base of Cambrian Series 2 and Stage 3. *Earth-Science Reviews*, 172:124-139. <https://doi.org/10.1016/j.earscirev.2017.07.017>

Zhou, B. and Xiao, L. 1984. Early Cambrian monoplacophorans and gastropods from Huainan and Huoqiu counties, Anhui province. *Professional Papers in Stratigraphy and Palaeontology*, 13:125-140.